Patrícia Raquel dos Santos Rodrigues

Licenciada em Bioquímica

Development of oxidoreductase based electrochemical biosensors

Dissertação para obtenção do Grau de Mestre em Biotecnologia

Orientadores : Profª Doutora Maria Gabriela Machado de Almeida, Investigadora associada, FCT-UNL
Profª Doutora Sofia de Azeredo Pereira, Investigadora auxiliar, FCM-UNL

Júri:

Presidente: Prof. Doutor Rui Manuel Freitas Oliveira

Arguente: Profª Doutora Ana Pimenta da Gama da Silveira Viana Semedo, Professora Auxiliar convidada, Faculdade de Ciências da Universidade de Lisboa

Vogal: Doutora Maria Gabriela Machado de Almeida, Investigadora Auxiliar, FCT-UNL

FACULDADE DE CIÊNCIAS E TECNOLOGIA
UNIVERSIDADE NOVA DE LISBOA

Maio, 2013

Development of oxidoreductase based electrochemical biosensors

Acknowledgements

First and foremost, I'd like to thank my supervisor, Prof. M. Gabriela Almeida for all her hard-work and support, the work developed during this year wouldn't have been the same without her constant presence, commitment and all the opportunities she made possible; I might not always show it but deep down I'm truly grateful for working to/with her. But above all else I'm indebted to her for all the faith she has put in me since the beginning.

I would like to acknowledge all the collaborators, which have contributed for this work and made it possible.

Dr. Michel Kranendonk, from Instituto de Higiene e Medicina Tropical, for providing the CYP samples used during this work.

To Dra. Sofia Azeredo Pereira for all her help and know-how in the early stages of the project.

A huge thank you to Dr. Mathieu Etienne who kindly received me in his lab in Nancy and always had an open door when I needed it.

To the ERASMUS program for enabling me to travel to France and perform such a great part of the work in this thesis.

I can't help mentioning my appreciation towards my office partners, Claúdia Nóbrega and Humberto Pedroso, for bearing with me even when I'm at my most despicable and can't stop ranting and venting for the life of me. If indeed someone deserves a place in heaven it's the both of them for being so patient xD

Like Norma Jean would say "I'm selfish, impatient and a little insecure. I make mistakes, I am out of control and at times hard to handle. But if you can't handle me at my worst, then you sure as hell don't deserve me at my best." Butterfly you both *

A very special thank you to Célia Silveira, even though she didn't have any obligation to listen to me, always did so with a lot of patience and helped me in any way she could. I can't seem to find the right words to thank you enough. I know you like to think of yourself like a cold person but I know the truth, deep down you're one tiny softy =P

I have thank César, if it wasn't for him I'd have been left stranded on the wrong side of the river for a good portion of the year. For that and everything else, thank you.

Last but not the least I'd like to thank everybody who has at some point wished me well (if you don't anymore I might have done something to deserve it), you probably know who you are better than I do ;)

Abstract

This thesis is divided in 2 sections, each describing the development of an oxidoreductase based biosensor. In the first part human Cytochrome P450 1A2 (CYP1A2) electrochemistry was studied, while the second is focused on the optimization of immobilization platforms and operation methods for amperometric biosensors, using cytochrome c nitrite reductase (ccNiR), (*Desulfovibrio desulfuricans* ATCC 27774) as a model enzyme.

The direct electrochemistry of P450s immobilized in water-based sol-gel thin films was described for the first time. The optimization of the film showed that only the combination of the inorganic matrix and the PEG400 enabled the direct electron transfer reaction and electrocatalytic activity towards oxygen. The amount of dissolved oxygen in solution revealed itself a significant feature in CYP's electrochemistry – in anaerobic conditions, when small amounts of oxygen are added the $PFe^{III/II}$ signal's intensity increased, while in aerobic conditions it disappeared; probably PFe^{III} is not being regenerated. However, this was not observed with the CYPOR complex, indicating that the reductase has an essential role in the CYP's catalytic cycle completion; this was also sustained by the fact that only in its presence organic substrates catalysis (caffeine) occurs.

The hybrid sol-gel developed for CYP, was optimized for a nitrite biosensor. ccNiR was successfully incorporated while promptly displaying catalytic currents. Although the bioelectrode's response decreases after day one, it was able to maintain a reasonable catalytic activity over a time span of 2 weeks. Another electrode modification strategy, studied with ccNiR, was based on the electrophoretic deposition of macroporous assemblies of single-walled carbon nanotubes. The macroporous structure was created as a result of the presence of polystyrene beads co-deposited with the carbon nanotubes. An increase in the amount of material was correlated with a higher enzyme activity.

Finally, an oxygen scavenger system consisting of glucose oxidase, glucose, and catalase was employed for oxygen removal in an open electrochemical cell. The system completely removed oxygen for over 1 h and was successfully applied to a ccNiR based nitrite sensor.

Keywords: biosensors, cytochrome *c* nitrite reductase, cytochrome P4501A2, sol-gel, carbon nanotubes, electrophoretic deposition.

Resumo

O presente trabalho encontra-se dividido em duas secções, cada um descrevendo o desenvolvimento de um biossensor baseado em oxidorredutases. Na primeira secção, foi estudada a eletroquímica do citocromo P450 1A2 (CYP1A2), enquanto que a segunda se foca na otimização de plataformas de imobilização e métodos de operação para biossensores amperométricos, usando a redutase do nitrito multihémica (ccNiR) extraída de *Desulfovibrio desulfuricans* ATCC27774 como um enzima modelo.

A electroquímica direta de P450 imobilizado em filmes à base de filmes de sol-gel aquoso foi descrita pela primeira vez. A otimização da composição do material mostrou que a combinação da matriz inorgânica e o PEG400 facilitava grandemente a transferência de electrões directa. A quantidade de oxigénio dissolvido na solução revelou-se uma característica importante em electroquímica do CYP - em condições anaeróbicas, em que as pequenas quantidades de oxigénio foram adicionados, a intensidade do sinal $PFe^{III/II}$ aumentou, enquanto que em condições aeróbicas desapareceu; provavelmente o PFe^{III} não estava a ser regenerado. No entanto, o mesmo não foi observado com o complexo CYPOR, indicando que a redutase tem um papel essencial na conclusão do ciclo catalítico do CYP, o que também foi sustentado pelo facto de apenas na sua presença ocorrer a catálise de substratos orgânicos (cafeína).

O sol-gel híbrido desenvolvido para o CYP, foi adaptado para um biossensor de nitrito no qual a ccNiR foi incorporada com sucesso. Embora a resposta do bioeléctrodo tenha diminuido após o primeiro dia, a atividade catalítica foi mantida a um nivel razoável ao longo de um intervalo de tempo de 2 semanas. Outra estratégia de modificação do eletrodo estudada com ccNiR, foi baseada na deposição eletroforética de nanotubos de carbono macroporosos. A estrutura macroporosa foi criado como resultado da presença de esferas de poliestireno co-depositadas com os nanotubos de carbono. Um aumento na quantidade de material foi correlacionado com o aumento da actividade enzimática.

Finalmente, um sistema eliminador de oxigénio consistindo em glucose oxidase, glucose e catalase, foi empregue para a remoção de oxigénio de uma célula electroquímica

aberta. O sistema removeu completamente o oxigénio durante mais 1 h e foi aplicado com êxito a um sensor de nitrito baseado na ccNiR.

Palavras-chave: biosensors, reductase do nitrito multihémica, citocromo P4501A2, transferência electrónica, sol-gel, deposição electroforética.

Contents

List of Figures

List of Tables

1

Introduction

1.1 Electrochemical Biosensors

1.1.1 Importance

The sensitive and selective determination of a large number of compounds is of great relevance, and has always been a problem of the utmost importance scientific research. In the field of health-care, it is indispensable for the diagnosis of diseases. Biotechnology, too, requires the analysis of complex media. High selectivity, even in trace analysis, has been achieved by the considerable progress in analytical instrumentation, as is reflected by modern gas chromatography, high-pressure liquid chromatography, mass spectrometry and atomic absorption spectroscopy. However, due to the high costs associated with these powerful instrumental techniques they are only used in specialized laboratories. The development of methods highly selective and easy to handle is thus a key issue in analysis. Whereas reliable sensors are available for the determination of physical parameters, e.g. temperature, pressure, or sound energy, the qualitative and quantitative analysis of chemical composition remains difficult. Electrochemical sensors, such as pH electrodes and Clark-type electrodes for oxygen measurement are widely used for this purpose[1-3]. Biosensors may be the answer to these problems.

1.1.2 History

The term biosensor was devised by Karl Camman in 1977. He defined it as a chemical sensor where the recognition system uses a biochemical mechanism. However, the IUPAC did not agree on the implementation of the term until 1997. Whereupon, the IUPAC

committee came up with their own definition, comprising Camman's definition plus several parameters that must be fulfilled (see below)[2].

Even though Karl Camman was the one who laid claim to the term, Leland C. Clark is considered by many the father of biosensors. He had developed the first bubble oxygenator for use in cardiac surgery. Conversely, when he came to publish his results, his article was refused by the editor since the oxygen tension in the blood coming out from the device could not be measured. This instigated Clark to develop the oxygen electrode4, with which he meant to measure the reduction of oxygen with a platinum electrode in order to determine the oxygenation of blood[5]. His first sensor failed because the blood components would adsorb on the electrode's surface, which in turn distorted the signal. Later on, Clark had the idea, which would change the history of biosensors, of using the cellophane wrapper of a cigarette packet on his sensor, making it so that only low molecular weight substances, mainly oxygen, could reach the electrode surface and be measured. The reduction current indicated the oxygen concentration, and so the Clark electrode was created[2]. Nowadays, Teflon is used as the membrane and this sensor remains a key tool in medicine and environmental monitoring. Afterwards, Clark developed the sensor further by entrapping concentrated glucose oxidase (GOx) with another semi-permeable membrane in front of the electrode, which could then be used for multiple glucose measurements based on the monitoring of the reaction described on equation 1.1[6].

$$glucose + O_2 \xrightarrow{glucose\ oxidase} gluconic\ acid + H_2O_2 \tag{1.1}$$

The enzyme layer became an integrated part of the sensor. Lee Clark went on to coin the term *"enzyme electrode"* at a meeting of the New York Academy of Sciences in 1962[2]. It was this electrode arrangement that introduced the new sensor concept - the biosensor. A few years later, hydrogen peroxide reduction was detected on the electrode instead of oxygen, due to limitations concerning this particular system, namely, oxygen fluctuations, substrate limitations/sensitivity, electrochemical interferences, among others[7].

Clark's system has been thoroughly studied and modified throughout the years, for several different purposes, one of which – an oxygen scavenging system – will be explored in this thesis.

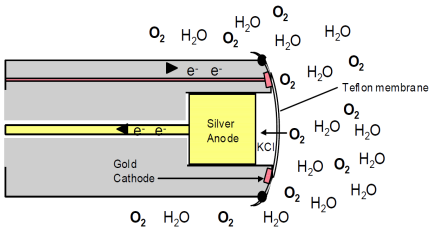

Figure 1.1: Clark electrode functioning.

Because of the volume of the literature regarding amperometric biosensors as well as space limitations it is not possible to cite all contributions to the field. It was selected representative work in the field of electrochemical biosensing. General milestones and achievements relevant to biosensor research and development are listed in Table 1.1.

Table 1.1: Historical landmarks in the development of enzyme based electrochemical biosensors.

Date	Event	References
1962	First glucose enzyme electrode	Clark, L. C. & Lyons, C.[5]
1973	Glucose enzyme electrode based on peroxide detection	Guilbault, G. G. & Lubrano, G. J.[8]
1975	Launch of the first commercial glucose sensor system	YSI Inc.
1977	Karl Cammann introduced the term " biosensor "	Cammann, K.[9]
1977	Reversible ET of cytochrome c was obtained employing tin-doped indium oxide electrodes and 4,4′ - bipyridiyl as a promoting monolayer on gold electrodes.	Eddowes, M. J. & Hill, H. A. O.[10] Eddowes, M. J., Hill, H. A. O. & Uosaki, K.[11]
1981	Oxidation of NADH at graphite electrodes is described for the first time.	Huck, H. & Schmidt, H.-L[12] Jaegfeldt, H. *et al*[13]
1982	Demonstration of in vivo glucose monitoring	Shichiri, M. *et al.*[14]
1984	First ferrocene - mediated amperometric glucose biosensor by Cass et al. The work led to the development of the first electronic blood glucose measuring system which was commercialized by MediSense Inc. (later bought by Abbott Diagnostics) in 1987.	Cass, A. E. G. *et al.*[15]
1987	Launch of the first glucose meter	Medisense Inc.
1987	Electrical wiring of enzymes	Degani, Y. & Heller, A.[16]
1988	Adam Heller and Yinon Degani introduced the electrical connection ("wiring") of redox centers of enzymes to electrodes through electron - conducting redox hydrogels. This work was the basis for continuous glucose monitoring employing subcutaneously implanted miniaturized glucose biosensors.	Degani, Y. & Heller, A.[17] Forster, R. J. & Vos, J. G.[18]; Csöregi, E., Schmidtke, D. W. & Heller[19] Schmidtke, D. W.[20] Wagner, J. G. et al.[21]
1988	Direct ET by means of immobilized enzymes was introduced	Frew, J. E. *et al.*[22–28]
1997	IUPAC introduced for the first time a definition for biosensors in analogy to the definition of chemosensors	Zayats, M. *et al.*[29]
1999	Launch of a commercial in vivo glucose sensor	Minimed Inc.
2000	Introduction of a wearable noninvasive glucose monitor	Cygnus Inc.
2002	Schuhmann et al. introduced the use of electrodeposition paints (EDPs) as immobilization matrices for biosensors. Following work enabled the incorporation of redox mediators into the polymer structure of EDPs	Kurzawa, C. *et al.*[30–32]
2007	An implanted glucose biosensor (Freestyle Navigator System) operated for five days	Weinstein, R. L. *et al.*[33]

1.1.3 Biosensor components

Nowadays, biosensors are characterized by the direct spatial combination of a matrix-bound biologically active substance - the so-called receptor - with a transducer component. For molecular recognition, biosensors may also be equipped with other biologic elements instead of enzymes. Besides nearly all kinds of electrodes, various other signal transducers have been combined with the immobilized bio-material[34]. Examples of these components are given in Figure 1.2; this compilation helps one to understand which parameters change during a biological recognition event in a biosensor. The choice of the transduction process and transduction material is dependent on this knowledge as well as the chemical approach to construct the sensing layer on the transducer surface.

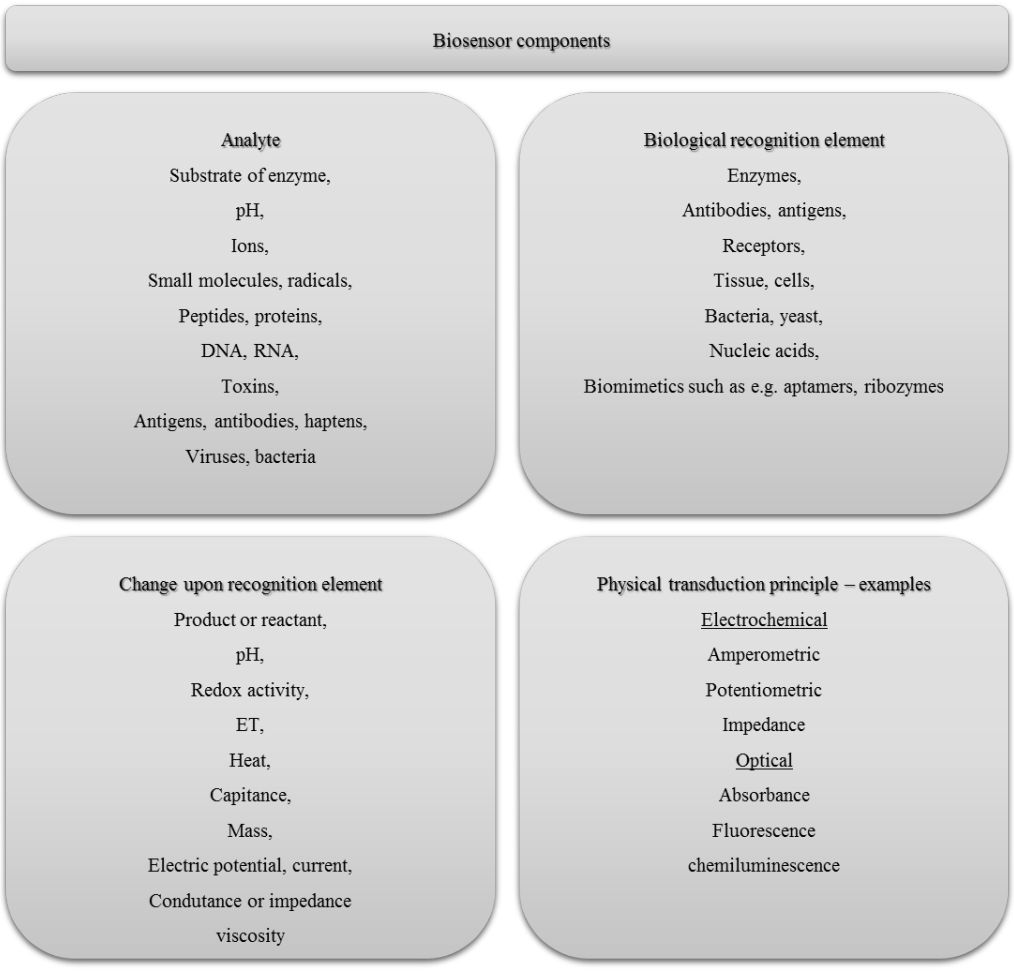

Figure 1.2: Examples for biosensor components and measured analytes[1].

The choice of the biological recognition element is the crucial decision when developing a novel biosensor device. Most importantly, the bioreceptor needs to selectively react with the analyte of interest. The bioreceptor needs to be stable under the operation and should provide a reasonable long-term stability. In Table 1.2 it is possible to see different types of receptors used in biosensors, that recognize specific species, and the

electrochemical measurement techniques linked to them[29].

Table 1.2: Types of receptors used in biosensors[a].[35]

Analytes	Receptor: Chemical recognition Measurement technique: Transduction mode system	Measurement technique: Transduction mode
1. Ions	mixed valence metal oxides	potentiometric, voltammetric
	permselective, ion-conductive inorganic crystals	
	trapped mobile synthetic or biological ionophores	
	ion exchange glasses	
	enzyme(s)	
2. Dissolved gases, Vapors, odors	bilayer lipid or hydrophobic membrane	in series with 1. amperometric
	inert metal electrode	amperometric or potentiometric
	enzyme(s)	amperometric, potentiometric or impedance, piezoelectric, optical
	antibody, receptor	
3. Substrates	enzyme(s)	amperometric or potentiometric in series with 1. or 2. or metal or carbon **electrode, conductometric,** piezoelectric, optical, calorimetric
4. Antibody: antigen	whole cells	as above
	membrane receptors	as above
	plant or animal tissue	as above
	antigen/antibody oligonucleotide duplex, aptamer	amperometric, potentiometric or impedimetric, piezoelectric, optical, surface plasmon resonance
	enzyme labelled	in series with 3. optical
	chemiluminescent or fluorescent labelled	
5. Various proteins and low molecular weight substrates, ions	specific ligands	as 4.
	protein receptors and channels	
	enzyme labelled	
	fluorescent labelled	

Enzymes are by far the most commonly used biological components in biosensors. Furthermore, electrochemical transduction is the most popular signaling method, with amperometry (measurement of electric current) the favored configuration. It is advantageous if the chemical structure of the enzyme allows the introduction of additional functionalities for chemical modification with redox mediators, binding, or crosslinking with the immobilization matrix. In addition, the potential for tuning the properties of the redox enzyme by means of genetic or chemical techniques can be helpful for biosensor optimization. An important factor, especially with respect to potential commercialization, is that the redox enzyme is available at reasonable costs and effort. This work will focus on membrane-bound enzymes as the bioreceptor, therefore they will be given special attention in this section.

The main advantages of employing enzymes in biosensor architectures are the following:

i) They can exhibit a very high catalytic activity with a turnover on a per mole basis which makes them not only exceptional bioelectrocatalysts for effective signal amplification in biosensors but also for biofuel cells. Good turnover frequencies k_{cat} are in the range of up to, at least, 100 s^{-1}.

ii) Typically, enzymes have a high selectivity for their substrates.

iii) The driving force - redox potential needed to achieve enzymatic biocatalysis - is often very close to that of the enzyme's cofactors. Therefore, biosensors can operate at moderate potentials.

iv) In several cases, an improvement of the enzyme stability is found when enzymes are immobilized on transducer surfaces[36,37].

Key parameters of biosensor performance

- Analyte
- Employed biocomponent for recognition of analyte
- Type & composition of sample matrices
- Selectivity
- Sensitivity
- Dynamic range
- Detection limit
- Reproducibility
- Precision
- Stability (in use, long-term, storage)
- Calibration approach (requirements, intervals, drift)
- Duration to reach baseline

Additional parameter of biosensor performance, e.g. relevant for commercialization

- Cost per measurement
- Duration of measurement
- Turnover of measurements (time resolution
- Warm-up time
- Sample volume
- Measuring temperature
- Size, weight & price of the device
- Costs, size & weight of required instrumentation
- Delivery time
- Development status of the device/procedure (commercial product, standard procedure, basic research, proof-of-principle)
- Time between maintenance checkspotential to be coupled with other analytical techniques
- Data storage and processing

Figure 1.3: Key features of amperometric biosensors[1].

Knowing the most influential parameters on a specific biosensor is the basis to understand and fine tune the performance of these devices in a rational manner. Figure 1.3 summarizes several analytical features of typical biosensors; selectivity, sensitivity, accuracy, response and recovery times, as well as operating lifetime are some of the most significant key factors.

An essential aspect of biosensor optimization is the elimination/reduction of the impact of interferences. In most samples there are components that either directly react at the electrode surface or at the involved redox centers, or interfere with the biological

recognition reaction (e.g., inhibitors or other enzyme substrates). Additional problems such as leakage from the sensing layer, loss of enzyme activity or electrode fouling may occur. Therefore, changes in sensitivity and baseline drifts are bound to arise during biosensor operation. Suitable strategies are needed to ensure reproducible and quantitative results[38]. For applications aimed for the general public, it is imperative to characterize and optimize the biosensor architecture under actual measuring conditions.

Besides dictating the efficiency of electrochemical transduction, the biosensor design also plays a fundamental role in defining the response features. For example, sensitivity and response time, which strongly depends on mass transfer limitations, are particularly influenced by the characteristics of the immobilization matrix[39].

1.1.4 Immobilization techniques

The main limitation for successful applications comes from the difficulty to elaborate reagentless devices in which all components enabling the bioelectrochemical detection (i.e. enzyme(s), cofactor and electro-catalytic system for cofactor detection and regeneration) are immobilized in a durable and active form[40]. The immobilization of biomolecules permits the re-use of costly biological molecule and allows a significant simplification of the analytical apparatus.

Controlled immobilization techniques are useful to more than allowing the re-use or continuous use of industrial enzymes. The immobilization and subsequent post-immobilization techniques can be very advantageous to greatly increase activity–stability properties of enzymes[41]. For example, inactivation of multimeric enzymes may be strongly influenced by the dissociation of subunits. On the other hand conformational changes promoted by any denaturing agent (heat, pH, organic solvents) on the small fraction of dissociated monomers could be much more rapid and intense[42,43].

The use of biological species such as proteins, peptides, nucleic acids and even whole cells in biosensors relies largely on the successful immobilization of the bioreceptor in a physiologically active form. Typical methods to immobilize bioreceptor onto inorganic, organic or polymeric surfaces have been based on physical adsorption[44], covalent binding[45], entrapment in semi-permeable membranes[46] and microencapsulation into polymer microspheres and hydrogels[47,48]. Notwithstanding problems such as leaching and desorption[44], denaturation and difficulty controlling the orientation of the biomolecule[49], these methods have proven to be amenable to the immobilization of a large number of biomolecules.

Various methods have been described for protein immobilization (Table 1.3). In general, biosensors using adsorbed enzymes or proteins are insensitive and unstable, except for a few cases, this procedure alone is rarely used in biosensor construction.

The relative lack of long-term stability in biological molecules is the most serious limitation in commercializing biosensors. Under some circumstances, the immobilized

Table 1.3: immobilization procedures for enzymes[50].

Method	Advantages	Disadvantages
Adsorption on insoluble matrices (e.g. by Van der Waals forces, ionic binding or hydrophobic forces)	Simple, mild conditions, less disruptive to enzyme protein	Enzyme linkages are highly dependent on pH, solvent and temperature; insensitive
Entrapment in a gel (eventually behind a semipermeable membrane)	Universal for any enzyme, mild procedure	Large diffusional barriers, loss of enzyme activity by leakage, possible denaturation of the enzyme molecules as a result of free radicals
Crosslinking by multifunctional reagent (such as glutaraldehyde bis-isocyanate derivatives or bis-diazobenzidine)	Simple procedure, strong chemical binding of the biomolecules; widely used in stabilizing physically adsorbed enzymes or proteins that are covalently bound onto a support	Difficult to control the reaction, requires a large amount of enzyme, the protein layer has a gelatinous nature (lack of rigidity), relatively
Covalent bonding onto a membrane, insoluble supports	Stable enzyme-support complex, leakage of the biomolecule is very unlikely, ideal for mass production and commercialization	Complicated and time-consuming: possibility of activity losses due to the reaction involving groups essential for the biological activity (can be minimized by immobilization in the presence of the substrate or inhibitor of the enzyme)

preparation displays a decrease in stability. Chibata[51] reports that, of 50 enzyme immobilizations studied, 60% showed an increase in stability, 24% were unaffected and 16% showed a decrease in stability.

As it is, in this thesis, special attention will be given to sol-gel immobilization and surfactant films. The interest of **sol–gel** chemistry for bioencapsulation has been largely discussed in the literature[52] for several types of biosensors, but most importantly it has been successful in protein immobilization on electrode surfaces[53,54]. Sol-gel matrices are produced from a starting colloidal suspension of sol-gel precursors –the sol – which undergoes hydrolysis and condensation reactions to form the gel (Figure 1.4).

The sol-gel entrapment can be a relatively gentle chemical procedure that is carried out at room temperature so that many of the molecules can endure the entrapment. The sol-gel methodology has been extensively used to immobilize soluble proteins showing that the majority of them can be encapsulated with retention of their native structure and functionality and an enhanced stability[52,55–58].

Bioencapsulation within these materials is usually obtained from the hydrolysis of alkoxide precursors (usually tetraethyl orthosilicate, TEOS, or tetrametyl orthosilicate, TMOS) resulting in a colloidal sol solution. Subsequently, a buffered aqueous solution containing the biomolecule of interest is added to the sol producing a polycondensation reaction that leads to the formation of a transparent highly porous gel that encloses the species within its pores. The popularity of sol-gel materials can be attributed to this and other significant factors, namely[54]:

(a) The ability to generate an almost infinite number of organic- inorganic hybrids that

display both the mechanical stability of a rigid inorganic framework and the particular reactivity (e.g., selective recognition, optical properties) of the organic component;

(b) The fact that sol-gel-derived materials can be used to encapsulate biomolecules (e.g., enzymes, antibodies, or other proteins) in a functional state;

(c) The discovery of the supramolecular template approach, which can generate ordered mesostructures over long length scales.

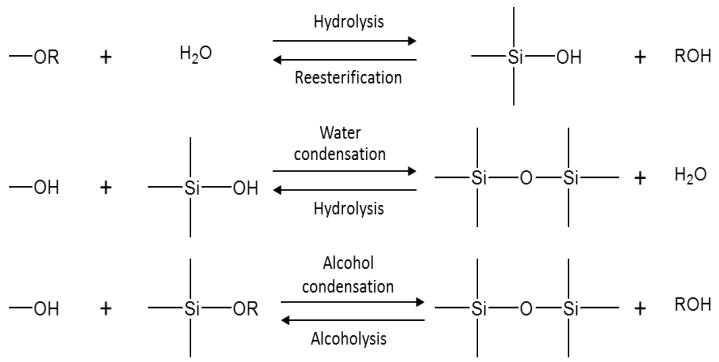

Figure 1.4: Sol-gel formation reactions from silica based alkoxide precursors.

Surfactants are surface active agents composed of a charged or polar head group and a hydrophobic nonpolar tail. The tail is generally a hydrocarbon chain with 6-22 carbon atoms. The hydrophilic region of the molecule – the head group – may be positive, negative, neutral or zwitterionic, thus categorizing the surfactant as cationic, anionic, non-ionic or zwitterionic[59,60]. Surfactants with longer hydrocarbon chains are also less prone to denature proteins than short chained compounds. Zwittergents like amphoteric sulfobetaines are usually more inactivating than non-ionic reagents[59,60]. Surfactant molecules can be adsorbed at the interface between two bulk phases such as the electrode/solution interface; lowering the interfacial tension between the two and facilitate the contact. Therefore, these surface active agents are capable of modifying and controlling electrode surface properties[61]. Surfactant molecules can aggregate to form supra-molecular structures with specific regions of hydrophilic and hydrophobic character. In aqueous solution, above the critical micellar concentration (CMC), they form spherical micelles with the hydrophilic head groups facing the solution and the hydrocarbon chains oriented towards the interior of the structure Figure 1.5 [59]. The CMC is characteristic of each surfactant and in addition to micelle formation it is also correlated with abrupt changes or sharp discontinuities in the physical properties of the surfactant, such as conductivity and surface tension[62,63].

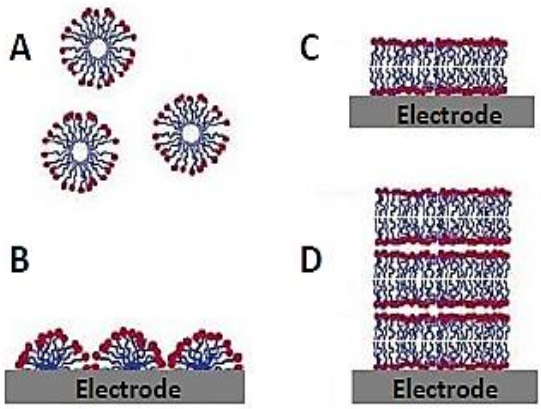

Figure 1.5: Schematic representations of surfactants in various forms, the headgroups are represented by the red circles and the hydrophobic tails are in blue. A) Spherical micelles, B) hemimicelles, C) bilayers and D) multilayers on electrode surfaces[39].

Electrochemistry mainly takes advantage of two properties associated with these surface active agents: their ability to adsorb at interfaces and to generate membrane-like structures[61]. In particular the membrane bound proteins incorporated in surfactant films are expected to experience a more natural environment, closer to the physiological surroundings they are taken from. Accordingly, surfactant films can help to promote and enhance protein electrochemistry and catalysis. Obvious cases are membrane-bound proteins[62], such as the enzyme employed in this thesis. Various soluble proteins have also shown enhanced electron transfer in surfactant films[61,64-66]. Myoglobin and some cytochrome P450 isoforms, for example, have showed good reversible electrochemistry in surfactant films of DDAB (Dodecyldimethylammonium bromide) at PG electrodes, as opposed to the bare ones, where no DET was observed. According to spectroscopic studies, both proteins were also able to keep their native conformations while embedded in the films[62,63,67].

The good performance of proteins in surfactant films has been associated to the strong adsorption of the surfactant at the electrode-film interface, therefore avoiding the denaturative adsorption of proteins or of other macromolecules that could block electron transfer[63]. Also, the well-defined microstructure and dynamics of the surfactant films allows good diffusion within the layer. These films can also help to guide the orientation of immobilized proteins. Which may not be related with the surfactant headgroup charge but with the interaction between the protein and the hydrophobic bilayers[68].

Rusling has pioneered the use of surfactant films on carbon surfaces for direct electrochemistry of heme proteins[69-71]. The surfactant is deposited onto the electrode, resulting in the formation of bilayers and micelles into which the protein is incorporated. The end result is a system that supports rapid and reversible ET between the electrode and the enzyme; typically, standard rate constants between 50 and 300 s^{-1} are observed. Protein-surfactant film voltammetry is now a routine method for studying the redox chemistry of

Heme transfer proteins: flavocytochromes[72], engineered mutants[73], as well as bacterial[74] and mammalian[75] variants, have been investigated.

1.1.5 Amperometric biosensors

As previously mentioned, a biosensor is generally defined as a sensing device consisting of a biological recognition element in intimate contact with a suitable transducer which is able to convert the biological recognition reaction, or eventually the biocatalytic process, into a measurable electronic signal. In the particular case of an amperometric sensor, the redox species in the sensing layer are oxidized or reduced at the transducer surface generating a current through the electrode. Assuming an enzyme catalyzed oxidation of a substrate (e.g. glucose, lactate, alcohol, etc.), either a prosthetic group integrated within the enzyme (e.g. FAD, PQQ, heme, transition metals) or a co-substrate (e.g. FMN, NAD+, NADP+) has to be reduced, intermediately storing the transferred redox equivalents. A measurable current through the electrode is related to the re-oxidation of the prosthetic group or the co-substrate in order to regenerate the enzyme and make it available for further substrate recognition and conversion reactions. Hence, a signal is only obtained if the transfer of electrons between the intermediately reduced enzyme (i.e. the prosthetic group or the co-substrate) and the electrode is possible. From this discussion it is evident that the specific features of the biosensor are highly dependent on the kinetics of this electron transfer process. Consequently, an essential prerequisite for the development of amperometric biosensors with high sensitivity and fast response characteristics is to establish a fast electron transfer (ET) from the biological component to the electrode.

1.1.5.1 Electron transfer

At a first glance, the easiest ET mechanism in an amperometric biosensor would be the direct electrochemical recycling of the enzyme's prosthetic group at the electrode surface involving electron tunneling mechanisms (Figure 1.6). However, according to the Marcus theory[76], the ET kinetics between two redox species is determined by the driving force (i.e. the potential difference), the reorganization energy (which qualitatively reflects the structural rigidity of the redox species) and the distance between the two redox centers. Obviously, the ET distance between the prosthetic group and the electrode surface is rather long due to the shielding by the protein shell, and direct ET via a tunneling mechanism is therefore rarely encountered.

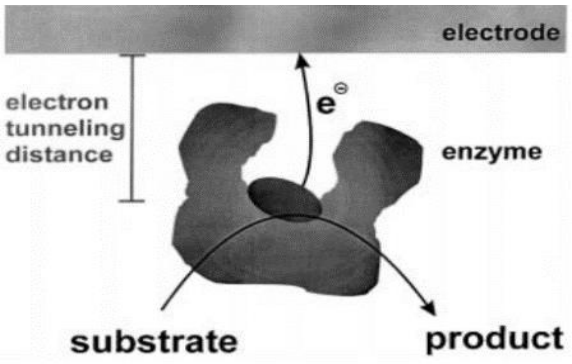

Figure 1.6: Direct ET (tunneling mechanism) from the active site of an enzyme to the electrode surface[77].

Thus, the main aim in the design of optimized amperometric biosensors is to ensure fast ET processes based on electrode architectures with predefined ET pathways interconnecting the redox site within the enzyme and the electrode surface. The electron transfer in biology usually involves initial protein-protein complex formation based on the complementarity of the docking sites. Efficient protein-electrode reactions appear to have some similarities to the way in which proteins act with their natural redox partner[78]. Therefore, methods for chemically modifying electrode surfaces as to mimic the biological situation were developed. The heterogeneous electron transfer between proteins and electrodes may be coupled with other reactions where the proteins act as vectorial mediators[79,80].

The principle of direct electrochemistry of redox proteins, can be explained by comparing this technique to the more traditional solution essays of enzyme activity. In homogeneous enzyme kinetics, the enzyme may be mixed in a cuvette with its substrate and a redox partner (otherwise called a mediator or co-substrate), providing a source/sink of electrons for the redox transformation of the substrate and whose absorbance depends on its redox state. In the steady state, the rates of substrate and co-substrate transformations are equal to the turnover rate of the enzyme and can therefore be determined by following the absorbance change of the solution[81].

In direct electron transfer (DET) the increase in catalytic currents is a result of the enzyme's cofactors direct regeneration (Figure 1.7A). This type of communication with the electrode, is typically harder to achieve due to the insulating nature of protein polypeptide chains and the location of redox centers, which are commonly deeply buried within the protein structure. Furthermore, the protein molecules can have an unfavorable orientation on the transducer surface, sometimes contributing to an increased distance between the electroactive centers and the electron transfer partner (the electrode) and thus hindering the electron exchange[39].

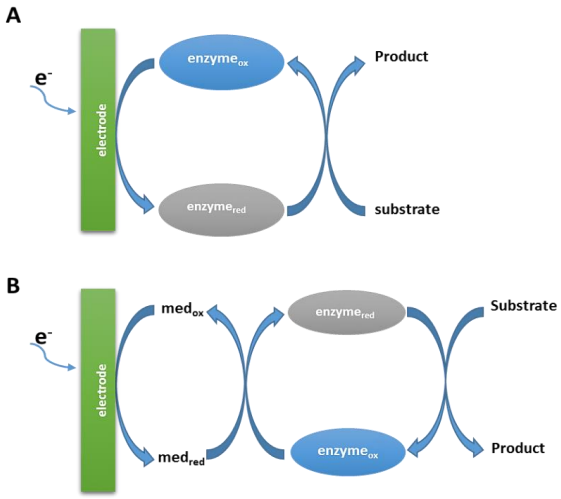

Figure 1.7: Schematic representations of the working principles of enzymatic biosensors with a reductase as biologic component: **A)**Mediated transduction, **B)** Direct transduction. (medox – mediator in the oxidized form; medred –mediator in the reduced form; enzymeox – reductase oxidized state; enzymered – Reductase reduced state).

Nowadays is still common to think that oxireductases are too large and too fragile to interact directly with a solid electrode without being at least partly denaturated. It is usually held that because the active site of these enzymes is deeply buried in the protective protein matrix, direct electron exchange at an electrode can only occur under exceptional conditions. However, more than 20 years have passed since it was shown that direct electron transfer (DET) can occur between an electrode and a large, catalytically active enzyme,[82,93] and about one hundred examples have already been reported[81,94].

Unlike in DET, the use of redox mediators takes control over the protein reaction center away from the electrode[95](Figure 1.7B). On the one hand, this can be detrimental to the selectivity of detection, because the mediator can react with other species present, and, for biosensors, can require a more complex manufacturing process, additional reagents, and sophisticated immobilization methods. On the other hand, redox mediation can overcome the frequently sluggish electron communication of enzyme redox centers with electrodes, thus increasing ET rates[96]. Mediated transfer of redox equivalents is the working principle of second-generation amperometric biosensors. Mediators are characterized by having a high heterogeneous ET rate that does not compromise electrochemical reversibility and, at the same time, homogeneous, rapid electron exchange with the enzyme. Both oxidized and reduced forms of the mediator should be stable and unreactive with oxygen; also, the reaction should not depend on pH. Furthermore, when selecting a redox mediator for biosensor applications it is important to consider toxicity, biocompatibility, ease of immobilization, and, very importantly, the redox potentials. Low operating potentials are preferred, enabling appropriate enzyme reaction transduction while avoiding side reactions. In other words, a mediator should shift redox potentials from the extreme values necessary to detect target analytes, to values near zero, at which

fewer interfering species are reduced or oxidized[95,97,98]. In mediated electrochemistry, the consumption of the redox partner is detected as a current wave resulting from its electrochemical recycling on the electrode; only the mediator interacts with the electrode, and the homogeneous catalytic process which occurs in the bulk of the electrochemical cell is fundamentally the same as that in solution assays[81].

Biosensors can be grouped into generations according to the modes of signal transfer between a redox enzyme and an electrode, i.e., via the natural secondary substrates or products of the enzyme reaction (first generation), via artificial (either synthetic or biological) electron mediators (second generation) or via direct electronic contact (third generation)[34,99,100]. A typical first generation biosensor is a glucose sensor with gel entrapped glucose oxidase on a Clark-type electrode[101,102] and also many variants of coupled enzymes on oxygen-sensitive electrodes[103].

Table 1.4: Generations of enzyme based amperometric and voltammetric biosensors MET, mediated electron transfer; DET, direct electron transfer[96].

Generation	ET mode	Electroactive species	Examples
1st	MET	Natural Co-substrates Products	O_2
			H_2O_2
2nd	MET	Artificial Natural ET molecules	Ferrocene, Viologens
			Cytochrome c
3rd	DET	Enzyme redox cofactores	Laccase, hemoglobin, peroxidades, nitrite Reductase

1.2 Nitrite Reductase based electrochemical biosensor

1.2.1 Nitrite assessment

Nitrate (NO_3^-) and nitrite (NO_2^-) are rarely found without each other, because their chemistries are practically indissociable.

Nitrate occurs naturally in soils containing nitrogen-fixing bacteria, decaying plants, septic system effluents, and animal manure. Among the artificial sources of nitrate there are nitrogenous fertilizers and airborne nitrogen compounds emitted by industry and motor vehicles. Nitrate penetrates through the soil and remains in groundwater for decades[104]; groundwater is the source for >50% of drinking water supplies, 96% of private water supplies, and an estimated 39% of public water supplies[105].

Water containing a high concentration of nitrite can create serious problems, for example, eutrophication of aquatic systems and potential hazards to human health[106]. The eutrophication in rivers, lakes, and coastal waters has become one of the most prevalent

environmental problems in recent years[106,107]. The health implications of exposure to nitrate in drinking water were first reported in 1945 by Comly after observing cyanosis in infants in Iowa, where well water was used in formula preparation[108]. These implications made it so that nitrite has been considered an important toxic agent[109]. However, as of late, there have been many new findings that imply the nitrite's role in the human organism may not be so straightforward, the main controversy is that nitrite's ingestion might be beneficial for human health despite it's being considered solely hazardous since the 1940's[110-122].

In order to manage environmental and health risks, deriving from exposure to these ions, governmental agencies have implemented rules and directives to restrict the levels of NO_3^- and NO_2^- in drinking waters and food products. European directive 98/83/EC has established the maximum admissible levels of nitrate and nitrite in drinking water at 50 and 0.1 ppm, respectively. Likewise, the World Health Organization has set these limits at 50 ppm (NO_3^-) and 3 ppm (NO_2^-) (WHO/SDE/WSH/07.01/16). More recently, following the European Food Safety Authority recommendations, 2006/52/EC directive has reduced the authorized levels for these ions in meat and other food products, which should be controlled on the basis of added rather than residual amounts (e.g. 150 mg/kg of nitrites in meat products). Furthermore, the determination of nitrite in human physiological fluids is also commonly used for clinical diagnosis. As a result, there is a growing demand to detect nitrite in food, drinking water and environmental samples[123].

1.2.2 Nitrite Biosensors

In the last decades, biosensor technology has been exploited as a route to provide reliable nitrite quantification in complex samples. Hence, several protein electrodes and optical devices are described in the literature[2,34,39,124-130].

When it comes to nitrite biosensors, the bulk of the approaches make use of mediated electron transfer by employing redox mediators (e.g. viologen derivates) that display a fast and reversible electrochemical response and are able to shuttle electrons rapidly to the redox centers of the proteins[39].

As transducing modes one could find a vast predominance of electrochemical approaches, the largest group being the voltammetric and/or amperometric ones and a small number being based on potentiometric or conductimetric platforms. Alternatively, the spectroscopic changes that take place during the catalytic cycle were also employed in the construction of optical biosensors. The strategies proposed for protein immobilization have relied on a variety of materials, ranging from non-conducting polymers, electropolymerized films, redox active clays, sol-gel silica glasses, carbon nanotubes, metal nanoparticles and DNA tethers, either alone or in composite formulations. Although the construction of these sensing devices is far from trivial, major progresses have been made over the last decade. After the preliminary studies carried out using non-immobilized electron carrier species, fully integrated biosensors based on mediated electrochemistry

have become a common configuration. More advanced strategies operating in the unmediated mode via DET[131] and exploiting nanostructured materials as electrodes interfaces were recently proposed[35]. In parallel, stability has been substantially improved through the construction of leak free devices and the use of protecting coats. Very recently, the screen printing technology was successfully employed, opening up the route for miniaturization[132].

The less used, mediatorless approaches - the ones on which this thesis will focus - are based on the direct electron transfer between the nitrite reductases and the electrode material.

Table 1.5 summarizes some of the most recent and representative works done in the field. A detailed analysis of this table clearly demonstrates that although electrode modifications are made with all sorts of materials, combined with polymers, silicates, surfactants or ionic liquids, the systems share many common features. Direct electron transfer between proteins and electrodes is frequently promoted by the modifying matrix and the intensity of the catalytic currents is correlated with nitrite concentration; amperometric transduction is a frequent option; and the working electrodes are always made of carbon materials (usually, glassy carbon (GC)).

Overall, the tabulated analytical parameters were highly variable. For instance, the detection limit can be as low as 0.06 μM and go up to 700 μM. Though, the substrate promiscuity of all these heme containing proteins puts in risk the selectivity of determination, so they are not recommended for the construction of a selective nitrite biosensor. Instead, much more selective biocatalysts should be employed. The next section aims to describe all nitrite biosensing systems reported hitherto that make use of highly selective enzymes for nitrite reduction.

1.2.3 Nitrite reductases

Nitrite reducing enzymes (NiRs) are the natural candidates for playing the role of biorecognition element in the nitrite biosensing devices. Four classes of NiRs have been recognized so far (Figure 1.8), all of which have already been used in biosensor applications. They can be grouped according to the type of co-factors and reaction product[133,134].

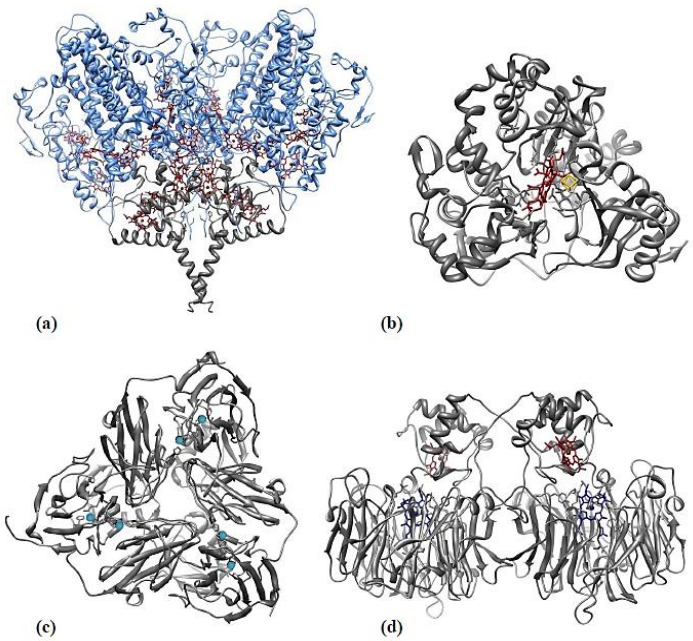

Figure 1.8: Three-dimensional structures of nitrite reductases. **(a)** Desulfovibrio vulgaris Hildenborough multiheme c nitrite reductase (NrfA4NrfH2 complex); the catalytic subunit (NrfA) is depicted in blue and the electron donor subunit (NrfH) in gray; heme groups are shown in dark red. **(b)** Spinach nitrite reductase; siroheme is shown in dark red and iron-sulfur cluster in yellow. **(c)** Achromobacter cycloclastes copper nitrite reductase (trimer); the copper centres are shown in blue. **(d)** Pseudomonas aeruginosa cytochrome cd1 nitrite reductase (dimer); heme c is depicted in dark red and heme d in blue[125].

There are two types of ammonia forming nitrite reductases: cytochrome c nitrite reductases (ccNiRs), which are multi-heme enzymes isolated from sulfate or sulfur reducing bacteria, and sirohemic nitrite reductases, which contain a siroheme and an iron-sulfur cluster and are commonly purified from photosynthetic organisms such as plants, algae and cyanobacteria. This group of enzymes is able to catalyze the six electron reduction of nitrite to ammonia, according to the following equation:

$$NO_2^- + 8H^+ + 6e^- \rightarrow NH_4^+ + 2H_2O \tag{1.2}$$

The nitric oxide forming nitrite reductases are dissimilatory NiRs involved in bacterial denitrification; they catalyze the one electron reduction of nitrite to nitric oxide.

$$NO_2^- + 2H^+ + e^- \rightarrow NO + H_2O \tag{1.3}$$

There are two different types: the copper-containing nitrite reductases (CuNiRs), with type-I and type- II copper centers, and the cytochrome cd1 nitrite reductases (cd1NiRs) that comprise a c-type and a d1-type heme[134].

Table 1-5 Description and analytical parameters of nitrite reductase based biosensors (N.A.—not applicable; N.D.—not determined;

Enzyme	Source	Sensor preparation	Transducing mode	Electron transfer	Linear Range	Detection Limit	Sensitivity	Reference
Sirohemic NiR	Spinach leafs	enzyme + BSA + glutaraldehyde	Potentiometric	N.A.	0.1–50 mM	N.D.	N.D.	[135]
*cc*NiR	D. desulfuricans	GC/casting of enzyme + polyacrylamide (mediator in solution)	Voltammetric	MET (methyl viologen)	up to 200 µM	N.D.	N.D.	[136]
*cc*NiR	D. desulfuricans	GC/casting of enzyme + polyacrilamide		DET	up to 200 µM	N.D.	N.D.	
*cc*NiR	D. desulfuricans	GC/dispersion of poly(pyrrole-viologen) + enzyme mixture followed by electropolymerization	Voltammetric	MET (poly(pyrrole-viologen))	5.4–43.4 µM	5.4 µM	1,721 mA $M^{-1}cm^{-2}$	[128]
*cc*NiR	D. desulfuricans	GC/casting of Nafion + enzyme/ incorporation of mediator	Voltammetric	MET (methyl viologen)	75–800 µM	60 µM	445 mA $M^{-1}cm^{-2}$	[130]
*cc*NiR	D. desulfuricans	GC/casting of [ZnCr-AQS] LHD + enzyme/ glutaraldehyde vapor cross-linking	Amperometric	MET (AQS)	0.015–2.350 µM	4 nM	1,824 mA $M^{-1}cm^{-2}$	[132]
*cc*NiR	D. desulfuricans	gold/casting of Nafion + enzyme + mediator + glycerol + BSA/ glutaraldehyde vapor cross-linking	Conductimetric	MET (methyl viologen)	0.2–120 µM	0.05 µM	0.194 µS/µM	[137]
*cc*NiR	D. desulfuricans	pyrolytic graphite/casting of EETMS sol/ casting of enzyme	Amperometric	DET	0.25–50 µM	120 nM	430 mA $M^{-1}cm^{-2}$	[124]

c*c*NiR	D. desulfuricans	graphite/casting of SWCNTs dispersion/casting of enzyme	Voltammetric	DET	up to 150 µM	N.D.	2,400 mA $M^{-1}cm^{-2}$	138
c*c*NiR	S. deleyianum	graphite and mediator composite/casting of enzyme + poly(carbamoyl sulfonate) hydrogel membrane	Amperometric	MET (phenosafranin)	up to 250 µM	1 µM	446.5 mA $M^{-1}cm^{-2}$	139
cd$_1$NiR	P. denitrificans	graphite/enzyme entrapment through dialysis membrane (mediator in solution)	Amperometric	MET (1-methoxy PMS)	4.35–65.2 µM*	N.D.	N.D.	140
cd$_1$NiR	P. denitrificans	graphite/enzyme entrapment with dialysis membrane (mediator in solution)	Amperometric	MET (1-methoxy PMS)	up to 750 µM	10 µM	33 mA $M^{-1}cm^{-2}$	139
cd$_1$NiR	P. pantotrophus	enzyme incorporated in bulk sol-gel monoliths of TEOS	Optical	N.A.	0.075–1.250 µM	0.075 µM	N.D.	141
cd$_1$NiR	P. pantotrophus	enzyme in controlled pore glass beads of isothiocyanate	Optical	N.A.	0–4 mM	0.93 µM	19.5 nM^{-1}	142
cd$_1$NiR	M. hydrocarbono-clausticus	graphite/casting of polyvinyl alcohol + enzyme + mediator followed by photopolymerization	Amperometric	MET (cyt-c_{552})	10–200 µM	7 µM	2.49 A cm^2 μM^{-1}	129
CuNiR	R. sphaeroides	GC/electropolimerization of PPB/ casting of enzyme + PBV	Voltammetric	MET (PPB)	up to 50 µM	1 µM	789 mA $M^{-1}cm^{-2}$*	143
CuNiR	R. sphaeroides	GC/casting of poly(vinyl alcohol) + mediator + enzyme/ casting of poly(allylamine hydrochloride)/ casting of hydrophilic polyurethane	Amperometric	MET (methyl viologen)	1.5–260 □M	1.5 µM	170 mA $M^{-1}cm^{-2}$*	144

CuNiR	A. faecalis	gold/enzyme entrapped with dialysis membrane (mediator in solution)	Amperometric	MET (1-methoxy PMS)	0–22 µM*	0.22 µM*	N.D.	[145]
CuNiR	A. faecalis	gold/dip-coating in (cysteine) thiolated hexapeptide (enzyme and mediator in solution)	Voltammetric	MET (pseudoazurine)	200–1,500 µM	N.D.	N.D.	[146]
		gold/dip-coating in (cysteine) thiolated hexapeptide (enzyme and mediator in solution)		MET (ruthenium hexamine)	1–100 µM	N.D.	N.D.	

1.2.3.1 Cytochrome c Nitrite Reductase

The cytochrome c nitrite reductase from *D. desulfuricans* was used as biorecognition element, in the experiments addressed in this thesis. This enzyme is involved in the pathway of dissimilatory nitrite reduction to ammonia thereby playing a crucial role in the biogeochemichal nitrogen cycle.

As mentioned above, ccNiR catalyzes the six-electron reduction of nitrite to ammonia (NH_4^+) using electrons from the oxidation of formate or hydrogen, mediated through a menaquinone and a quinol- oxydizing system[147].

ccNiR also catalyzes the reduction of nitrite oxide and hydroxylamine to ammonia and of sulfite to sulfide It is usually found as a membrane associated complex with a transmembrane subunit. The physiological form of the enzyme is believed to be a double trimer of 2 NrfA and 1 NrfH subunits[148] (Figure 1.9) in vitro, the protein complexes associate each other forming large aggregates (min. 890 kDa)[149].

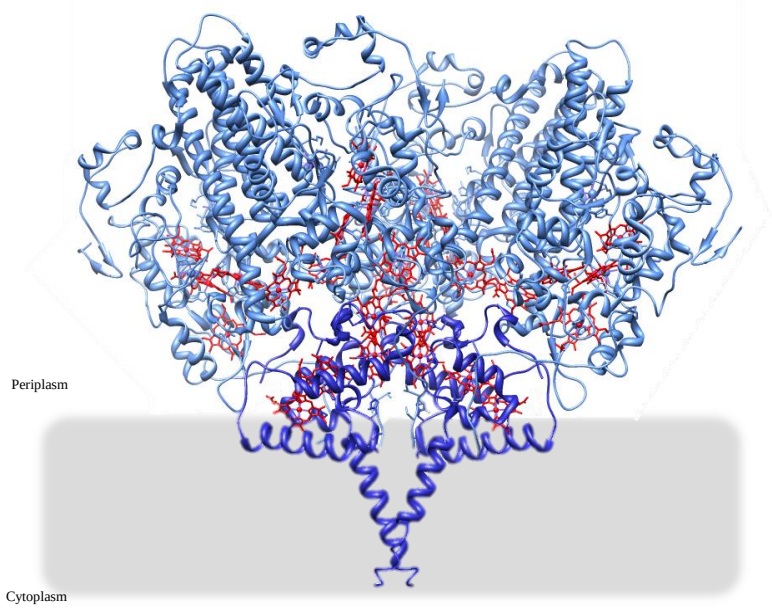

Figure 1.9: Secondary structure of NrfHA viewed parallel to the membrane (grey rectangle) with haems drawn as red sticks[148].

The catalytic subunit NrfA (61 kDa), which is associated to the periplasmic membrane, is a pentaheme cytochrome c-type where the short distances between hemes allow a fast and efficient electron transfer[150,151]. It can be assessed by two channels that reach the protein surface.

They were proposed to be the substrate and product channels because they have an overall electrostatic charge opposed to the anion NO_2^- substrate and cation NH_4^+ product that should flow through them. This is thought to contribute to the high catalytic activity of this enzyme[151-153] . The product channel in *D.desulfuricans* ccNiR is partially blocked

by a polypeptide segment; accordingly, the product may have to find a different route to exit the active site or a conformational change may allow this to occur through the designated product channel[151]. NrfH (19 kDa) is a small membrane-bound cytochrome comprising four c-type heme groups and it serves a double purpose; it anchors the catalytic subunits to the membrane and serves as a quinol oxidase, transferring electrons from the quinone pool to the catalytic subunits[148,149]. It is composed of a transmembrane helix and a globular hydrophilic domain that houses the four hemes. The NrfH subunit interacts with the NrfA dimmer in an asymmetrical way, with only one of the catalytic monomers receiving electrons directly from NrfH.

1.3 Cytochrome P450 based biosensors

1.3.1 Cytochromes P450

he cytochromes P450b (CYP) are a ubiquitous superfamily of mixed function oxidases. They play an important role in the detoxication of bioactive compounds and hydrophilic xenobiotics being formed inside cells in living organisms (cholesterol, saturated and unsaturated fatty acids, steroids, prostaglandins and others) or from external souces (medicines, drugs, food supplements, and environmental pollutants)[166,167]. These enzymes represent a superfamily of b-type hemeproteins with a catalytic activity towards two substrates: oxygen and organic substances The general monooxigenase reaction by which the CYPs metabolize their substrates is the following.

$$RH + O_2 + NA(P)H + H^+ \rightarrow ROH + H_2O + NAD(P)H^+ \tag{1.4}$$

The generic reaction catalyzed by P450 (Figure 1.11) implies the reduction of molecular oxygen with two electrons that are supplied by various redox partners[168].

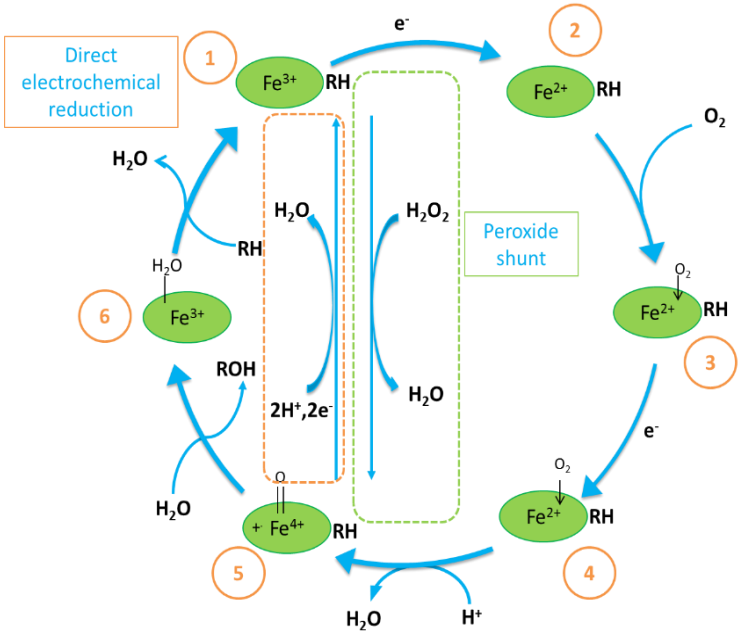

Figure 1.10: Proposed Cyt P450 Catalytic Cycle. RH: lipophilic compound in which an oxygen atom derived from O_2 is introduced.

These enzymes are unique in being able to hydroxylate non activated carbon atoms (C-H bonds)156,166,167. The products of substrates' metabolism usually serve as regulators in cells or are excreted from organisms. Cytochromes P450 are capable of metabolizing over 1,000,000 chemicals and involve about 60 distinct classes of biotransformation reactions, e.g. hydroxylation, N-, O- or S-demethylation, dealkylation, epoxydation among others[169,170]. This particular feature of P450s makes them one of the most studied proteins as they are highly promising for use in farmaceutical drug assays and in stereo-directed synthesis of steroids[171]. For eukaryotic microsomal P450, the membrane-bound form of NADPH cytochrome P450 reductase (CPR) is the primary source of electrons[168]. Electrons from NAD(P)H flavins ferric form of cytochrome P450 ($Fe3^{+}$). Resting P450s are in the ferric form (Fe_3^+), one electron reduction of ferric form leads to ferrous state (Fe_2^+) of hemoprotein, which can bind oxygen[172]. During reduction of P450s according to the scheme $Fe_3^+ + e^- \rightarrow Fe_2^+$ NADPH or NADH are exhausted[159]. The P450s share a common fold that is unique to this enzyme class. P450s are mainly β-helical, with the heme cofactor sandwiched between a larger helix-rich (alpha) domain and a small β-sheet-rich (beta) domain. A core structure around the heme cofactor provides the scaffold that allows oxygen activation by the P450s. The heme iron is equatorially coordinated by four pyrrole nitrogens from the heme b macrocycle, and axially coordinated by a conserved cysteine as the proximal ligand and typically by a water molecule as the distal ligand (in the P450 resting state).

1.3.2 NADPH-cytochrome P450 reductase

As previously mentioned, for eukaryotic microsomal P450s, the membrane bound form of cytochrome P450 reductase (CPR) orchestrates the stepwise electron transfer from NADPH to the cytochrome P450 heme center[168,173,174]. NADPH-cytochrome P450 oxidoreductase transfers electrons from NADPH to cytochrome P450 and catalyzes the one-electron reduction of many drugs and foreign compounds. CPR is a 78 kDa membrane anchored multidomain enzyme composed of a FMN-containing flavodoxin like domain associated with a FAD-containing ferrodoxin reductase like domain175 probably originating from horizontal gene transfer or exon fusion. A folded connecting domain joins the two sections. By using its two flavin cofactors and a peculiar electron transfer cycle, CPR is able to split the dielectronic flux of NADPH by sequential electron transfer to external acceptors[176].

Electron transfer in biological systems occurs in the presence of electron donors such as NADPH and NADP, and is generally affected by electron transfer mediators, such as flavin nucleotides. In the presence of substrate and dioxygen, the monooxygenation reaction of the CPR-CYP enzyme system is dependent on the binding of NADPH to CPR. Electrons, in the form of a hydride anion are transferred from NADPH to FAD. Reduced FAD then transfers single electrons to FMN, which in turn reduces the prostetic heme iron of the CYP[178,179].

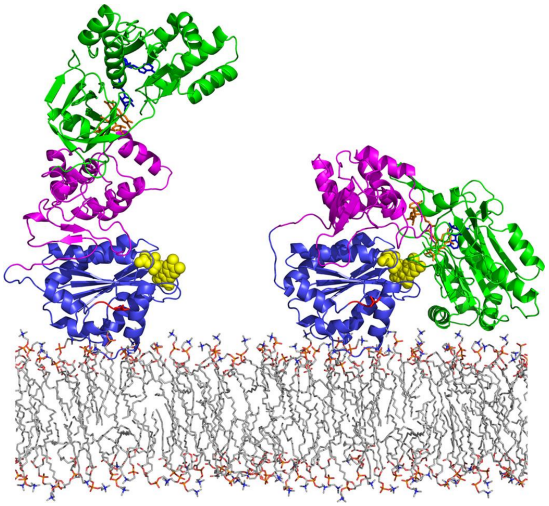

Figure 1.11: Model of the conformational equilibrium in CPR[177].

1.3.3 Cytochrome P450 1A2

Human CYP1A2 is one of the major CYPs in human liver; it metabolizes a variety of clinically important drugs (e.g., clozapine, tacrine, tizanidine, and theophylline), a number of procarcinogens (e.g. benzo[a]pyrene and aflatoxin B1), and several important endogenous compounds (e.g. steroids and arachidonic acids). Like many other CYPs, CYP1A2 is subject to induction and inhibition by a number of compounds, which may provide an explanation for some drug interactions observed in clinical practice. A large interindividual variability has been observed in the expression and activity and in the elimination of drugs that are mainly metabolized by CYP1A2. This is largely caused by genetic (e.g., Single-nucleotide polymorphisms) and epigenetic (e.g., DNA methylation) and environmental factors (e.g., smoking and comedication). CYP1A2 is primarily regulated by the aromatic hydrocarbon receptor (AhR). It is induced through AhR-mediated transactivation following ligand binding and nuclear translocation. To date, more than 15 variant alleles and a series of subvariants of the CYP1A2 gene have been identified and some of them have been associated with altered drug clearance and response to drug therapy[180].

1.3.4 P450 based electrochemical Biosensors

Investigation of the catalytic activity of isolated cytochromes from the P450 superfamily requires the obligatory presence of redox partners and electron donors (NADPH) (see section 1.3.3). However, redox partners are not obligatory for the electrochemical reduction of P450 family hemoproteins, so the catalytic system is essentially simplified. The electrochemical approach is especially important in the case of unknown physiological partners (e.g. CYP51 MT, systematic name CYP51b1)[154]. Electrochemical systems execute a dual function: substitute partner proteins and serve as a source of electrons for redox enzymes. Electrochemistry permits to study the whole catalytic cycle of P450s

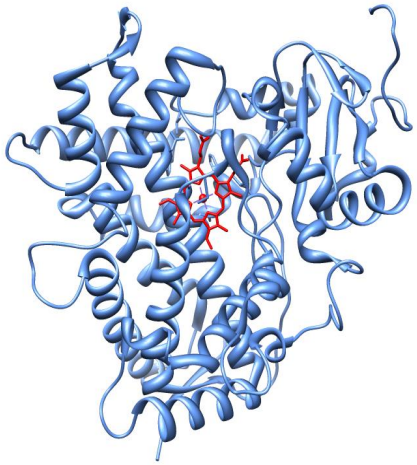

Figure 1.12: The secondary and tertiary structure of human P450 1A2 is shown in two views. The α-helices are colored blue, and the β-strands are colored brown. These secondary structure elements are designated A-L and 1-4, respectively, and are sequentially identified from the N terminus. The heme prosthetic group is represented in sticks and is colored red. The substrate binding cavity is illustrated as a red mesh surface.

from different viewpoints. On the one hand, the enzyme P450-electrodes are power tools for investigation of the catalytic properties of P450s towards new chemicals (i.e. for the search of new drugs with the properties of substrates or inhibitors). On the other hand, the stoichiometry of the P450's catalytic cycle and the thermodynamics of electrochemical reduction of P450s can also be assessed. Additionally, electrochemistry can allow the investigation of the peroxide shunt pathway with the help of bifunctional electrodes, therefore permitting the direct registration of hydrogen peroxide consumption by the hemeprotein[155].

As mentioned above P450 enzyme electrodes aim to eliminate the complex electron transfer machinery of the P450-reductase required in nature. For their successful electrochemical response two points must be addressed. First of all, the enzyme should be in its native conformational state and retain its catalytic activity after the adsorption or immobilization procedure, i.e. it should maintain its active P450 form and not convert to the inactive P420 one. The P420 form results from the weakening or distortion of the thiolate bond of the cysteine residue that is the fifth ligand of the heme[156]. This bond weakening can occur upon immobilization on electrode surfaces. Secondly, care must be taken on the coupling of the electron consumption that must be linked to the conversion of the substrate into its product(s). The fine-tuning of electron delivery and proton flow is crucial for the efficient conversion of substrate to product by cytochrome P450 enzymes. Ideally all the electrons provided by the electrode should be used in the formation of the product and not wasted on the production of oxygen reactive species in uncoupled reactions. Unfortunately this phenomenon does occur and it is well-documented for the

human drug metabolizing P450 enzymes[157]: oxygen and NAD(P)H are largely used by these enzymes to produce hydrogen peroxide and superoxide anion radical or water.

The relevance of such an approach is obvious: cytochrome P450 and P450-based enzyme electrodes may be used as biosensors in patient-tailored (personalized) medicine, high- throughput screening and drug interference studies.The biotechnological interest related to these enzymes in the development of biocatalysts or biosensors[158-160] is due to their versatility in the recognition of a vast array of compounds, many of which are relevant to the development of fine chemicals, new drugs and drug products and even environmentally important compounds (detected or degraded through bioremediation). However, in spite of the huge biotechnological interest, their use in bioelectrochemical devices has proven to be highly challenging.

The progression of P450-electrode systems into amperometric biosensors is largely dependent on the efficiency of the electrode-driven P450 activity and therefore the immobilization. Which is why a large part of this work is centered on immobilization strategies. However, there are two technical difficulties in handling P450s based electrochemical biosensors. The first problem is the complexity in the measurement of their enzymatic activity.

Most P450s need another redox protein as an electron donor for their activity besides the lipophilic substrate, O_2 and NADPH or NADH. Pathways of electron transfer to P450s are shown in Figure 1.10.

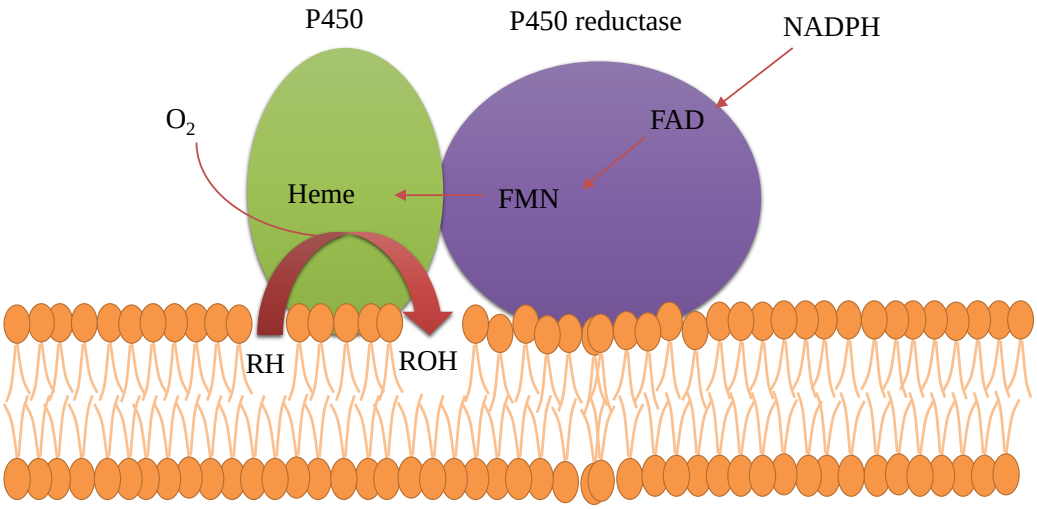

Figure 1.13: schematic representation of electron transfer in microsomal membrane. Electron transfer from P450 reductase to P450 (adapted from Hara (2000).[161]).

For example, P450 reductase transfers electron to microsomal type P450 as shown in the scheme in Figure 1.10. Usually, two electrons are supplied from NADPH to P450

through P450 reductase containing both FAD and FMN as shown in the upper part of this scheme.

Kinetic parameters such as Michaelis constant (KM) of the substrate highly depend on the microenvironment of the lipid membrane on which the P450 is bound. Both isolated P450 and P450 reductase should be coreconstituted into the same liposomes for expressing its full enzymatic activity.

The second problem is the stability of the enzyme. Many P450s, especially membrane-bound enzymes from microsomes or mitochondria are labile. Some can be partly stabilized in the presence of glycerol[161].

The types of electrode modifications used in CYP biosensor studies vary, as shown in Table 1.6, ranging from thin films with opposite charge adsorbed onto graphite to conductive polymers deposited onto noble metals such as gold or platinum. Most of these studies rely on a combination of electrochemical and analytical techniques to show that the CYP biosensor is electroactive and can detect different drug compounds via electrochemically-driven catalysis. Nevertheless, a number of recent studies characterizing the active site structure and redox potential of CYPs immobilized on electrodes have shown that much of the CYP immobilized on the electrode is in an inactive form and call into question the results from previous CYP biosensor studies[162-164].

In addition, some CYP biosensor studies are missing crucial substrate turnover data and instead rely on electrochemical experiments alone to indicate that the immobilized CYP is capable of electrochemically- driven catalysis[157].

Table 1-6 Summary of different electrode types and electrode modifications used to construct CYP electrodes and biosensors[165].

CYP enzyme	Electrode material	Electrode modification	Result	Reference
Adsorption to bare electrodes				
CYP101 ($P450_{CAM}$)	Edge-Plane Pyrolytic Graphite	None	Reversible peaks for FeIII/FeII seen in anaerobic CV Increased reduction peak area in presence of D-(þ)-camphor	Kazlauskaite et al., 1996
CYP101 Mutant SCF-K344C	Gold	None	Enhanced electroactivity of the SCF-K344C mutant	Lo et al., 1999
CYP2E1	Gold	None	Reversible peaks for Fe^{III}/Fe^{II} seen in anaerobic CV, k_s=5 s^{-1}	Fantuzzi et al., 2004
CYP199A2	Basal-Plane Pyrolytic Graphite	None	Quasi-reversible peaks for Fe^{III}/Fe^{II} seen in anaerobic CV, k_s=550 s^{-1}	Fleming et al., 2007
CYP101	Glassy Carbon	None	Increased reduction peak area in presence of D- (þ)-camphor, k_s=0.016 s^{-1}	Mhaske et al., 2010
Layer-by-Layer Adsorption				
CYP101	Gold	Multilayer films of PSS and PDDA on an MPS SAM	Reversible peaks for Fe^{III}/Fe^{II} seen in anaerobic CV Electrochemically-driven styrene epoxidation (turnover 9.3 h^{-1})	Lvov et al., 1998
CYP3A4	Gold	MPS SAM followed by PDDA	Reversible peaks for Fe^{III}/Fe^{II} seen in anaerobic CV Electrochemical detection of the 3A4 substrates verapamil and midazolam	Joseph et al., 2003
CYP1A2	Carbon Cloth	Alternate adsorption of PSS and 1A2	Reversible peaks for Fe^{III}/Fe^{II} seen in anaerobic CV Electrochemically-driven styrene epoxidation (turnover 39 h^{-1})	Estavillo et al., 2003
CYP1A2 and CYP3A4 microsomes	Pyrolytic Graphite	Multilayer films of PEI and PSS	Reversible peaks for FeIII/FeII seen in anaerobic CV Electrochemically-driven styrene epoxidation	Sultana et al., 2005
CYP1A2 and CYP2E1	Basal-Plane Pyrolytic Graphite	Multilayer films of CYP and CPR/b5	Reversible reduction and oxidation peaks visible in anaerobic CV	Krishnan et al., 2011

			Evidence that electron transfer follows natural catalytic pathway from CPR Electrochemically-driven catalysis of NNK to HPB by 2E1 electrode	
Adsorption to Thin Films				
CYP101	Glassy Carbon	Pretreated sodium montmorillonite clay colloid	Reversible peaks for Fe^{III}/Fe^{II} seen in anaerobic CV Fast electron transfer (5 to 152 s^{-1} for scan rates of 0.4 to 12 V/s)	Lei et al.,2000
CYP2B4	Glassy Carbon	Mixture of sodium montmorillonite clay colloid, 2B4, and Tween 80	Reversible peaks for Fe^{III}/Fe^{II} seen in anaerobic CV Amperometric detection of the 2B4 substrates aminopyrine and benzphetamine	Shumyantseva etal., 2004
CYP101	Pyrolytic Graphite	DDAB or DMPC	Reversible peaks for Fe^{III}/Fe^{II} seen in anaerobic CV Relatively fast electron transfer with DDAB (k_s=26 s^{-1}) and DMPC (k_s=25 s^{-1})	Zhang etal.,1997
CYP2C9, 2C18, and 2C19	Edge-Plane Pyrolytic Graphite	DDAB	Reversible peaks for FeIII/FeII seen in anaerobic CV for all three enzymes Weak signal-to-background current and only 1–3% of enzyme is electroactive	Shukla etal.,2005
CYP2C9	Edge-Plane Pyrolytic Graphite	DDAB	Reversible peaks for Fe^{III}/Fe^{II} seen in anaerobic CV Anodic shift in redox potential with 2C9 substrates torsemide, warfarin, and tolbutamide and with CO	Johnson etal.,2005
CYP27B1	Edge-Plane Pyrolytic Graphite	DDAB	Reversible peaks for FeIII/FeII seen in anaerobic CV (k_s=3.5 s^{-1}) No product formation observed during electrolysis with 27B1 substrate 25(OH)D3	Rhieu etal.,2009
CYP3A4 fusion protein	Glassy Carbon	PDDA	Electrochemically-driven catalysis with the 3A4 substrate erythromycin	Dodhia etal.,2008
CYP101	Glassy Carbon	Covalent attachment to thin film of pyrene maleimide	Increased reduction peak area in the presence of D-(þ)-camphor	Mhaske etal.,2010
Screen-Printed Electrodes				

Riboflavin-conjugated CYP1A2, 2B4, and 11A1	Rhodium-graphite	Mixture of CYP, BSA, glutaraldehyde, sodium cholate, and phospholipid	Electrochemically-driven catalysis with respective 1A2, 2B4, and 11A1 susbstrates Amperometric detection of the substrates aminopyrine (2B4) and cholesterol (11A1)	Shumyantseva etal., 2001
CYP1A2	Riboflavin-graphite	Glycerol and agarose	Amperometric detection of the 1A2 substrate clozapine	Antonini etal.,2003
CYP11A1	Rhodium-graphite	Gold nanoparticles	Amperometric detection of the 11A1 substrate cholesterol Enhanced electroactivity and sensitivity with inclusion of gold nanoparticles	Shumyantseva etal., 2005
CYP2B4	Carbon	Covalent attachment via EDC/NHS to a COOH-functionalized electrode	Amperometric detection of the 2B4 substrate cocaine in confiscated cocaine samples	Asturias-Arribas et al.,2011
CYP1A2, 2B4, and 51b1	Graphite	Mixture of gold nanoparticles and DDAB	Increased reduction peak area in the presence of substrates for 2B4 (benzphetamine) and 51b1(lanosterol) Enhanced electroactivity with inclusion of goldnanoparticles	Shumyantseva etal., 2007
CYP2B4	Graphite	Mixture of gold nanoparticles and DDAB	Electrochemically-driven catalysis with benzphetamine exhibits similar uncoupling behavior to catalysis with 2B4 in solution	Rudakov etal.,2008
CYP2B4, 3A4, 11A1, 51b1	Graphite	Mixture of gold nanoparticles and DDAB	Amperometric detection of multiple substrates and inhibitors	Shumyantseva et al., 2011
Encapsulation in Polymers of Gels				
CYP101	IndiumTinOxide	Polypyrrole	Electrochemically-driven catalysis with D-(þ)-camphor	Sugihara et al.,1998
CYP102 ($P450_{BM3}$) Mutant	Platinum and Glassy Carbon	Polypyrrole	Compared chemical vs. Electrochemical polymerization of polypyrrole for effect on enzyme catalysis	Holtmann et al., 2009
CYP2B4	Gold	Polypyrrole	Amperometric detection of the 2B4 substrate phenobarbitol	Alonso-Lomillo et al.,2008
CYP101	Glassy Carbon	Methyltriethoxysilane sol-gel and DDAB	Reversible peaks for FeIII/FeII seen in anaerobic CV in aqueous and organic media Amperometric detection of camphor and pyrene	Iwuoha et al.,2000

CYP2B6	Glassy Carbon	Mixture of chitosan and gold	Enhanced electroactivity within clusion of chitosan and goldnanoparticles	Liu etal.,2008
			Electrochemically-driven catalys is of the 2B6 substrate bupropion	
Covalent Attachment to Self-Assembled Monolayers on Gold				
CYP2C9	Gold	Amine coupling via EDC/NHS to a mixed SAM of OT and MUA	Quasi-reversible peaksforFeIII/FeII seen in anaerobic CV	Yang et al.,2009
			Electrochemically-driven catalysis with the 2C9 substrate warfarin	
CYP3A4 fusion protein	Gold	Amine coupling via EDC/NHS to a mixed SAM of 6HT and 7MHA	Microfluidic cell made of the 3A4 electrode amperometrically detected the 3A4 substrates quinidine, nifedipine, alosetron, and ondansetron	Fantuzzi et al.,2010
CYP2C9n1, 2C9n2, and 2C9n3 CYP2D6n1, 2D6n2, and 2D6n17	Gold	Amine coupling via EDC/NHS to a mixed SAM of 6HT and 7MHA(2C9)Maleimide/thiol coupling to maleimide-terminated SAM (2D6)	Micro-machined eight-electrode array used to amperometrically measure the KM and kcat values for the 2C9 substrate warfarin and the 2D6 substrate bufuralol	Panicco et al.,2011
CYPc17	Gold	His-tag attachment via modified Ni-NTA on na MPASAM in the presence of DDAB	Redox peaks for FeIII/FeII seen in anaerobic CV	Johnson and Martin, 2005
			Enhanced electroactivity when using His-tag attachment vs.amine-coupling	
CYP2E1	Gold	Maleimide/thiol coupling to maleimide-terminated SAM	Redox peaks for Fe^{III}/Fe^{II} seen in anaerobic CV Faster (k_s=10 s^{-1}) electron transfer with maleimide/thiol coupling compared to adsorption to thin films	Fantuzzi et al.,2004
CYP2E1 Single-Cysteine Mutants	Gold	DTME SAM	Electrochemically-driven catalysis with the 2E1 substrate p-nitrophenol	Mak et al.,2010
CYP3A4 fusion protein	Gold	Maleimide/thiol coupling to maleimide-terminated SAM	Electrochemically-driven catalysis with the 3A4 substrate erythromycin	Dodhia et al.,2008

Future Directions/Nanostructured Electrodes

CYP11A1	Rhodium-graphite	MWCNTs on screen-printed electrodes	Enhanced amperometric detection (improved linearity) of cholesterol within clusion of MWCNTs	Carrara et al.,2008
CYP2B4, 2C9,3A4	Graphite or Gold	MWCNTs on screen-printed electrodes	Amperometric detection of benzphetamine (2B4), naproxen (2C9), and cyclophosphamide Enhanced limits of detection with inclusion of MWCNTs	Cararra, et al.,2011
CYP3A4	Sputtered Gold	Adsorption to thin film of napthalene thiolate SAM	Enhanced electroactivity on sputtered gold electrodes (k_s=340 s^{-1})	Mie et al.,2010
CYP3A4 microsomes	Microfabricated Gold Nanodomes	Adsorption to thin film of napthalene thiolate SAM	Enhanced electroactivity on nanostructured gold electrodes	Ikegami et al.,2011
CYP3A4	Gold	Amine coupling to ZnSe quantum dots covalently coupled to na MPASAM	Amperometric detection of the 3A4 substrate 17β-estradiol Anodic shift in the redox potential with inclusion of quantum dots	Ndangili et al.,2011

1.4 Heme proteins

Both enzymes addressed in this thesis fall into the heme proteins category; Cytochrome P450 (CYP) and Cytochrome c Nitrite Reductase (ccNiR).

Heme is perhaps the most ubiquitous cofactor found in nature and the most functionally diverse. Proteins containing a heme group constitute a heterogeneous family whose functional impact in living organisms is exceedingly high, due to their involvement in a large range of biological processes. By taking part in several metabolic processes within living creatures, heme proteins play a key role in the maintenance of life on earth [181] . Hemoproteins are involved in cell respiration (cytochromes), oxygen-binding and transport (hemoglobin and myoglobin), oxidative biotransformations (cytochrome P450 and peroxidases), and most recently discovered, as sensors in 2-component regulatory systems (guanylate cyclase, FixL, and CooA).

The ability of hemoproteins to carry out extremely diverse reactions arises largely from the protein environment in which the heme molecule resides and specifically the nature of the heme-ligands. Other factors that contribute to the reactivity of the heme are intrinsic to the heme itself, including the substituents on the heme periphery and, in some cases, the covalent attachment of the heme to the protein[182].

2

Experimental

2.1 Part A- Cytochrome P450 1A2

The cytochrome P450 1A2 (protein 10 mg/mL; CYP1A2 122 pmol/mg) was provided by the Centro de Investigação em Genética Molecular Humana from IHMT. The protein was purified as previously described in Palma et al.[183], and stored in TGE buffer (75 mM Tris.HCl, 10 % (v/v) Glycerol and 25 mM EDTA, pH 7,5) at -80 °C.

Caffeine was purchased from Sigma-Aldrich, the solutions were prepared in deionized water (18MΩ/cm) from Millipore MilliQ or Purelab Option (Elga) water purification systems.

2.1.1 Electrochemical measurements

A conventional three-electrode electrochemical cell was used, with an Ag/AgCl reference electrode, a Pt counter electrode and a PGE (ϕ=3mm) modified with the enzyme/sol-gel film, as working electrode. The electrochemical cell, containing 10mL of 0.5M PBS buffer, pH 7 as supporting electrolyte, was thoroughly purged with argon before and an argon atmosphere was maintained inside the cell during the experiments. Measurements were performed with a potentiostat Autolab PSTAT 12 (Eco-Chemie) monitored by the control and data acquisition software NOVA 1.6. In cyclic voltammetry experiments, a 50mV/s scan rate was used unless otherwise stated. All potentials were quoted against the Ag/AgCl reference electrode.

2.1.2 Mediated electrochemistry of cytochrome P450

Before modification the PG working electrodes (self-made with 3 mm diameter disks in glass tubes) were polished with alumina slurry (0.3 μm) from Buehler, thoroughly washed with water and ethanol and ultra-sonicated in deionized water for 5 min. Finally, the electrodes were washed with water and dried with compressed air.

The mediators used, 1,1'-dimethyl-4,4'-bipyridinium dichloride (methyl viologen, MV) and 3,7-bis(Dimethylamino)-phenothiazin-5-ium chloride (methylene blue MB) were purchased from Sigma. All chemicals were of analytical grade.

Table 2.1: Mediators structure and formal reduction potential.

Mediator	structure	E°' (mV)vs NHE
Methylene Blue[184]	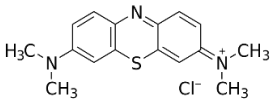	-426
Methyl Viologen[130]	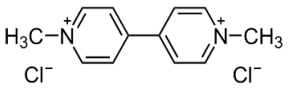	-440

2.1.2.1 Mediator in solution

The electrode was prepared by depositing 7.5 μL of CYP1A2 on the PGE and drying at room temperature for ca. 45 min. The assays were performed in the presence of 100 mM of mediator (either MB or MV) in the electrochemical cell.

2.1.2.2 Electropolymerized mediator

Electropolymerization of methylene blue was performed by cyclic voltammetry (11 scans); the CVs were traced at a scan rate of 100 mV/s in the potential window -0.6 to 1.2 V vs Ag/AgCl , mediator concentration in solution was 100 mM.

After the mediator polymerization, a 7.5 μL drop of CYP1A2 was applied to the PGE and left to dry at room temperature for ca. 45 min.

2.1.3 Direct electrochemistry

2.1.3.1 Direct adsorption

The PG working electrodes were cleaned as described above, subsequently a 7.5 μL drop of CYP1A2 was applied on the electrode surface and left to dry at room temperature for ca. 45 min.

2.1.3.2 Surfactant films

The surfactant films were usually prepared from aqueous solutions which were cast onto the electrode surfaces. After solvent evaporation, a water-insoluble multi-bilayered film structure was formed (selfassembled). The structures of the surfactants used in the work described in this section are shown in Figure 2.1.

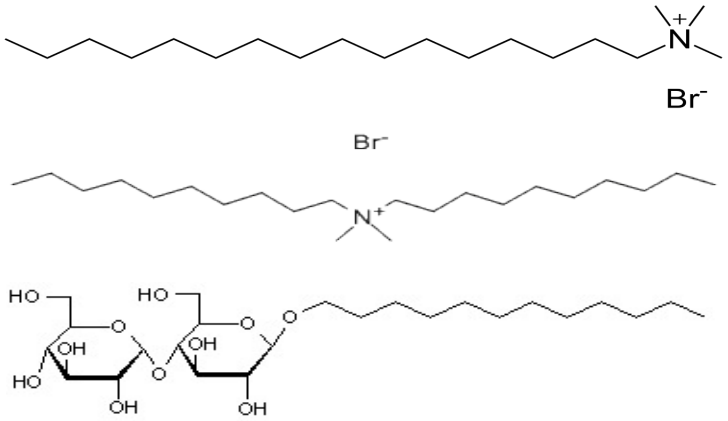

Figure 2.1: Surfactant structures. Cationic head group: A) CTAB, B) DDAB; C) DDM (n-dodecyl-b-D-maltoside).

The protein (CYP1A2) was confined within different surfactant films (Dodecyldimethylammonium bromide (DDAB) and Cetyl Trimethyl Ammonium Bromide (CTAB) purchased from Sigma-Aldrich and n-Dodecyl β-D-maltoside (DDM) from CalBiochem®), on the surface of basal-plane graphite electrodes (PGE) which were analyzed by cyclic voltammetry. All chemicals were of analytical grade.

CYP1A2–surfactant solutions were prepared by mixing 1.0 mg/mL of enzyme with 2 times the CMC of each surfactant (see Table 2.2). These mixtures were then incubated at room temperature (22 $\pm$ 2 °C) for 30 minutes. A 7.5 μL drop of mixture was then applied to the PGE. The electrodes were dried at room temperature for ca. 45 min.

Table 2.2: Surfactant critical micelar concentrations.

Surfactant	Type	MW (g/mol)	CMC (mM)
DDM	Non ionic	510.6	0.18
CTAB	Cationic	364.45	0.16
DDAB	Cationic	322.37	1

2.1.3.3 Sol-gel matrices

Sodium Silicate (Figure 2.2A) (Sigma-Aldrich), Tetraethoxysilane (TEOS, 98%, Alfa Aesar) and Tetramethyl orthosilicate (TMOS 98%, Sigma-Aldrich) were used as the silica precursor. Poly(ethylene glycol) (PEG, MW 400 and 6000)(Figure 2.2B) were purchased from Prolabo.

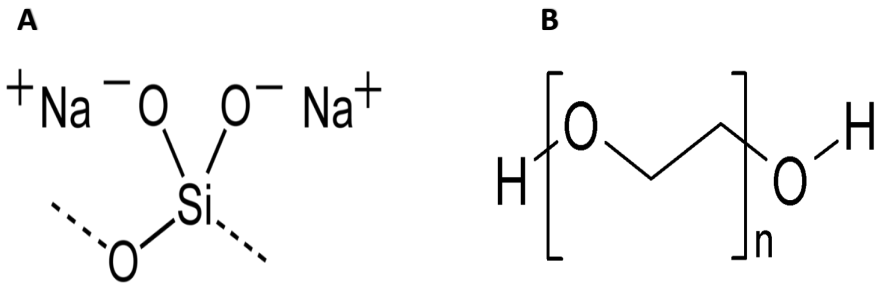

Figure 2.2: A) structure of sodium silicate; B) structure of poly(ethylene glycol).

Phosphate buffer solutions (PBS) were prepared with Na2HPO4•2H2O (99.5%, Merck) and KH2PO4 (99.9%, Prolabo). Tris–HCl buffers were prepared using Tris(hydroxymethyl)aminomethane (Sigma, 99.8%) and HCl (36%, Prolabo). All solutions were prepared with high purity water (18MΩ/cm) from a Purelab Option water purification system (Elga).

The PG working electrodes were cleaned as described above. For the sol-gel modified electrodes the surfaces were first treated by abrasion with sandpaper followed by the regular procedure. The optimized hybrid sol-gel was prepared by mixing Sodium Silicate 55 mM and PEG400 6% at pH 7. Protein films were applied onto the electrode surface by placing 10 μL of a solution containing equal parts of CYP1A2 and sol-gel. The electrodes were left to air dry for 1h.

Table 2.3: Compositions of sol-gel based matrices using TMOS and CTAB.

[TMOS] (mM)	*100*	*100*	*100*	*100*	*100*	*80*	*60*	*40*	*20*
[CTAB] (mM)	20	15	10	5	3	4	4	4	4
Ratio (TMOS/CTAB)	5/1	100/75	10/1	20/1	100/3	20/1	15/1	10/1	5/1

Table 2.4: Compositions of sol-gel based matrices using Sodium silicate and CTAB.

[Sodium silicate] (mM)	*82*	*16*	*9*	*20*	*16*	*100*
[CTAB] (mM)	1.5	2	4	5	4	5
Ratio (Sodium silicate/CTAB)	164/3	8/1	9/4	4/1	4/1	20/1

Table 2.5: Compositions of sol-gel based matrices using Sodium silicate and PEG400.

[Sodium silicate] (mM)	*55*	*55*
[PEG400] (v/v%)	30	6.25
Ratio (Sodium silicate/PEG400)	11/6	44/5

2.2 Part B- Cytochrome c Nitrite Reductase

The protein Cytochrome c Nitrite reductase from *Desulfovibrio desulfuricans* ATCC 27774 was purified at Requimte, FCT-UNL, according to the procedure described by Almeida et al.[149] and stored in 0.1 M phosphate buffer pH7.6, at -20°C. The specific activity was 300 U/mg and the protein content 1.0 mg/mL.

2.2.1 Electrochemical measurements

conventional three electrode electrochemical cell was used, with an Ag/AgCl reference electrode (Radiometer), a Pt counter electrode (Radiometer) and a PG electrode (ϕ= 3mm) modified with the sol- gel/ccNiR film, as working electrode. The electrochemical cell, containing 10 mL of PBS pH 7.0 as supporting electrolyte, was thoroughly purged with argon before and an argon atmosphere was maintained inside the cell during the experiments. Measurements were carried out with a potentiostat Autolab PSTAT 12 (Eco-Chemie) monitored by the control and data acquisition software NOVA 1.6 (EcoChemie). Cyclic voltammetry experiments were performed with a 50 mV/s scan rate in a potential window of -0.1 to -0.8 V.

2.2.2 Response to nitrite

To evaluate the biosensors response to nitrite, the electrochemical cell was successively spiked with standard solutions of sodium nitrite (0.01, 0.1 and 1 M). After each addition, the cell was again purged with argon for ca. 30 s and the CV was recorded. Nitrite

catalytic currents were determined at the inversion potential (-0.8 V) unless stated otherwise. All potentials were quoted against the Ag/AgCl reference electrode (-197 mV vs NHE).

2.2.3 Hybrid sol-gel matrix

The sol-gel precursor Sodium Silicate was purchased from Sigma-Aldrich and the Poly(ethylene glycol) (PEG, MW 400 and 6000) was acquired from Prolabo. Solutions were prepared with deionized water (18 MΩcm) from a Millipore MilliQ water purification system. All chemicals were analytical grade and were used without further purification.

The PGE working electrodes were cleaned as described in section 2.1.2). Protein films were prepared by depositing a 10 μL drop of the preparation, containing the enzyme solution (1.0 mg/mL) and the sol-gel (sodium silicate and PEG, either or kDa, were prepared according to the formulation described in Table 2.5 with a ratio of 44/5, on the electrode surface. After 60 minutes, the electrode was washed with buffer and placed in the electrochemical cell.

2.2.4 Macroporous Carbon Nanotubes

ingle-walled carbon nanotubes functionalized with carboxylic groups (CNT, >90%, 4–5nm 0.5-1.5 lm) were obtained from Sigma. Polystyrene beads (PS, $\phi \approx 500$ nm, 50mg/mL) were prepared by emulsion polymerization in water solution following a protocol from the literature M. Nagai et. al.[185].

Glassy carbon plates used as working electrodes (GC, Sigradur®, HTW Hochtemperatur-Werkstoffe, Germany) were polished before and after modification by wet emery paper 4000 with Al_2O_3 powder (0.05 μm, Buehler).

Electrophoretic deposition of carbon nanotubes and polystyrene-beads was performed using a cell consisting of stainless steel plate as cathode and glassy carbon plate as anode. The two electrodes were placed parallel to each other and separated by 6 mm Figure 2.3. The area of contact of each electrode with the dispersion was 1 cm^2. The adequate voltage was applied using a DC power supply.

Prior to enzyme coating, the GC plates working electrodes previously functionalized with carbon nanotubes (as described in section 2.1.2) were rinsed with deionized water. A drop of enzyme (7 μL) was then applied onto the modified electrodes which were left drying for 40 min under an argon flux.

The carbon nanotubes dispersion (0.1 mg/mL) was obtained by sonication in an ultrasonic bath for 12 hours. The PS-beads were added under gentle stirring to the carbon nanotubes dispersion prior to the deposition in order to achieve a final concentration of 0.025mg/mL . The two parallel electrodes were introduced in a 4mL aliquot of the CNT or CNT-PS dispersion and a constant voltage of 60 V was applied for the required time. The electrode dipping was kept constant in order to ensure the same area of contact with

the dispersion and therefore improve the reproducibility of the deposition. After deposition, the glassy carbon plate was carefully removed from the remaining dispersion and dried horizontally at room temperature. The electrodes prepared in such way were thereafter after called GC-CNT or GC-CNT-PS. The template (PS-beads) removal was carried out in an oven at 450 °Cfor 1 hour with 15 °C/min ramp resulting in electrodes called GC-CNT-(macroporous).

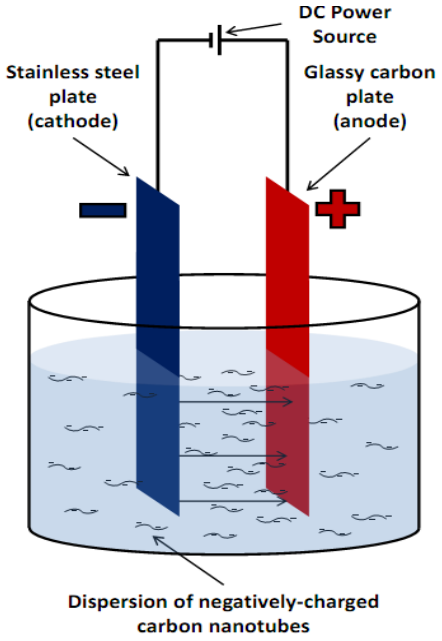

Figure 2.3: Scheme of the experimental device used for the electrophoretic deposition of carbon nanotubes[201].

A three electrode electrochemical cell was used Figure 2.4, with an Ag/AgCl reference electrode (Radiometer), a Pt counter electrode (Radiometer) and a modified glassy carbon plate as working electrode. The electrochemical cell containing 0.1 M KCl in 0.05 M Tris-HCl buffer pH 7.6 as supporting electrolyte, was thoroughly purged with argon before and during the experiments. Measurements were carried out with a potentiostat Autolab PSTAT 12 (EcoChemie) monitored by the control and data acquisition software NOVA 1.6 (EcoChemie). Cyclic voltammetry experiments were performed with a 50 mV/s scan rate in the potential window -0.1 to -0.8 V.

To evaluate the biosensors response to nitrite, the electrochemical cell was successively spiked with standard solutions of sodium nitrite (0.01, 0.1 and 1 M). After each addition, the cell was again purged with argon for ca. 30 s and the CV (cyclic voltammogram) was recorded. Nitrite catalytic currents were determined at the inversion potential (-0.8 V) unless stated otherwise. All potentials were quoted against the Ag/AgCl reference electrode (-197 mV vs NHE).

The electrochemical experiments were performed according to section 2.2.1) except for a few changes: namely, the electrochemical cell (Figure 2.3); the working electrode,

and a modified glassy carbon plate as working electrode.

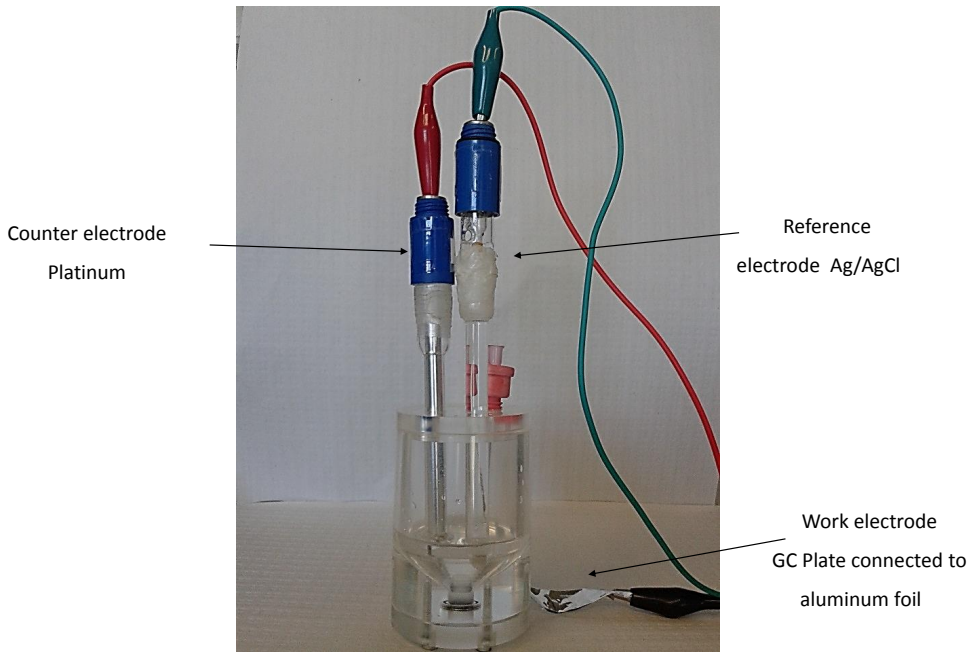

Figure 2.4: Electrochemical cell.

2.2.5 Oxygen scavenger system

Glucose oxidase (Type II from Aspergillus niger 17.3 U.mg-1) and catalase (from bovine liver, 2-5kU mg^{-1}) were purchased as lyophilized powders from Sigma and used as received. All other chemicals were of reagent grade. Deionized water (18 MΩcm) was used in all experiments.

Prior to modification the PG electrodes were cleaned as previously described. Protein films were prepared by depositing a 10 μL drop of the preparation, containing the enzyme solution(s) and the sol-gel, on the electrode surface. After 60 minutes of air drying, the electrode was washed with buffer and placed in the electrochemical cell.

The enzymatic scavenger system constituted by glucose oxidase and catalase was tested in different ways: 1) with sol-gel immobilized ccNiR (4.5 U) and GOx (9.3 U/mL) and catalase (650 U/mL) in solution in the electrochemical cell; 2) sol-gel immobilized ccNiR (4.5 U) and catalase (41.7 U) with GOx (9.3 U/mL) in solution and.

3

Results and discussion

3.1 Cytochrome P450 1A2

Aiming at the development of an electrochemical CYP1A2 based biosensor, P450 enzyme was used either in presence or absence of its natural redox partner (CYPOR complex). The different strategies were investigated using cyclic voltammetry. The experimental design has taken into account the need to establish an effective electronic communication between the enzyme and the electrode and, at the same time, preserve the biological activity. It is important to note that to probe the catalytic activity of CYP1A2, caffeine was selected from a plethora of substrates due to its low cost, availability and moderate water solubility. In general, the co-substrate - molecular oxygen - was provided to the medium dissolved in the caffeine aqueous stock solutions or, alternatively, in deionized water. Unless stated otherwise the experiments were carried out in a purged electrolyte solution in order to remove oxygen which exhibits a broad waved that might mask the non-catalytic signals of P450.

3.1.1 Cytochrome P4501A2 in the absence of CPR

The following section describes several strategies tested with the purpose of establishing the electronic communication between the cytochrome and the electrode. At an initial stage, a mediated approach was used that later proved itself inadequate to our goals. This approach was discarded in favor of direct electrochemistry.

3.1.1.1 Mediated electrochemistry

Selection of a suitable mediator Three mediators were selected and tested as electron shuttles, namely methyl viologen, methylene blue and methylene green (either in monomeric or polymeric forms). These substances have sufficient negative potentials compared to the redox potentials of the active sites of P450 (-0.4V $\pm$ 0.1V) and might reduce the oxidized form (PFe^{III}) of the enzyme. In a first approach CVs were recorded with the CYP immobilized on the PG electrode in the presence of dissolved mediators.

Following the addition of a caffeine stock solution, catalytic reduction currents could clearly be observed (Ic increases while Ia decreases); to illustrate this behavior Figure 3.2 and Figure 3.3 show the CV of methyl viologen and methylene blue in the presence of an electrode with membrane entrapped-CYP. This means that the reduced forms of each mediator were able to deliver electrons to a CYP which in turn, passes the electrons to the substrate (MV Figure 3.2 and MB Figure 3.3). However, control experiments done in the absence of caffeine (additions of non-purged water aliquots) produced a similar behavior. It became clear that the catalytic response was due an increase in the oxygen concentration (water dissolved) and not the caffeine's (Figure 3.1). On the other hand, control experiments performed in the absence of protein did not show significant current variations. Apparently, despite CYP being able to reduce molecular oxygen, the organic substrate caffeine is not participating in the catalytic reaction.

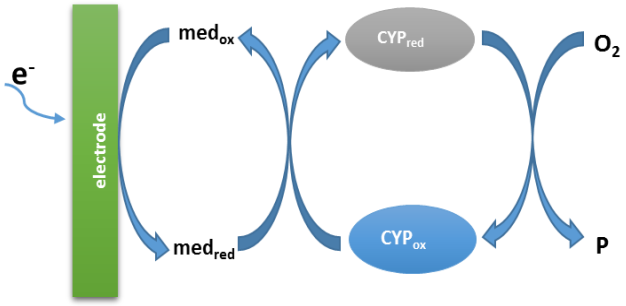

Figure 3.1: Schematic representations of the working principles of a CYP Bioelectrode with mediated transduction.

Because at this stage the focus was on the catalytic response of CYP to caffeine only, this approach was abandoned.

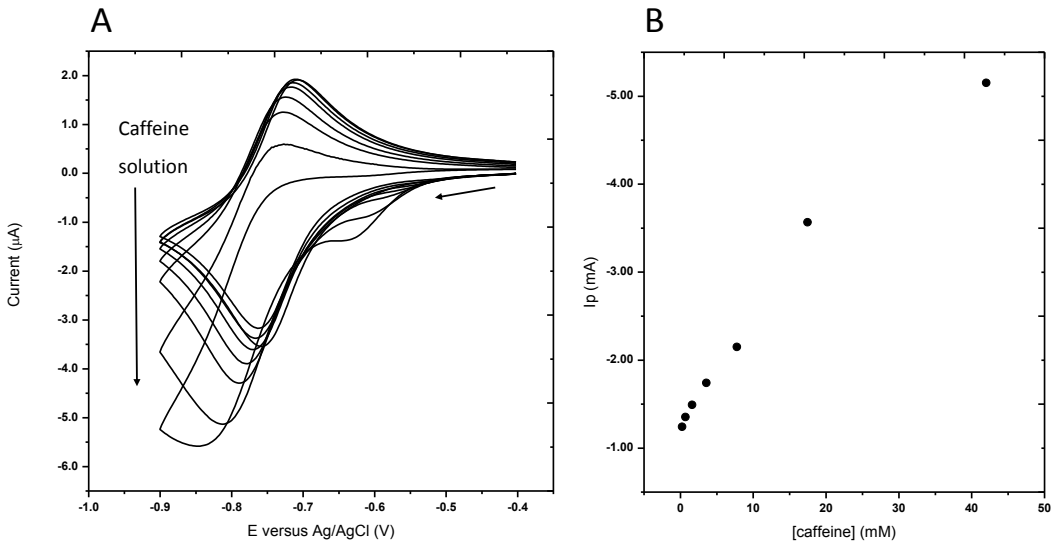

Figure 3.2: A) Cyclic voltammograms of methyl viologen in the presence of CYP membrane entraped on a PG electrode, buffer solution 0.1 M MV, 0.1 M KCl and tris-HCl buffer 50 mM pH 7.6. in the presence of varying caffeine concentrations (0-42mM).Scan rate: 50mV $s^{-1.B}$ Icat variation with nitrite concentration.

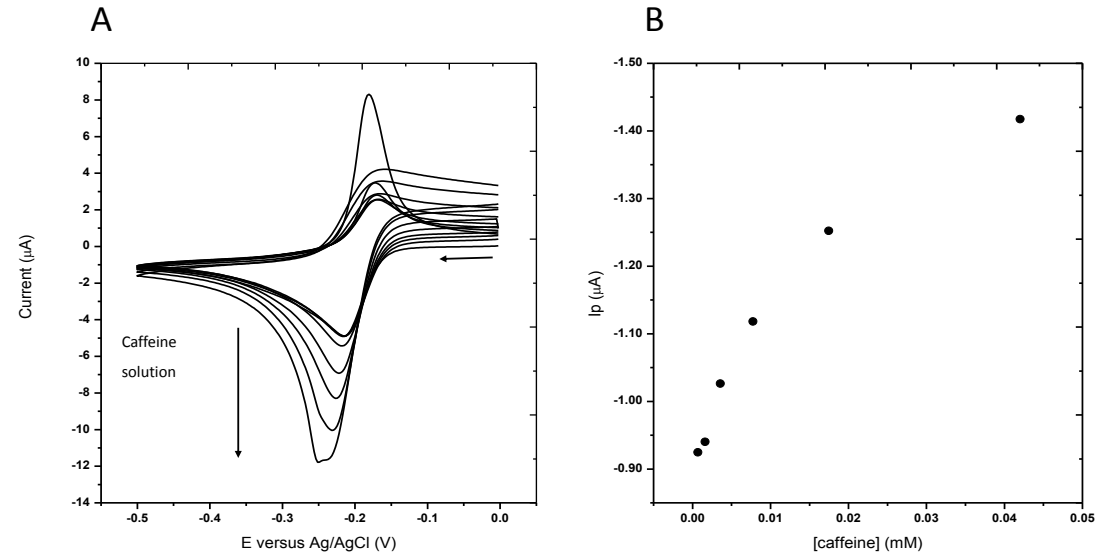

Figure 3.3: 3 A) Cyclic voltammograms of methylene blue in the presence of CYP on a PG electrode, buffer solution 0.1 M MV, 0.1 M KCl and tris-HCl buffer 50 mM pH 7.6. in the presence of varying caffeine concentrations (0–42mM).Scan rate: 50mV $s^{-1.B}$. B) Icat variation with nitrite concentration.

3.1.1.2 Direct electrochemistry of cytochrome P450

Direct electrochemistry of cytochrome P450 in surfactant films Because the electrochemically mediated experiments did not give the expected full catalytic response, it was decided to use a DET approach. In fact, direct electrochemical reduction has the potential to provide P450s with reducing equivalents, thereby eliminating the native ET machinery.

The first attempt at direct electrochemistry was carried out in the absence of surfactants or other stabilizing components. The successive voltammograms depicted in Figure 3.4A show the change in the non-catalytic signals of cytochrome P450 1A2 with time.

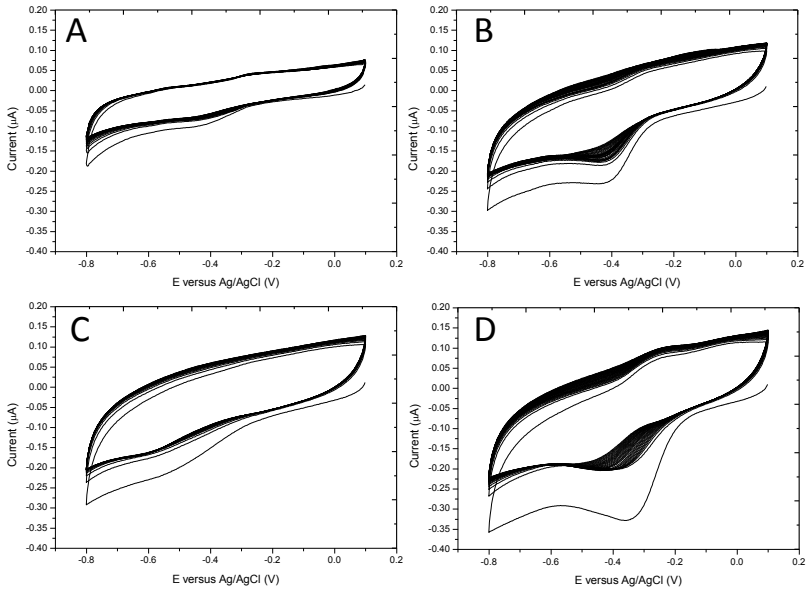

Figure 3.4: Consecutive cyclic voltammograms of CYP1A2–surfactant films casted on PG electrodes in 0.1 M KCl and tris-HCl 50 mM pH 7.6; scan rate 50 mV/s. A) Control electrode with CYP1A2 only, B) DDM C) DDAB, D) CTAB.

Although a small and broad redox wave could be observed in the range -0.3;-0.5 V the signal promptly disappeared; this signal is similar to the ones observed in electrochemical experiments using other cytochromes P450[75,163,186,187], leading to the conclusion that this non-catalytic signal is correlated with the reduction and reoxidation of P450Fe^{III}/Fe^{II}. This signal was not systematically observed and, when observed, was of very small intensity, probably due to of the small amount of protein that was able to reach the required orientation to keep the conformation for direct electron transfer reaction and/or to a small ET rate.

In order to improve the protein stabilization and subsequent direct electron transfer it was decided upon the use of surfactants. This CYP is a membrane-bound protein for which a more hydrophobic environment could be beneficial. Surfactant assemblies on carbon electrodes have been shown to facilitate direct ET with various P450s[74,188,189]. The

protein was therefore incorporated into surfactant layers deposited on the electrode.

All the surfactants tested were used in a concentration corresponding to 2xCMC to ensure that micelles could be formed on the electrode and, in this way, equivalently compare the effects of the surfactants on the enzyme's electrochemical response.

Cyclic voltammograms of CYP1A2–surfactant films casted on PG electrodes are shown in Figure 3.4. The peak potential was never shifted, no matter the surfactant type. The voltammograms depicted in Figure 3.4 show a consistency in the electrochemical behavior of the protein in different surfactant films. It is easier to observe in Figure 3.4 B and D, that the peak potential is in the -0.350 to -0.400V range, and that it shifts slightly to more negative potentials over time.

The reported studies on heme proteins, like hemoglobin and myoglobin, considered that the DDAB surfactant films could favor a specific orientation of the proteins embedded in them, due to interaction with the cationic head group or the hydrocarbon chains of DDAB[63,68]. However, in this study DDAB did not provide the best results. On the contrary, DDM and CTAB enabled a better electrochemical response. CTAB in particular, a cationic surfactant such as DDAB, greatly enhanced the DET of CYP with the PG electrode, therefore, it was selected for further studies.

The effect of the scan rate is shown in Figure 3.5. The cathodic peak currents increased linearly with the scan rate up to 1 V/s which is consistent with a diffusionless electrochemistry (Figure 3.5); only CVs with a scan rate up to 0.5 V are shown). The absence of the symmetrical counterpart of the peak located at -375 mV indicates that the electrode reaction is nonreversible.

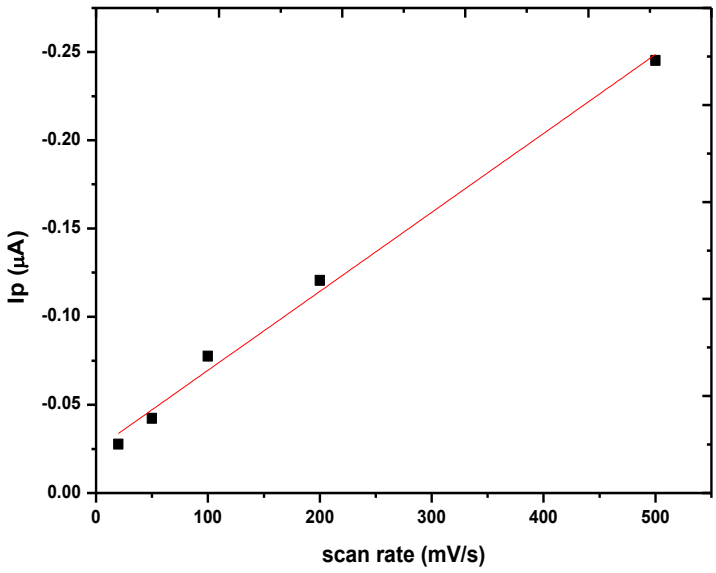

Figure 3.5: Variation of the cathodic peak currents on the potential with the scan rate (5-500 mV/s) (y=-2.48*10-8-4.48*10^{-10}x; r^2=0.992)

The catalytic activity of the CYP1A2-CTAB films towards caffeine was investigated; substrate solutions were deoxygenated before addition to the electrochemical cell. Once again, no relevant changes could be detected in the voltammograms, i.e., there was no catalytic activity (results not shown).

Stabilization of membrane-bound P450 protein for bioelectrochemistry

Sensor optimization The optimum membrane composition was selected from a group of sol-gel formulations prepared with different precursors, water: monomer molar ratios and enzyme quantities. The bioelectrodes were characterized by cyclic voltammetry.

The first efforts were based on formulations containing CTAB, due to the results obtained in the previous section. The formulations based on the sol-gel precursors TEOS and TMOS had a tendency to precipitate, regardless the solvent/precursors/surfactant ratios tested (Table 2.3). The sol-gel films had a thin and glassy appearance, but a high tendency to fracture during the drying process, occasionally loosing small pieces of glass. For these reasons these precursors were discarded and it was decided to test a different type of precursor, sodium silicate.

The sol-gel matrices prepared by the combination of sodium silicate and CTAB (Table 2.4) provided fairly more positive results (20 mM sodium silicate, 5 mM CTAB). Still, the film was thin and brittle. Although it was possible to obtain an electrochemical response, it was lost once the film cracked. Besides PEG being known to improve sol-gel consistency, it has also been reported as a stabilizing agent for P450 in electrochemical experiments at high temperature[190]. Thus, it was tested here to immobilize CYP1A2 (Figure 3.6C). However, no signal was observed in these conditions. The immobilization in silicate was also considered (Figure 3.6B), leading to a slight improvement in the measured electrochemical signal.

Next, sol-gel/enzyme films were prepared with the combination sodium silicate and polyetilene glycol (Table 2.5). With the optimal formulation: 55 mM sodium silicate and 6.25% PEG400 it was possible to obtain a hybrid film stable enough to continue our work. These results lead to the assumption that the use of sodium silicate prevents the introduction of alcohol in the starting sol, while PEG improves the stabilization of the membrane protein. This hybrid sol-gel formulation has not been previously reported and its reaction mechanism is not yet been established.

As previously stated, only the combination of PEG and silicate led to well defined redox peak at -0.335 V versus Ag/AgCl. The redox signal decreased rapidly by a factor of three during the first minutes of placing the electrode in electrolyte solution (Figure 3.7). Most likely, the weakly immobilized protein molecules are leaching out from the film and only the stably encapsulated CYP remains attached in the hybrid sol-gel film for long time experiments. This set of results clearly show that neither PEG nor silicate are able to immobilize CYP1A2 in an electrochemically active form and only the synergetic effect from their combination allows the redox activity of the membrane-bound protein.

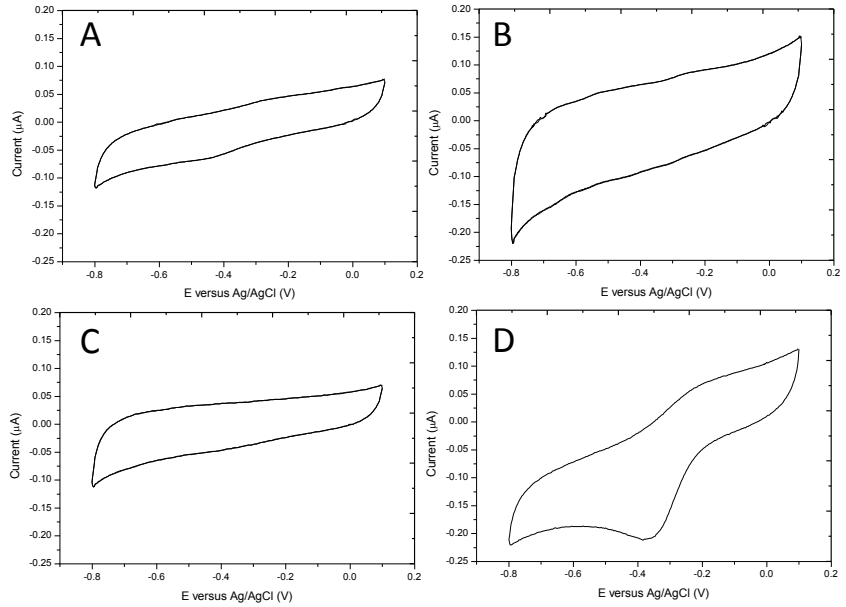

Figure 3.6: Cyclic voltammograms of CYP1A2 casted on PG electrodes, in 0.1 M KCl and tris-HCl 50 mM pH 7.6 purged electrolyte; scan rate 50 mV/s, in the presence of A only CYP; B CYP/Sodium Silicate; C CYP/Peg400; D CYP/Sol-gel(sodium silicate and PEG400).

Characterization of the non-catalytic signals The bioelectrodes, prepared with the hybrid sol-gel formulation described in the previous section were, characterized by cyclic voltammetry. A non-catalytic current-potential curve was always observed in purged electrolyte without caffeine (Figure 3.7); the peak potential is coherent with the one obtained in the presence of surfactants (previous section) as well as the potentials described in the literature for the heme iron reduction[191]. However, according to the literature, the CYP1A2 electrochemical signal in the absence of oxygen should depict the reversible electrochemical conversion of PFe^{III}/PFe^{II} indicating that perhaps the vestigial oxygen concentration present in the sol-gel film/electrolyte is causing the anodic signal to disappear. This phenomena will be further discussed in the next section.

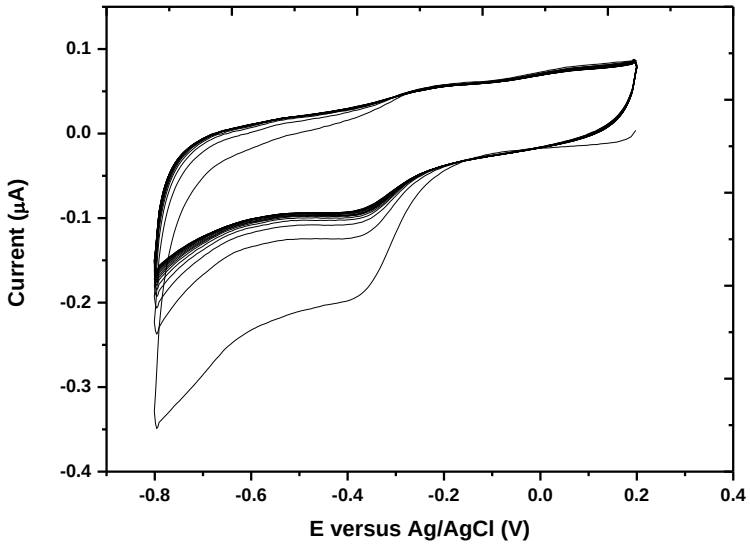

Figure 3.7: Consecutive cyclic voltammograms of PG/CYP1A2–sol-gel film electrode in 0.1 M KCl and 50 mM tris-HCl buffer pH 7.6 purged with argon. scan rate 50 mV/s.

The electrochemistry of sol-gel encapsulated CYP1A2 was studied by changing systematically the potential scan rate from 5 to 1000 mV s-1 as reported in Figure 3.8. Only one peak could be observed, and its current intensity increased linearly with scan rate's square root which is consistent with a diffusion controlled electrochemistry (Figure 3.8). The enzyme is thought to be immobilized in a matrix that does not prevent diffusion since no deviation from linearity is observed between peak current and square root of the scan rate up to 1 V/s (Figure 3.8 only shows up to 0.50 V/s).

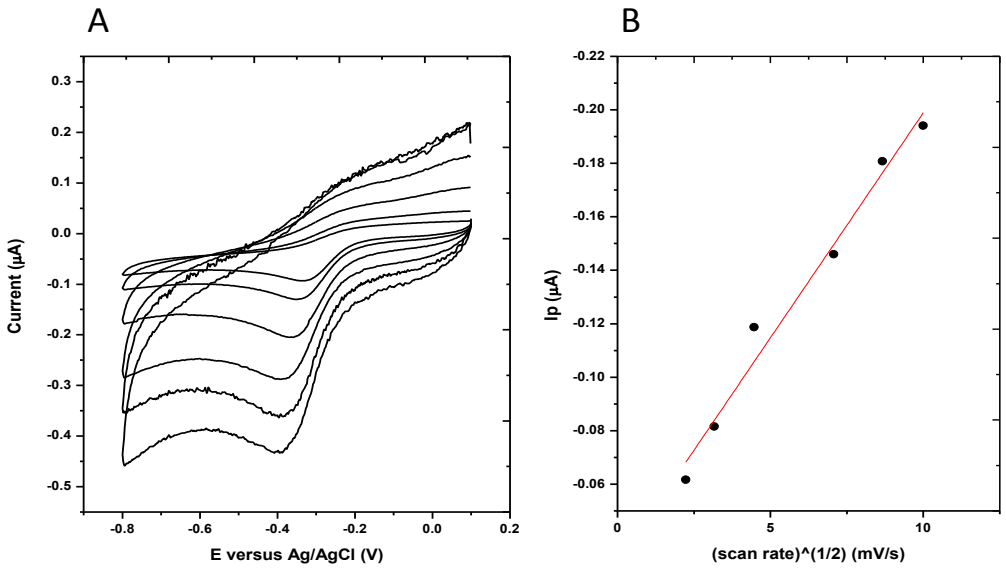

Figure 3.8: A) Cyclic voltammograms of PG/CYP1A2–sol-gel film electrode in 0.1 M KCl and 50 mM tris-HCl buffer pH 7.6 purged electrolyte at different scan rates; from inside to outside: 0.005, 0.01, 0.02, 0.05, 0.1, 0.2, 0.25 V.s^{-1}, respectively. B) Variation of the cathodic peak currents on the potential scan rate (y=-0.03-0.017x; r^2=0.98).

Response to oxygen and caffeine The chemistry of oxygen activation catalyzed by the P-450s has always been a topic of great controversy. The heme iron of P450 is coordenated by a cysteine as the fifth ligand. The sixth position is left vacant for oxygen binding during catalysis - but may be occupied by a water molecule in the resting state. The influence of dissolved oxygen on the electrochemical response of CYP1A2 immobilized in sol-gel (PEG400 and sodium silicate), observed in Figure 3.9 reveals that when the electrode is exposed to a high percentage of oxygen the cathodic signal, however intense in the first scan, quickly disappears. The electrochemical response measured for the first cyclic voltammogram showed a well-defined peak with a current intensity higher than 8 μA and maximum peak potential at -0.355 V vs Ag/AgCl. Still, continuous cycling at 50 mV s-1 leads to a continuous signal degradation and a peak shift to lower potentials. According to Rusling191, after electrochemical reduction of P450-Fe^{III} in aerobic solution, reduced form PFe^{II} is combined with dioxygen to form PFe^{II}-O2 complexes and this complex might be further reduced electrochemically, yielding hydrogen peroxide and regenerating the PFe^{II} heme[192,193]. The peroxide generated in this catalytic reduction of oxygen reacts with cyt P450Fe^{III} to form +•(P450-FeIV=O), which should be reduced at the electrode to regenerate cyt P450-Fe^{III} (Figure 3.10), the lectroactive species whose reduction is being monitored. Though, this regeneration does not appear to occur, which leads to the possible conclusion that the cycle described in the scheme is blocked in one of the steps. In such a case there are three hypotheses:

i) The window of potential in which the reaction was analyzed is not negative enough to reduce the +•(P450-Fe^{IV}=O), in other words, there is a lack of a driving force able to reduce this form of P450 making it impossible to regenerate the PFe^{III} (step 6 blocked);

ii) The PFe^{III} heme degradation due to hydrogen peroxide accumulation (c.f. 3.2.3) (step 5 blocked);

iii) The CYP's conformational change necessary for P450-Fe^{II}-O_2 conversion in hydrogen peroxide and P450-Fe^{II} does not occur (step 3 blocked).

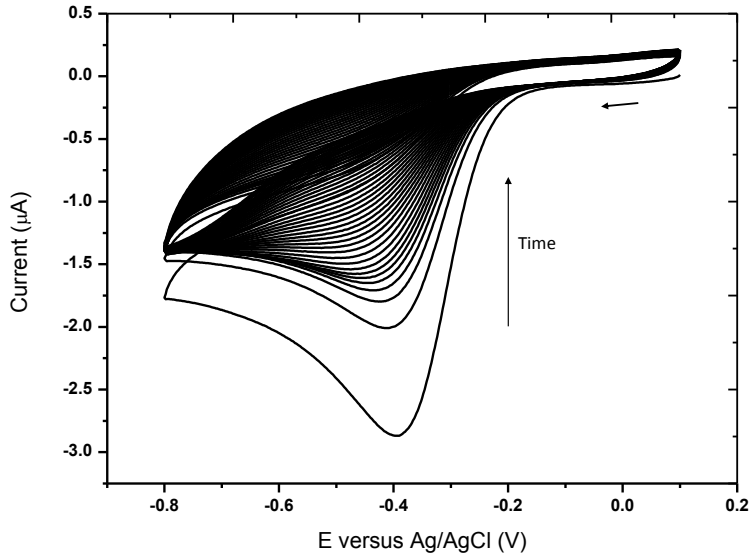

Figure 3.9: Consecutive cyclic voltammograms of PG/CYP1A2–sol-gel film electrode in 0.1 M KCl and 50 mM tris-HCl buffer pH 7.6 aerobic conditions. scan rate 50 mV/s.

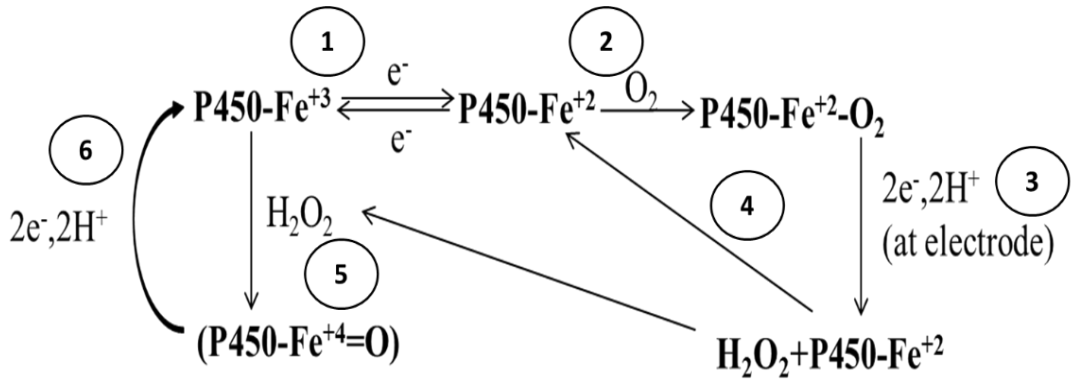

Figure 3.10: Pathways for Biocatalytic Activation of Cyt P450s by Peroxides, Oxygen Reduction Formed Peroxide.by P450s on Electrodes.

The results obtained upon the addition of purged caffeine aliquots turned out to be equivalent to the ones acquired when using redox mediators or DET with surfactants, meaning no catalytic response could be observed (Figure 3.11). This signal represents step 1 (Figure 3.10) in the presence of small amounts of oxygen (vestigial). If the conditions were completely anaerobic the signal should be reversible. However, in the presence of oxygen the equilibrium is shifted in the direction of $PFe^{II}O_2$ formation, turning the reaction (step 1) irreversible.

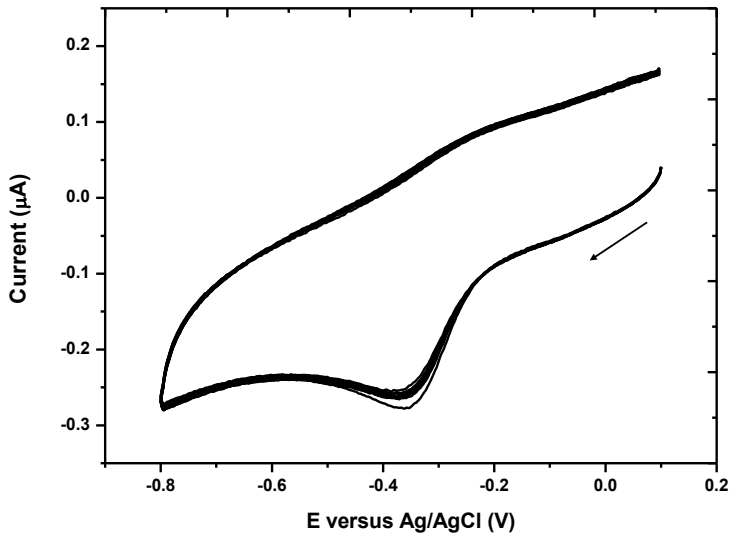

Figure 3.11: Cyclic voltammograms of CYP1A2–sol-gel film casted on PG electrode, buffer solution, 0.1 M KCl and tris-HCl 50 mM pH 7.6 purged with argon. In the presence of varying caffeine concentrations in the absence of oxygen. Scan rate: 50mV s^{-1}.

Figure 3.12 reports the electrochemical response of CYP1A2 immobilized in the sol-gel-PEG hybrid film to an increasing amount of non-deareated caffeine. The experiment was initiated in an oxygen free solution (purged with Argon). Then, small volumes of a non-purged caffeine solution were introduced in the cell, leading to the gradual increase in the cathodic peak intensity and a decrease in the anodic currents. It important to note that the data was plotted against the volume of caffeine added, in order to have a comparison term with the experiments where water additions were made.

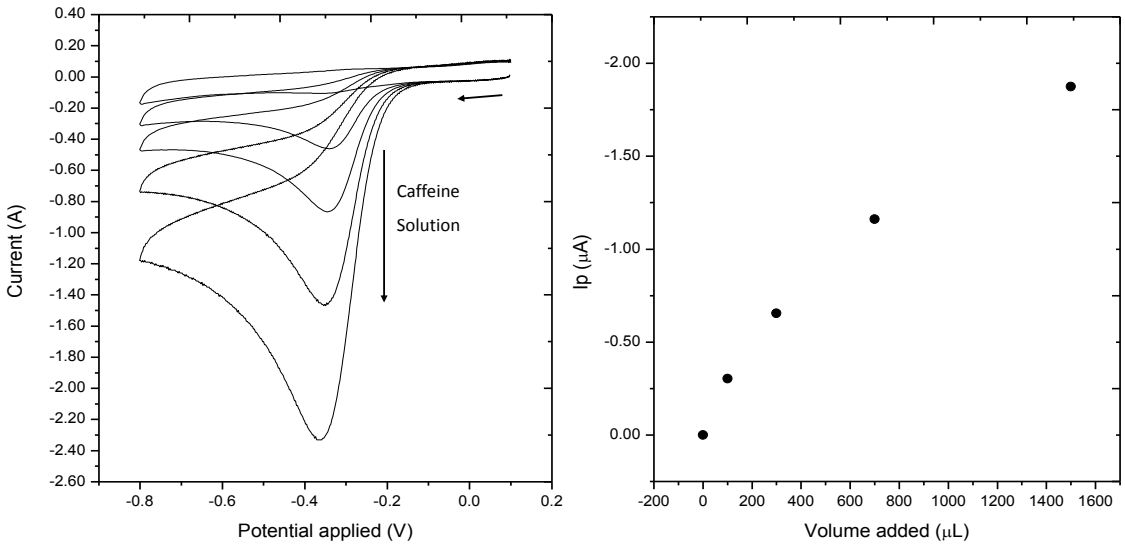

Figure 3.12: Cyclic voltammograms of CYP1A2–sol-gel film casted on PG electrode, buffer solution, 0.1 M KCl and tris-HCl 50 mM pH 7.6 purged with argon. In the presence of varying non-purged caffeine volumes (stock solution 60 mM). Scan rate: 50mV/s.

Conversely, control experiments carried out adding equivalent volumes of deareated water, provided the same results revealing that the responses observed was due to an increase in oxygen catalysis and not to caffeine's (Figure 3.13). The following experiment was initiated in an oxygen free electrolyte solution. When small non-purged water volumes were added to the solutions bathing CYP1A2/sol-gel/PG electrodes, the PFe^{III} reduction peak increased greatly (Figure 3.13). This is the classic voltammetric signature for electrochemical catalysis. Here, it the reflects reaction of PFe^{II} with dioxygen (step 2 of Figure 3.10) followed by reduction of the PFe^{II}-O_2 complex to give H_2O_2 , regenerating PFe^{II} to continue the reaction cycle (step 3 of Figure 3.10).

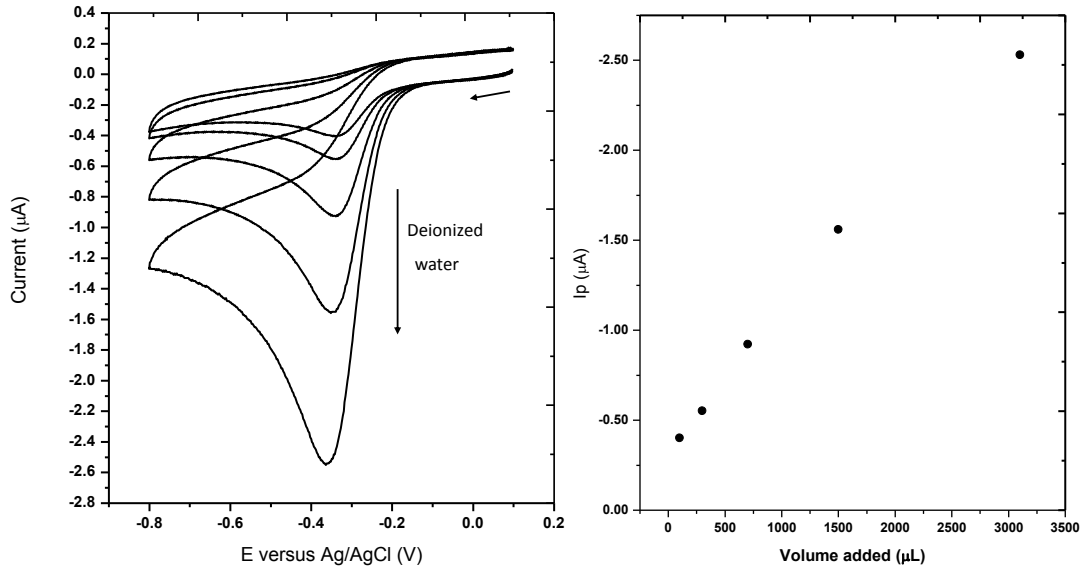

Figure 3.13: Cyclic voltammograms of CYP1A2–sol-gel film casted on PG electrode, buffer solution, 0.1 M KCl and tris-HCl 50 mM pH 7.6 purged with argon. Consecutive additions of non-purged water. Scan rate: 20mV s^{-1}.

3.1.1.3 Catalase

As previously mentioned, hydrogen peroxide formation might be one of the reasons why, in the presence of high concentrations of oxygen, the catalytic peak, corresponding step 1 (Figure 3.10), disappears after a few scans (Figure 3.9). In an attempt to avoid heme degradation from hydrogen peroxide exposure194 several experiments were carried out in the presence of catalase. This enzyme is a commonly found in nearly all living organisms exposed to oxygen. A number of recent studies indicate that catalase is the primary enzyme responsible for protecting the cells from hydrogen peroxide by catalyzing the fast decomposition of hydrogen peroxide to water and oxygen Equation 5.

$$H_2O_2 \rightarrow H_2O_2 + O_2 \tag{3.1}$$

Table 3.1 shows the experiments performed to diminishing the peroxide's impact in the P450's electrochemistry. It can be seen that the catalase addition to the cell does not prevent the decrease in the signal's intensity, regardless some assumptions can be made concerning the profile of the cyclic voltammograms. The twisted reverse trace phenomenon tends to increase in the presence of catalase at lower scan rates, according to what Limoges et al. reported194 this is characteristic of a chemical inactivation–redox reactivation mechanism. Additionally, when looking at the negative sweep and considering the results obtained by Butt *et al.*[195] when studying Nitrite reductase in the presence

of inhibitors, is possible to infer that the combination of the magnetic stirring and the lower scan rate promotes hydrogen peroxide removal of the electrode surface.

Table 3-1 Compilation of several electrochemical experiments with sol-gel/CYP1A2 in anaerobic conditions.

	50 mV/s without stirring	**50 mV/s stirring**	**10 mV/s stirring**
Without catalase	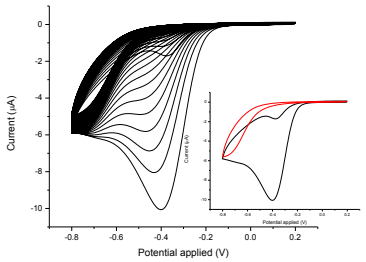	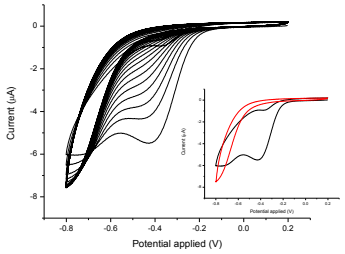	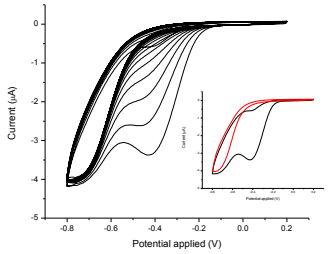
With catalase 1mg/mL	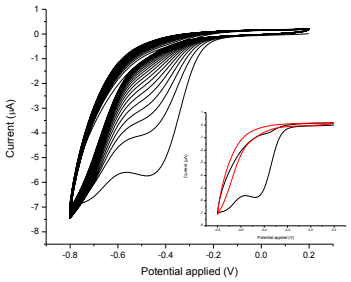	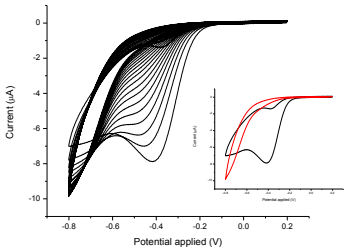	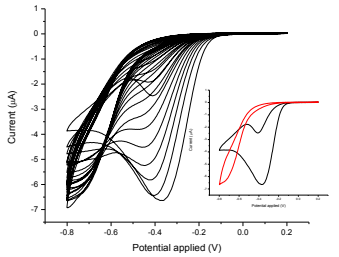

3.1.2 CYPOR complex

In order to better understand the results obtained with CYP1A2 namely, the lack of catalytic activity towards caffeine, similar experiments were performed with the CYPOR complex. Considering that in vivo, as previously discussed in section 1.3.1), the CPR transfers the electrons form NADPH to the cytochrome, it would be expected that, in the presence of the cytochrome P450 reductase there could be catalytic activity towards caffeine. For the immobilization of the CYPOR complex the same sol-gel was used as described in section 3.1.1.2)b)). The CVs revealed a cathodic peak at -0.2 V and a small anodic wave at -0.33 V. As observed in Figure 3.14 the cathodic peak currents vary linearly with the scan rate in a 5-500 mV/s range. This behavior indicates that the electrochemical reduction of CYPOR is not controlled by diffusion inside the sol-gel film. Although the cyclic voltammograms depicted in Figure 3.14 do not fulfil the reversibility criteria, we are now able to observe an anodic peak, unlike what happened in the absence of the CPR.

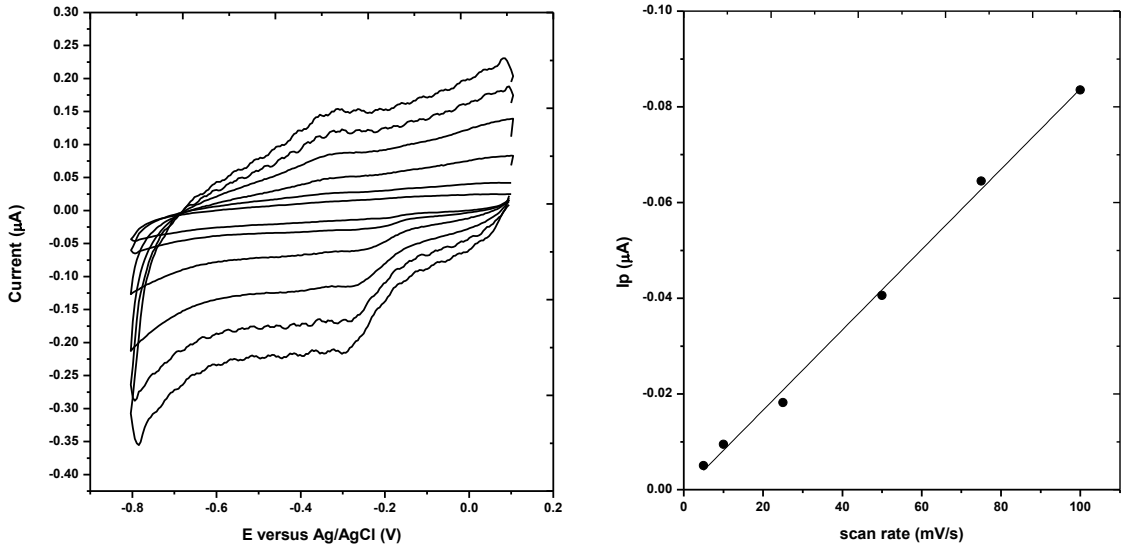

Figure 3.14: A) Cyclic voltammograms of PG/CYPOR–sol-gel film electrode in 0.1 M KCl and 50 mM tris-HCl buffer pH 7.6 in a purged electrolyte at different scan rates; from inside to outside: 0.005, 0.01, 0.02, 0.05, 0.1, 0.2, 0.25 V.s-1, respectively. B) Variation of the cathodic peak currents on the potential scan rate (y=1.85x10-10^{-8}.39x10^{-10}x; r^2=0.997).

In aerobic conditions, the CYP bioelectrode's CVs reveal a sharp catalytic peak. Heme–iron containing enzymes such as P450 have, not only, the ability to incorporate an oxygen atom from O2 into organic substrates, but also to utilize H_2O_2 and other peroxides in the one-electron oxidation of the different cosubstrates (peroxidase activity)[196]. This fact should account for the heme protection from degradation while exposed to hydrogen peroxide, but as it was discussed in the previous sections, this does not occur (Figure 3.15B). Nonetheless, in the experiments containing CPR (Figure 3.15A) it is possible to

observe that the catalytic activity does not disappear. In fact, although a decrease of current intensity occurs in the first 10 cycles, at that point the signal stabilizes still displaying a "strong" catalytic activity, leading to the supposition that the CPR is somehow related to the peroxidase activity of the cytochrome P450.

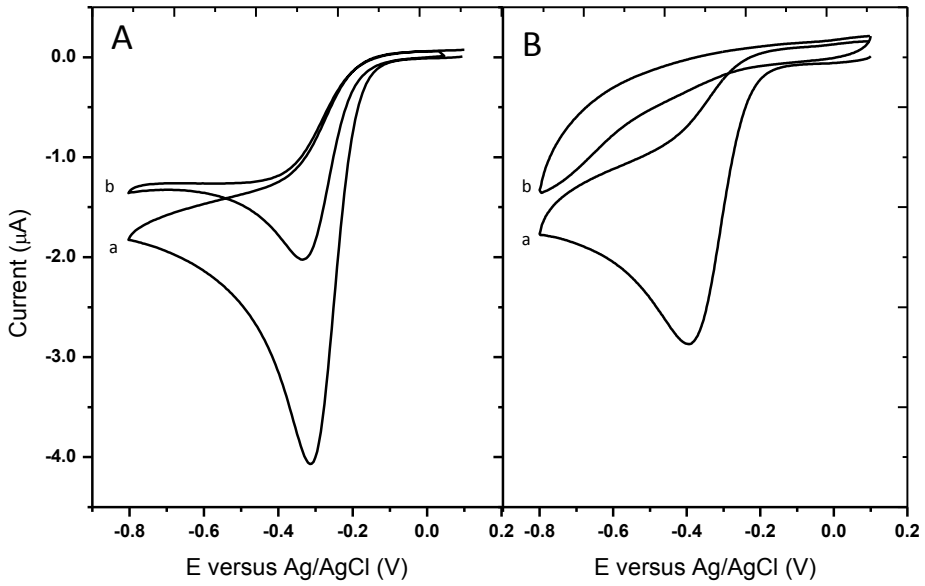

Figure 3.15: Cyclic voltammograms of films casted on PG electrode in aerobic conditions, buffer solution, 0.1 M KCl and tris-HCl 50 mM pH 7.6. Scan rate: 50mV s^{-1}.of A) CYPOR–sol-gel B) CYP1A2–sol-gel film. a) 1st scan b) 20^{th} scan.

The difference observed helps sustain the hypothesis postulated in the previous section, stating that a change in the CYP's conformation is required in order to perform the P450-Fe^{II}-O2 conversion in hydrogen peroxide and P450-Fe^{II} (step 3, Figure 3.7); therefore CPR is an essential element for the structural rearrangement. Upon the addition of small volumes of non-purged water to electrochemical cell an increase in the CYP's catalytic response is observed (Figure 3.16).

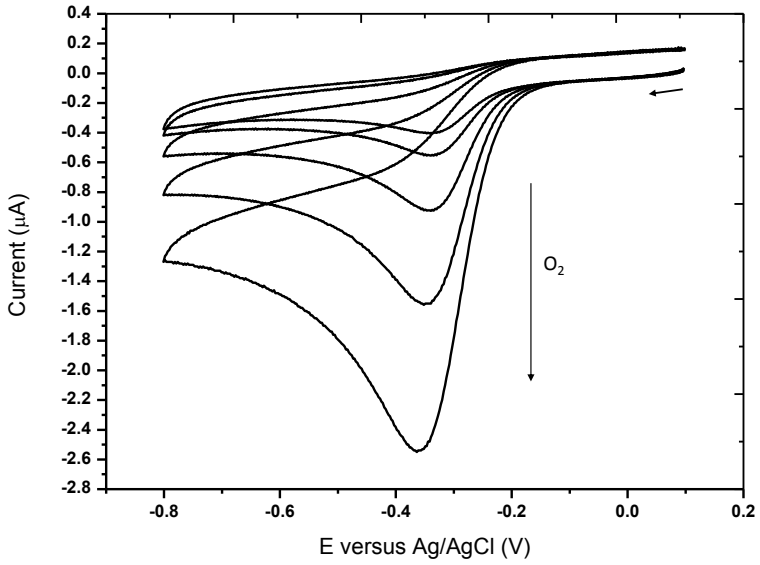

Figure 3.16: The effect of O2 binding on the electrochemistry of the CYPOR/sol-gel casted on a PG electrode, purged buffer solution, 0.1 M KCl and tris-HCl 50 mM pH 7.6. Consecutive additions of non-purged water. Scan rate: 50mV s^{-1}.

Interestingly, unlike what was observed in the previous experiments carried out, in the absence of CPR, when caffeine was added to the electrochemical cell, already containing a non-saturating oxygen concentration, a decrease in the catalytic current was observed (Figure 3.17). A similar catalytic current decreasing phenomenon has been described in the literature with glucose oxidase. Liu et al.197 for instance reported a decrease in the catalytic response upon glucose addition. In the work reported, GOD($FADH_2$), electrocatalyzes the reduction of dissolved oxygen according to following equations.

$$GOD(FAD) + 2e^- + 2H^+ \leftrightarrow GOD(FADH_2) \tag{3.2}$$

$$GOD(FADH_2) + O_2 \leftrightarrow GOD(FAD) + H_2O_2 \tag{3.3}$$

In the presence of glucose the electrocatalytic reaction is restrained due to the enzyme-catalyzed reaction between the oxidized form of GOD, GOD(FAD), and glucose, which then results in a decrease of electrocatalytic response (Equation 3.4).

$$Glucose + GOD(FAD) \rightarrow gluconolactone + GOD(FADH_2) \tag{3.4}$$

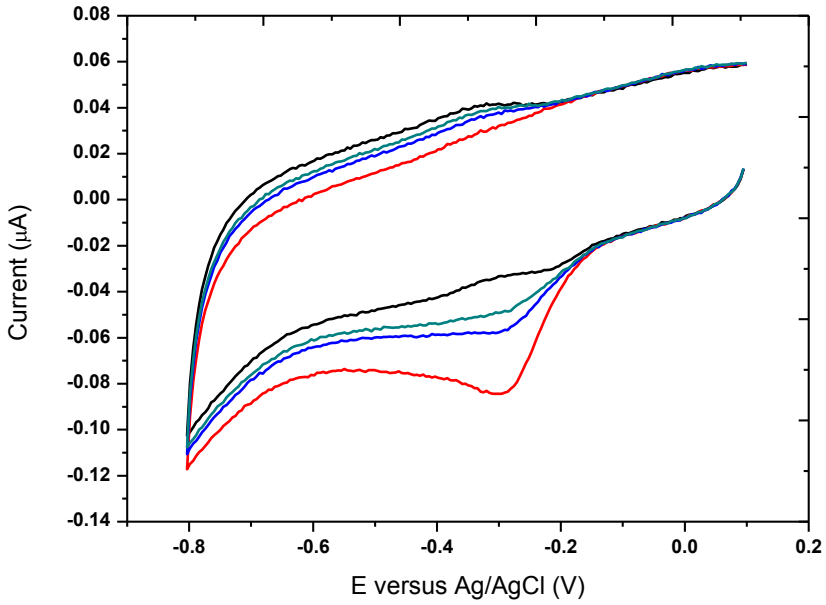

Figure 3.17: Cyclic voltammograms of CYPOR/sol-gel films casted on PG electrode in anaerobic conditions, buffer solution, 0.1 M KCl and tris-HCl 50 mM pH 7.6 purged with argon.scan rate, 50 mV/s.(black-line) without substrates (red-line) oxygen addition (blue and green lines) caffeine additions increased concentration.

3.2 Cytochrome *c* nitrite reductase

n recent years, several ccNiR (D. desulfuricans ATCC 27774) based electrochemical biosensors have been proposed[125]. Herein, this well-established biosensor system was used as a model to evaluate new immobilization platforms and operation methods. Unless stated otherwise, the experiments were carried out in a purged electrolyte solution in order to remove oxygen, which exhibits a broad waved that might mask the (non-) catalytic signals of ccNiR. In this section, several approaches will be presented, whose purposes were to improve the electronic communication and diminish the effect of interferences in the ccNiR based sensor. The first strategy focused on the optimization of the use of the sol gel formulation developed in section 3.1.1.2) using ccNiR as a model enzyme. In a second approach, the electrophoretic deposition of macroporous assemblies of single-walled carbon nanotubes (SWCNTs) was used with the goal of improving the sensitivity of ccNiR based nitrite biosensors. Lastly, an oxygen scavenger system was explored with the aim of avoiding the mandatory oxygen removal when working with reductase enzymes.

3.2.1 Hybrid sol-gel matrix

Like CYP1A2, ccNiR is a heme containing protein associated to the periplasmic membrane; for this reason, the matrix previously used for CYP immobilization was tested. This time, the sol-gel film was optimized by varying the polymer's size.

3.2.1.1 Non catalytic signals

As shown in Figure 3.18, the CVs of the PEG400 based films have higher cathodic peak currents, which can indicate that this matrix is more suitable for the detection of the electrochemical signals of ccNiR. The non-turnover currents should reflect the amount of immobilized enzyme molecules and their ability to interact with the electrode. The CVs of the PEG400 based films produce a higher cathodic peak currents, which can indicate that this matrix is more suitable for the direct ET with ccNiR. Though, the results were somewhat surprising because the higher polymer size of the PEG6000, is was expected to provide larger pore sized films which constitute a more appropriate environment for the incorporation of the large molecular weight aggregates of ccNiR (as purified this enzyme is normally found is aggregates of over 890 kDa)[149]. In effect, other sol-gel formulations tested in the past124, using diferent monomer precursors indicated that those providing the largest porosity delivered the best results. Such broad envelope comprises all hemes belonging to both NrfA and NrfH subunits (14 hemes, per NrfHA trimer) with reduction potentials ranging +150mV to 400mV vs NHE, as previously stipulated by protein film voltammetry, using an enzyme layer directly adsorbed on pyrolitic graphite electrode surface. Since the potential of the cathodic peak was more negative when ccNiR was entrapped in the PEG400 based formulations, perhaps in this case, the electrochemical reaction beneath is related with the reduction of the more negative hemes. This might be

a consequence of different molecular reduction within this sol- gel matrix. Future surface characterization of these two enzyme films should indicate if the protein is effectively encapsulated in both of them. If ccNiR is embedded only in the PEG6000 sol-gel, then the direct electrode contact on the PG surface may be somewhat impaired, and in contrast, with the PEG400 sol-gel but heterogeneously deposited on the electrode surface.

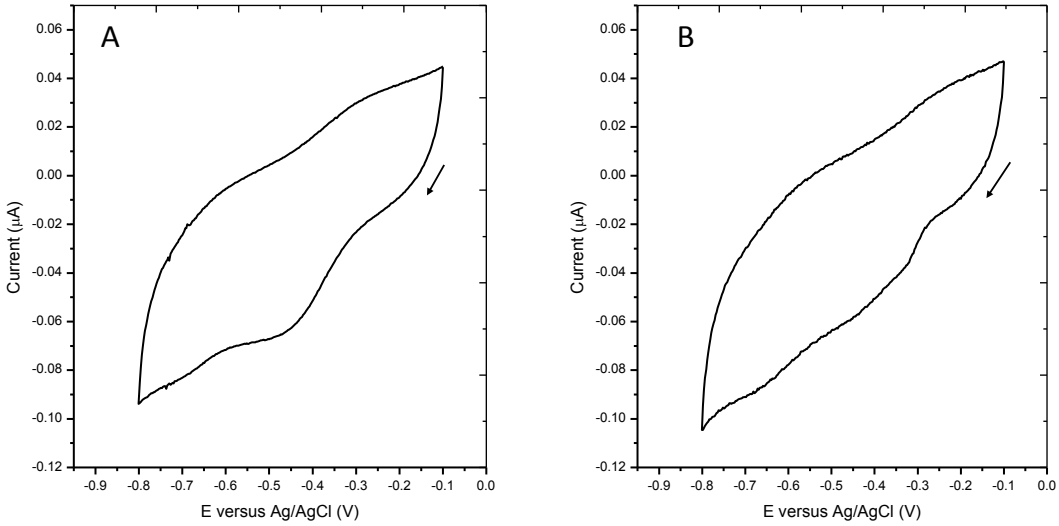

Figure 3.18: Cyclic voltammograms of ccNiR immobilized on sol -gel films, buffer solution, 0.1 M KCl and tris-HCl 50 mM pH 7.6 purged with argon.scan rate, 20 mV/s. A) ccNiR entrapped in a sodium silicate and PEG400 film B) ccNiR entrapped in a sodium silicate and PEG6000 film.

3.2.1.2 Response to nitrite

To assess the dependence of the catalytic current on the concentration of the substrate, cyclic voltammograms of the PG/ccNiR-PEG modified electrodes were registered at various nitrite concentrations. The correspondent cyclic voltammograms for a PG/ccNiR-PEG6000 electrode are presented in Figure 3.19; they show increased cathodic peak currents correlated with the substrate amount. This reflects the electroenzymatic reduction of nitrite to ammonium and hence, a direct electrical connection of ccNiR to the electrode surface.

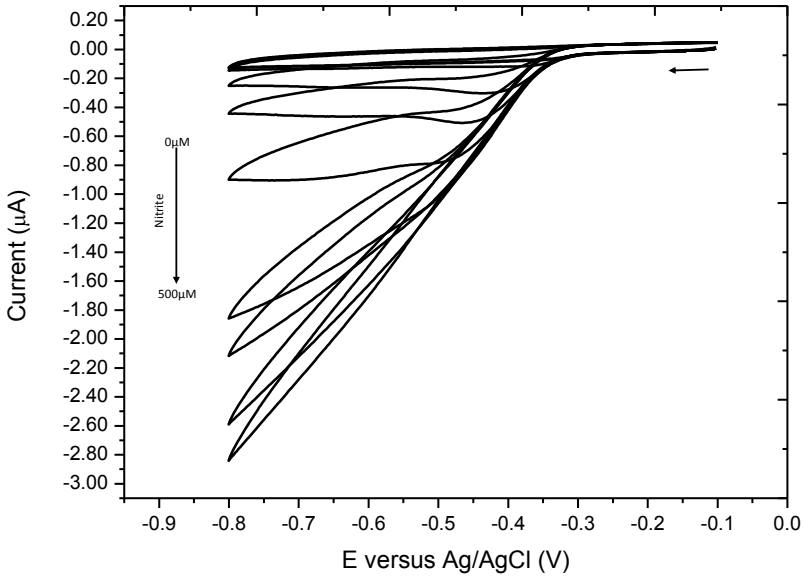

Figure 3.19: Electrochemical response of PG/ccNiR–sol-gel film(PEG6000) electrode to varying nitrite concentrations (0-500μM) in 0.1 M KCl and 50 mM tris-HCl buffer pH 7.6 purged with argon. Scan rate, 20 mV/s.

Figure 3.20 shows the relation between the catalytic currents and nitrite concentration for ccNiR/PEG400 and ccNiR/PEG6000 electrodes. Apparently, the nitrite reducing activity follows a typical Michaelis-Menten behavior, i.e. a steady increase of the catalytic currents is observed, with a linear range extending up to 100 μM of nitrite and reaching a plateau at higher concentrations.

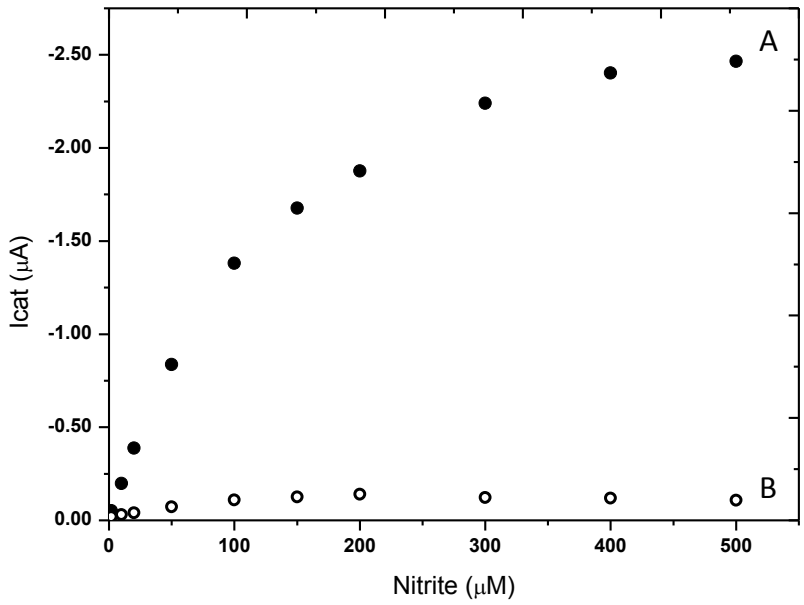

Figure 3.20: Variation of Icat with nitrite concentration of ccNiR immobilized on sol-gel films A) ccNiR entrapped in a sodium silicate and PEG6000 film B) ccNiR entrapped in a sodium silicate and PEG400 film.

The sensitivity of the bioelectrodes, as determined by the slope of the linear part of the calibration curve (Figure 3.20) is 197 mA/M.cm2 and 12.7 mA/M.cm2 for the ccNiR/PEG400 and ccNiR/PEG6000 bioelectrodes, respectively, while the maximum currents at saturating nitrite concentrations (500μM) are -0.109 μA and -2.47 μA, respectively. These results are somewhat contradictory when compared with the non-turnover signals seen in section 3.2.1)3.2.1.1), considering that ccNiR/PEG6000 gave a poor non- catalytic response and in the presence of nitrite, the catalytic response is more than ten-fold that of ccNiR/PEG400 electrode. Nonetheless, this result was anticipated because, as mentioned previously, a higher pore size was expected to be more suitable not only for the accommodation of the large ccNiR aggregates, as well as to guide protein molecules towards the electrode surface with PEG6000 based sol- gel., but also for the mass transport of the substrate. Another possibility for the improved behavior of PEG6000 lies on the assumption previously made, that the cathodic peak's potential is closer to that of the catalytic site. Within the 3Dmatrix, the sensitivity of the PEG6000 electrode is slightly lower than most of the values reported for the preceding nitrite biosensors constructed with the same enzyme 39(cf. Table 1.5).

The lower detection limit at a signal to noise ratio of 3 was 2 μM and 0.19 μM for ccNiR/PEG400 and ccNiR/PEG6000 bioelectrodes respectively; these values are similar to the previously reported LODs of ccNiR based biosensors and meet the requirements for nitrite monitoring in drinking waters according to European Union rules (maximum admissible level <0.1 ppm, i.e., 2.2 μM). Nevertheless, one should consider further optimization studies, using different amounts of enzyme and sol-gel concentrations.

3.2.1.3 Stability

The sol-gel/ccNiR modified electrodes were stored at 4°Cand tested for stability. Calibration curves were periodically traced and the maximum currents and sensitivity for nitrite were evaluated. Figure 3.21 shows the gradual decrease in the ccNiR's catalytic response to nitrite over time (80 days) in a ccNiR/PEG6000 bioelectrode. The ccNiR/PEG400 electrodes had a similar profile but maintained their catalytic activity for a shorter period (9 days).

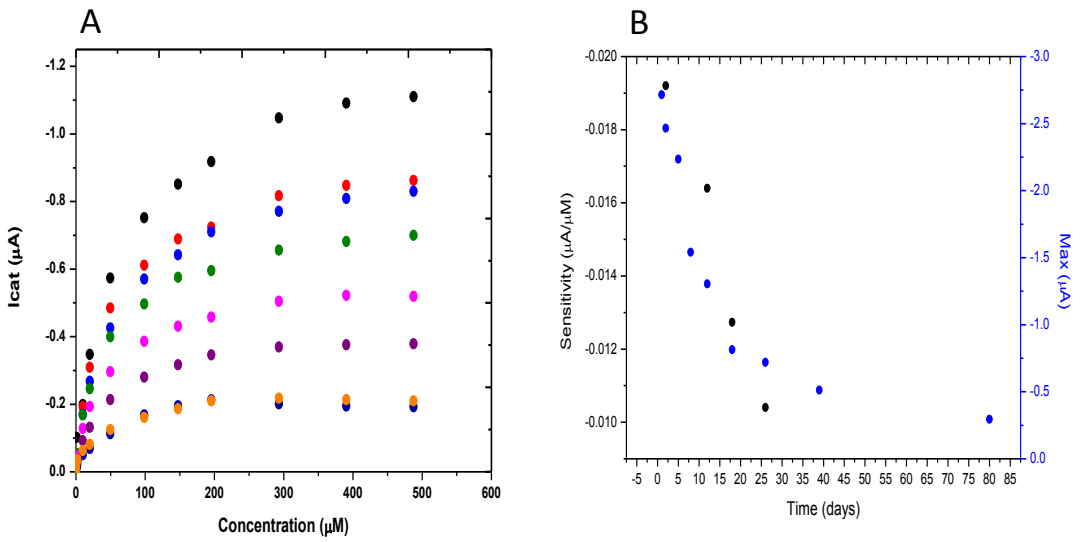

Figure 3.21: Variation of Icat with nitrite concentration of ccNiR immobilized on sol-gel films A) ccNiR entrapped in a sodium silicate and PEG6000 film B) ccNiR entrapped in a sodium silicate and PEG400 film.A) Variation of Icat with nitrite concentration of ccNiR immobilized on PEG6000 sol-gel films over time. B) Time effects on the biosensor sensitivity for nitrite determination. Sensitivity values were given by the slope of calibration curves performed periodically throughout 80 days. Catalytic currents wer e measured at - 0.8 V vs Ag/AgCl.

A steep decrease in maximum current and sensitivity occurs in the first day, with both matrices. Nevertheless, it is clear that the PEG400 leads to a complete loss of activity faster than the PEG6000 sensor (ccNiR/PEG400 loses activity after 9 days while ccNiR/PEG6000 keeps 50% of its initial activity after 2 weeks). Most likely this is due to denaturation or/and lixiviation of the enzyme in the sol-gel matrices. Though, it is worth mentioning that the long period in which the ccNiR/PEG6000 configuration remains active is quite promising, and a future optimized formulation possibly comprising enzyme stabilizing agents could originate a more reliable and stable biosensor.

3.2.2 Macroporous carbon nanotubes

The electrophoretic deposition allows the formation of macroporous CNTs layers from suspensions of charged particles on the electrode surface. The carbon nanotubes are negatively charged in a broad pH range198 due to the presence of carboxylic groups on their surface. They move to the anode during the deposition and form a dense interconnected network with a two-dimensional geometry and irregular mesopores caused by voids between the randomly distributed carbon nanotubes[199].The polystyrene beads are also negatively charged due to the presence of sulfonate groups on their surface (potassium persulfate was used as initiator of the polymerization in their synthesis[200]) and can be electrophoretically deposited as well. Variation of the deposition time affects thickness/amount of CNTs deposited.

The influence of the amount of deposited macroporous SWCNT on the catalytic response of ccNiR was evaluated by CV on glassy carbon plates. The deposition time was varied between 30s and 240s. Figure 3.22 depicts the effect of increasing nitrite concentrations on the ccNiR/CNT-PS electrode prepared with a 240s deposition time.

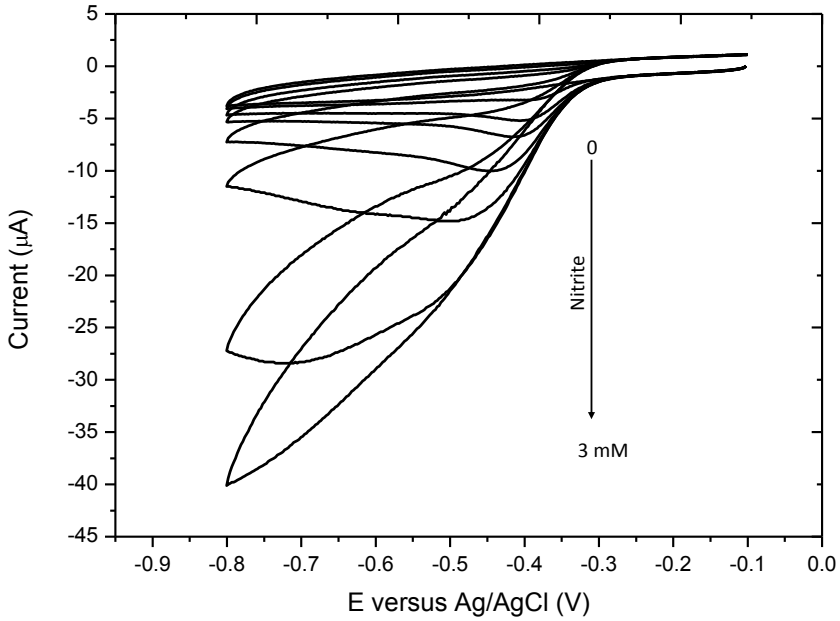

Figure 3.22: Electrochemical response of PG/CYP1A2–sol-gel film electrode to varying nitrite concentrations (0-300mM) in 0.1 M KCl and 50 mM tris-HCl buffer pH 7.6 purged with argon. Scan rate, 20 mV/s.

Figure 3.23 shows that higher deposition times, and consequent higher nanotubes amounts deposited on the electrode, results in an increased ccNiR response to nitrite. Yet, the sensitivity, as determined by the slope in the linear part of the catalytic current vs. substrate curve, did not improved with the amount of macroporous material (results not shown) and only a higher maximum current at saturating substrate concentrations

was observed.

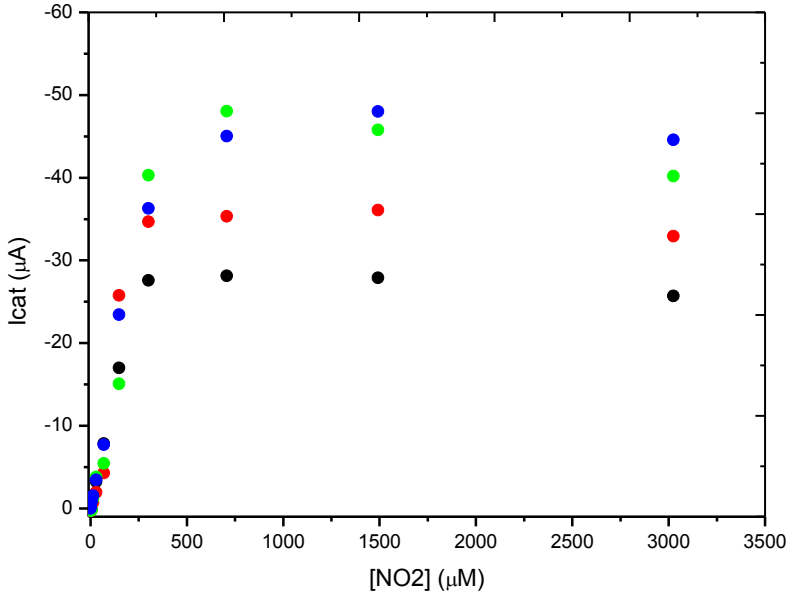

Figure 3.23: Catalytic current variation of the ccNir/CNT-PS layer as a function of nitrite concentration. Macroporous SWCNTs deposition time. (black) 30s; (red) 135s; (green) 180s; (blue) 240s.

The deposition times were chosen based on the work developed at LCPM-CNRS Nancy[201] , which demonstrated that above 240s the film stability starts to decrease. In the conditions tested in this work it was also possible to observe that there is hardly any difference between the 180s and 240s configurations. This behavior is in agreement with the results presented by Etienne et al.201 very recently, because the film thickness is expected to start stabilizing after 100s deposition time. Bearing in mind that there is an improved response with the amount of nanotubes, the results presented above are considered positive. Still, these experiments are preliminary and further work must be accomplished to better understand the system,for instance, the study of difference between the presence and absence of the PS beads would be quite interesting.

3.2.3 Oxygen scavenger system

The majority of electrochemical nitrite biosensors are used under anaerobic conditions, usually by eliminating the electrolyte's oxygen content by inert gas bubbling. Herein an enzyme-catalyzed O2 removal system, based on the protocol developed by Plumeré et al.202 will be studied, in order to use a nitrite reductase based biosensor under ambient air electrochemical cells. The glucose-GOx-CAT system (Figure 3.24) was thus tested with respect to its ability to remove oxygen and maintain anaerobic conditions in unstirred electrochemical cells open to ambient air.

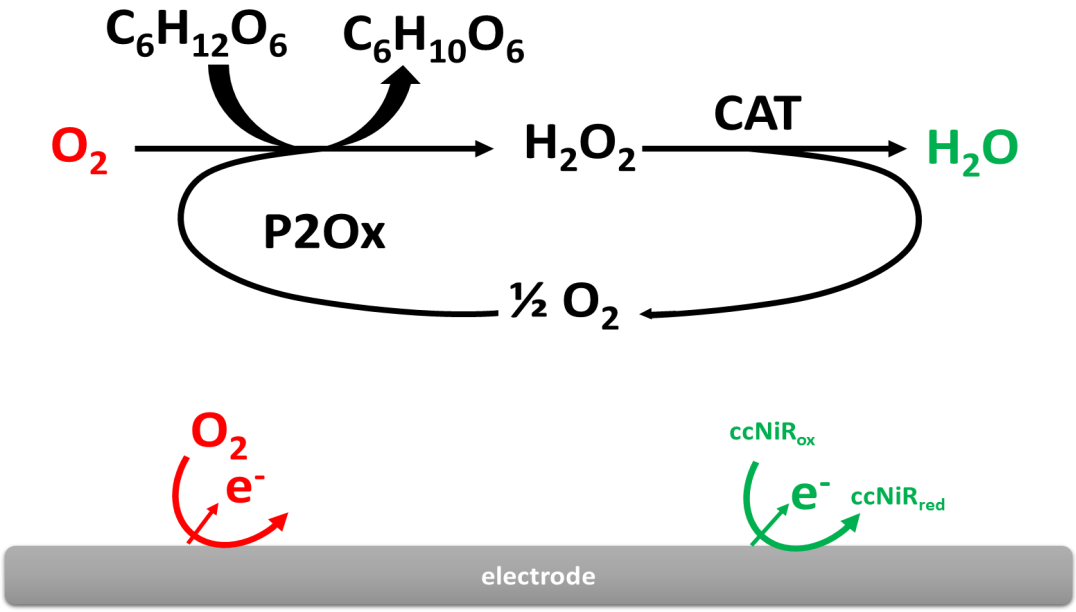

Figure 3.24: Scheme of the GOx-CAT scavenging system.

The oxygen scavenger system was tested with the sol-gel/ccNiR system described in section 3.1.1.2)b). In absence of GOx and CAT, the cathodic oxygen reduction signal appears at potentials lower than 600 mV vs Ag/AgCl at the PGE.

Figure 3.25 shows that after addition of glucose, GOx and CAT to the electrochemical cell oxygen is efficiently removed from the electrolyte. The remaining background current is comparable or even lower than the one obtained after purging the electrolyte with inert gas for 20 min (usual method for oxygen removal).

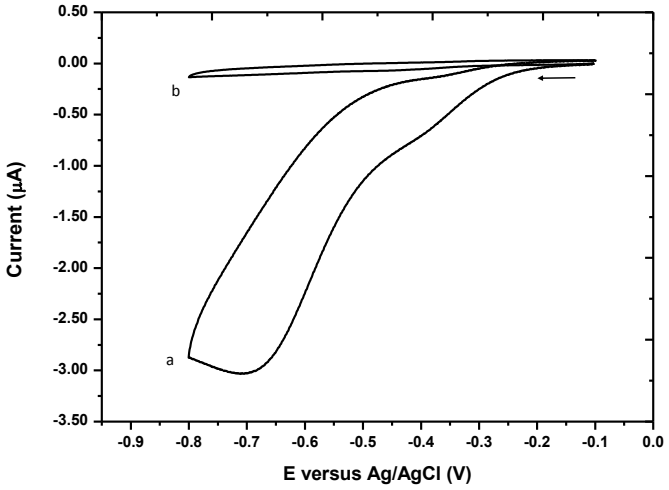

Figure 3.25: Cyclic voltammograms of PGE/ccNiR/PEG at 20 mV s -1 in 10 mL of 0.1 M KCl and tris-HCl 50 mM pH 7.6; (a) GOx (12.5 μM, 15 UmL -1) and CAT (16.6 μM, 2 kU mL -1) in solution (b) GOx (12.5 μM, 15 UmL-1), CAT (16.6 μM, 2 kU mL-1) and glucose (50 mM) in solution.

Next, the addition of nitrite to the cell reveals an increase in the catalytic current of ccNiR, indicating that the nitrite biosensor remains functional and is able to detect nitrite in the presence of the oxygen scavenging system. (Figure 3.26).

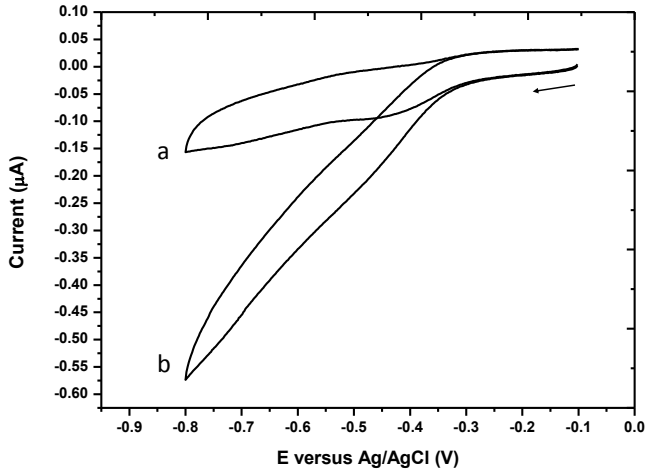

Figure 3.26: Cyclic voltammogram with PGE at 20 mV s -1 in 10 mL of 0.1 M KCl and tris-HCl 50 mM pH 7.6; (a) upon addition of GOx (12.5 μM, 15 UmL -1) and CAT (16.6 μM, 2 kU mL -1) and with the addition of glucose (50 mM).(b) addition of 100 mM Nitrite.

After confirming the GOx-Catalase-glucose ability to remove oxygen from solution, the efforts were focused on immobilizing the oxygen removal system on the ccNiR bio-electrode in order to constitute a fully integrated biosensor. As a first attempt, catalase was immobilized on the sol-gel matrix and GOx and glucose were added to the unpurged electrolyte. As can be observed in Figure 3.27, this system is not effective for oxygen removal, since the cathodic oxygen currents are still present. Most likely, catalase is not active in the sol-gel film or the amount of immobilized enzyme is not enough to complete the cycle of oxygen removal in the vicinity of the electrode surface. Next, the electrolyte solution was thoroughly purged with argon to remove oxygen from solution, however as confirmed by the green curve in Figure 3.27A the cathodic currents are not eliminated. At this point it is very likely that the GOx (and glucose in solution) has produced high amounts of hydrogen peroxide which, due to the lack of catalase in solution, is accumulating and originating the cathodic currents observed after purging the solution. In order to remove the accumulated peroxide, catalase was then added to the solution and, in effect, the cathodic currents were eliminated. Interestingly, upon nitrite addition to the cell, no nitrite reduction currents were observed, which could indicate that the hydrogen peroxide may have inactivated ccNiR.

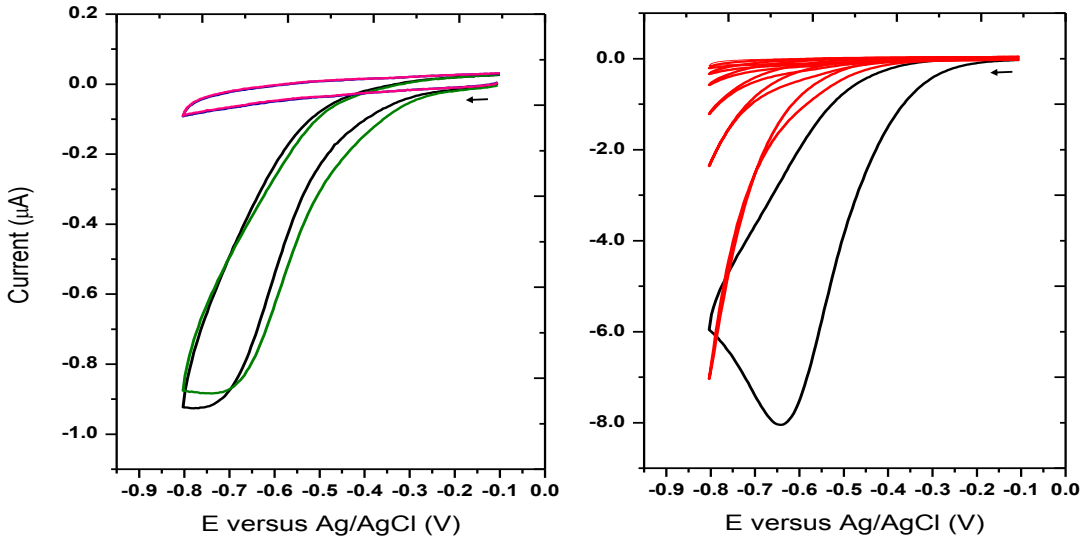

7

Figure 3.27: Cyclic voltammogram with ccNiR/CAT immobilized in PGE at 20 mV s^{-1} in 10 mL of 0.1 M KCl and tris-HCl 50 mM pH 7.6; A) (black) addition of GOx (12.5 μM, 15 UmL^{-1}) and of glucose (50 mM).(green) after purging the electrolyte solution with argon for 10 min (magenta) CAT (16.6 μM, 2 kU mL^{-1}) (blue) 100 mM Nitrite.B) control experiments performed in the absence of ccNiR. (Red line) increasing hydrogen peroxide concentrations (0-3mM); (black line) non purged electrolyte.

The precise chemical mechanisms of the heme destruction are probably very complex. The most plausible hypothesis is that hydrogen peroxide produced by GOx is the initiating agent in the degradative mechanism203,204. Studies on hydrogen peroxide-mediated heme degradation have implicated the hydrogen peroxide complex of ferryl (Fe4+) heme, the ferryl heme itself being produced from a peroxide complex of ferri- and ferrohemes. The peroxide complex of the ferryl heme readily autoxidizes to form the highly reactive superoxide radical[205,206]. The proposed mechanism via initially coordinated peroxide is consistent with the observations of a lack of reactivity of the heme group of ccNiR. Although there is still a lot of work to be accomplished regarding the system's immobilization, the results obtained are very promising from the oxygen scavenging system point-of-view. It must be taken into account that the phenomenon of heme degradation by hydrogen peroxide has yet to be reported with ccNiR.

4

Conclusion

4.1 Cytochrome P450 electrochemistry

The electrochemistry of P450 proteins is rather challenging. Several experimental approaches were tested in order to study this system, ranging from mediated electrochemistry with solution and electropolymerized electron shuttles, to direct electron transfer based systems using surfactants and/or sol-gel films. However, only a few of these methodologies were successful in channeling the electrons from the electrode to the CYP, namely, entrapment with long-chained surfactants, DDM and CTAB, and sodium silicate/PEG400 sol-gels.

In this work, P450 DET in a water-based sol-gel thin film is described for the first time. The electrochemistry of the heme center and the electrocatalytic reaction with O_2 was greatly improved in the presence of PEG400. From the wide range of film compositions tested, it was shown that only the combination of the sodium silicate inorganic matrix and the PEG additive enabled the direct electron transfer reaction and the electrocatalytic activity towards oxygen.

From this thesis, it becomes apparent that the amount of oxygen in the supporting electrolyte is critical to the PFe^{III}/PFe^{II} conversion being monitored on the electrode. In anaerobic conditions, a small non-reversible cathodic peak is observed, whose intensity increases with the oxygen concentration. On the other hand, in aerobic conditions, a cathodic peak with a high current value is initially observed, which completely disappears over time. This suggests that the PFe^{II} species is not being regenerated and subsequently electrochemically reduced.

The results obtained with CYP and CYPOR immobilized in sol-gel, in the presence of varying oxygen and caffeine concentrations raised several questions for which there is

not a definite answer - why is there no increase in the catalytic current in the presence of caffeine? What is the hydrogen's peroxide relevance for the CYP's activity? - nonetheless one thing is clear, the CYP's catalytic cycle is interrupted in the absence of CPR. One of the first hypothesis revolved on the prerogative that hydrogen peroxide might have a detrimental effect on the catalysis of oxygen by CYP, by promoting heme degradation. However, there was no improvement in the system's response in the presence of a peroxidase (catalase), from which it is possible to infer that if the hydrogen peroxide concentration was one of the issues, it certainly was not the only one. The next hypothesis - CYP needs an efficient electron donor, in order to proceed with the substrates conversion, as well as a specific conformation that may be induced by the interaction with CPR – was sustained by the results. In fact, in the presence of CPR a catalytic response to caffeine was observed. Most likely, the docking between the two partners (CYP and CPR) is necessary for CYP to adopt the right conformation. One the other hand, one should not discard the hypothesis that the stabilizing matrix is not fully biocompatible, hindering the CYP's catalytic activity. A decrease in the oxygen catalytic current was observed upon caffeine addition, indicating that its concentration is being translated into a variation in the oxygen response by, somehow, disturbing the CYP cycle. In contrast, Rusling reported an increase in the catalytic current while using the same P450 isoform and another substrate (styrene)[187], regardless in his work it is not mentioned if the substrate stock solution was purged prior to the addition.

4.2 Cytochrome c nitrite reductase electrochemistry

Aiming at the development/optimization of a fully integrated amperometric nitrite biosensor, the hybrid sol-gel used in the studies performed with CYP1A2 was optimized for ccNiR. The results observed with different sol-gel formulations are in accordance with the ones previously obtained with ccNiR, which indicate that large pore matrices are preferable for the enzyme's immobilization/activity[124]. Indeed, the PEG6000 polymer (expected to produce large pore films) is more favorable than PEG400 to maintain the electrocatalysis of nitrite over time. Also, a more favorable orientation might be attained in this sol-gel, as corroborated by the fact that the cathodic peak's potential is similar to the one reported for the catalytic site of ccNir as immobilized on a PG electrode[207]. Macroporous carbon nanotube assemblies have been successfully prepared by electrophoretic deposition in the presence of a polystyrene template. The quantity of carbon nanotubes and polystyrene beads in the deposition medium is critical for the proper self-assembly of the composite film in the 60 V potential field. Cytochrome c nitrite reductase was deposited on the surface of these macroporous CNT electrodes and then used for the electrocatalytic detection of nitrite. A direct correlation was observed between the deposition time and the ccNiR's electrochemical response to the substrate, as shown by an increase in the catalytic current with nitrite concentration. Most likely, the greater

nanotube surface area generated with longer deposition times allows the electrical connection of a higher amount of electroactive enzyme. There are still other venues that have to be followed in order to ascertain the real weight of this approach, namely the interference with the size of the PS beads in the ccNiR's response to substrate. An oxygen removal system based in an oxidase, in the presence of its aldohexose substrate, and catalase was investigated for field biosensor applications. Electrochemical measurements under ambient air were free of oxygen interferences, even for electrolyte volumes of 10 mL. Quantification of nitrite, in an open cell with an electrochemical biosensor based on ccNiR as the biorecognition element and GOx as O_2 reduction catalyst was demonstrated. Interestingly, the results obtained during the study of this oxygen scavenger system - the bioelectrode lost its activity after being exposed to a high concentration of peroxide - uphold previous theories postulating that hydrogen peroxide might contribute to heme group degradation[208]. Although, thus far it was not possible to immobilize the oxygen scavenger system, this approach was successful in maintaining anaerobic conditions in the model nitrite biosensor described, proving itself a promising, simple and inexpensive oxygen removal methodology.

5

Future work

5.1 Cytochrome P450 electrochemistry

Several authors have proposed that any electrochemical experiments of immobilized P450 should be accompanied by control experiments with P420 (the inactive form), as well as an iron-protoprofirin group or other heme proteins such as myoglobin. Therefore as future work we propose to repeat this experiments using two working electrodes, one with immobilized P450 and the other with immobilized P420. Voltammograms should then be measured under identical conditions by switching between the two working electrodes. This would allow us to assure that the P450 has not been inactivated and detect other possible electrochemical artefacts. Another interesting experiment would be to co-immobilized catalase with P450 and P420 with the aim of reducing or eliminating hydrogen peroxide.

Additionally, other immobilization matrices should be tested with the CYP/CYPOR system in order to improve the electrochemical response and catalysis. Furthermore, other P450 substrates should be tested, for example propanolol and paracetamol.

Seeing that, the electron tunneling with DET is not mimicking the physiological electron pathway, future parallel studies could be performed with different redox mediators and electrochemical potential windows in order to access CYP's activity.

5.2 Cytochrome c nitrite reductase electrochemistry

The hybrid sol-gel developed in this thesis is a very promising biocompatible matrix, mainly due to the fact that is a water based formulation. Therefore, future work should strive to improve this matrix, for instance for application in nitrite biosensors. These

attempts should comprise further optimization of the sodium silicate, PEG and ccNiR ratios in the sol-gel film, the use of different molecular weight PEGs or the incorporation of other sol-gel stabilizing agents, such as PEI. It would also be quite interesting to perform surface characterization, of these bioelectrodes, in order to confirm effective enzyme immobilization, by scanning electron microscopy or atomic force microscopy.

Regarding the macroporous nanotubes electrode modification system, future endeavors should cover a more detailed study of the importance of the CNT's film porosity. That being said, the GC-plates should be functionalized with varying deposition times with and without PS-beads.

In the future, whichever sensor platforms used, it will be beneficial to promote the enzyme molecules structural orientation on the bioelectrodes, which would guarantee a greater reproducibility in the amount of electrically-wired enzyme and, consequently, the biosensor's response. This could be achieved by the use of functionalized materials, such as self-assembled monolayers or gold nanoparticles.

In order to implement the enzymatic oxygen scavenger system in biosensors, its immobilization must be accomplished; the sol-gel matrix here described should be optimized for this purpose or a different encapsulation material could be tested.

6

References

1. Borgmann, S., Schulte, A., Neugebauer, S. & Schuhmann, W. Amperometric Biosensors. Advances in Electrochemical Science and Engineering: Bioelectrochemistry (2011).doi:10.1002/9783527644117.ch1

2. Urban, G. Reinhard Renneberg and Fred Lisdat (eds.): Biosensing for the 21st century. Analytical and Bioanalytical Chemistry 393, 777-778 (2008).

3. Zweier, J. L., Li, H., Samouilov, A. & Liu, X. Mechanisms of nitrite reduction to nitric oxide in the heart and vessel wall. Nitric oxide: biology and chemistry / official journal of the Nitric Oxide Society 22, 83-90 (2010).

4. Severinghaus, J. W. The invention and development of blood gas analysis apparatus. Anesthesiology 97, 253–6 (2002).

5. Clark, L. C. & Lyons, C. Electrode systems for continuous monitoring in cardiovascular surgery. Annals of the New York Academy of Sciences 102, 29–45 (2006).

6. Wang, J. Electrochemical glucose biosensors. Chemical reviews 108, 814–25 (2008).

7. Almeida, M. G. Electrochemical biosensors revisited: old solutions to new problems. Submited in Bioelectrochemistry (2013).

8. Guilbault, G. G. & Lubrano, G. J. An enzyme electrode for the amperometric determination of glucose. Analytica chimica acta 64, 439–55 (1973).

9. Cammann, K. Bio-sensors based on ion-selective electrodes. Fresenius' Zeitschrift for Analytische Chemie 287, 1–9 (1977).

10. Eddowes, M. J. & Hill, H. A. O. Novel method for the investigation of the electrochemistry of metalloproteins: cytochrome c. Journal of the Chemical Society, Chemical Communications 771b (1977).doi:10.1039/c3977000771b

11. Eddowes, M. J., Hill, H. A. O. & Uosaki, K. The electrochemistry of cytochrome c. Investigation of the mechanism of the 4,4′-bipyridyl surface modified gold electrode. Journal of Electroanalytical Chemistry and Interfacial Electrochemistry 116, 527–537 (1980).

12. Huck, H. & Schmidt, H.-L. Chloranil as a Catalyst for the Electrochemical Oxidation of NADH to NAD+. Angewandte Chemie International Edition in English 20, 402–403 (1981).

13. Jaegfeldt, H., Torstensson, A. B. C., Gorton, L. G. O. & Johansson, G. Catalytic oxidation of reduced nicotinamide adenine dinucleotide by graphite electrodes modified with adsorbed aromatics containing catechol functionalities. Analytical Chemistry 53, 1979–1982 (1981).

14. Shichiri, M., Yamasaki, Y., Kawamori, R., Hakui, N. & Abe, H. Wearable artificial endocrine pancreas with needle-type glucose sensor. The Lancet 320, 1129–1131 (1982).

15. Cass, A. E. G. *et al.* Ferrocene-mediated enzyme electrode for amperometric determination of glucose. Analytical Chemistry 56, 667–671 (1984).

16. Degani, Y. & Heller, A. Direct electrical communication between chemically modified enzymes and metal electrodes. I. Electron transfer from glucose oxidase to metal electrodes via electron relays, bound covalently to the enzyme. The Journal of Physical Chemistry 91, 1285–1289 (1987).

17. Degani, Y. & Heller, A. Direct electrical communication between chemically modified enzymes and metal electrodes. 2. Methods for bonding electron-transfer relays to glucose oxidase and D-amino-acid oxidase. Journal of the American Chemical Society 110, 2615–2620 (1988).

18. Forster, R. J. & Vos, J. G. Synthesis, characterization, and properties of a series of osmium- and ruthenium-containing metallopolymers. Macromolecules 23, 4372–4377 (1990).

19. Csöregi, E., Schmidtke, D. W. & Heller, A. Design and optimization of a selective subcutaneously implantable glucose electrode based on "wired" glucose oxidase. Analytical chemistry 67, 1240–4 (1995).

20. Schmidtke, D. W. Measurement and modeling of the transient difference between blood and subcutaneous glucose concentrations in the rat after injection of insulin. Proceedings of the National Academy of Sciences 95, 294–299 (1998).

21. Wagner, J. G. *et al.* Continuous amperometric monitoring of glucose in a brittle diabetic chimpanzee with a miniature subcutaneous electrode. Proceedings of the National Academy of Sciences 95, 6379–6382 (1998).

22. Frew, J. E. & Hill, H. a Direct and indirect electron transfer between electrodes and redox proteins. European journal of biochemistry / FEBS 172, 261–9 (1988).

23. Tarasevich, M. R., Yaropolov, A. I., Bogdanovskaya, V. A. & Varfolomeev, S. D. 293 - Electrocatalysis of a cathodic oxygen reduction by laccase. Bioelectrochemistry and Bioenergetics 6, 393–403 (1979).

24. IKEDA, T., FUSHIMI, F., MIKI, K. & SENDA, M. Direct bioelectrocatalysis at electrodes modified with D-gluconate dehydrogenase. Agricultural and biological chemistry 52, 2655–2658.

25. Ikeda, T., Miyaoka, S. & Miki, K. Enzyme-catalysed electrochemical oxidation of d-gluconate at electrodes coated with d-gluconate dehydrogenase, a membrane-bound flavohemoprotein. Journal of Electroanalytical Chemistry 352, 267–278 (1993).

26. Armstrong, F. A., George, S. J., Thomson, A. J. & Yates, M. G. Direct electrochemistry in the characterisation of redox proteins: Novel properties of Azotobacter 7Fe ferredoxin. FEBS Letters 234, 107–110 (1988).

27. Armstrong, F. A. Probing Metalloproteins by Voltammetry. Bioinorganic Chemistry 72, (1990).

28. Armstrong, F. A., Heering, H. A. & Hirst, J. Reaction of complex metalloproteins studied by protein-film voltammetry. Chemical Society Reviews 26, 169 (1997).

29. Zayats, M., Kharitonov, A. B., Katz, E., Bückmann, A. F. & Willner, I. An integrated NAD+-dependent enzyme-functionalized field-effect transistor (ENFET) system: development of a lactate biosensor. Biosensors & bioelectronics 15, 671–80 (2000).

30. Kurzawa, C., Hengstenberg, A. & Schuhmann, W. Immobilization method for the preparation of biosensors based on pH shift-induced deposition of biomolecule-containing polymer films. Analytical chemistry 74, 355–61 (2002).

31. Guschin, D. a, Shkil, H. & Schuhmann, W. Electrodeposition polymers as immobilization matrices in amperometric biosensors: improved polymer synthesis and biosensor fabrication. Analytical and bioanalytical chemistry 395, 1693–706 (2009).

32. Guschin, D. a, Castillo, J., Dimcheva, N. & Schuhmann, W. Redox electrodeposition polymers: adaptation of the redox potential of polymer-bound Os complexes for bioanalytical applications. Analytical and bioanalytical chemistry 398, 1661–73 (2010).

33. Weinstein, R. L. *et al.* Accuracy of the 5-day FreeStyle Navigator Continuous Glucose Monitoring System: comparison with frequent laboratory reference measurements. Diabetes care 30, 1125–30 (2007).

34. Scheller, Frieder W.; Schubert, F. *et al.* Biosensors. Journal of Chromatography A 510, 347–354 (Elsevier: 1992).

35. Thévenot, D. R., Toth, K., Durst, R. A., Wilson, G. S. & The, D. R. Electrochemical biosensors: recommended definitions and classification. Biosensors and Bioelectronics 16, 121–131 (2001).

36. Cracknell, J. a, Vincent, K. a & Armstrong, F. a Enzymes as working or inspirational electrocatalysts for fuel cells and electrolysis. Chemical reviews 108, 2439–61 (2008).

37. Guilbault, G. G. Use of immobilized enzymes in chemical analysis. Journal of Solid-Phase Biochemistry 2, 329–342 (1978).

38. Phillips, P. E. M. & Wightman, R. M. Critical guidelines for validation of the selectivity of in-vivo chemical microsensors. TrAC Trends in Analytical Chemistry 22, 509–514 (2003).

39. Silveira, C. M. C. F. Development of electrochemical nitrite biosensors using cytochrome c nitrite reductase from Desulfovibrio desulfuricans ATCC 27774. (2011).at <http://hdl.handle.net/10362/6811>

40. Wang, Z., Etienne, M., Quilès, F., Kohring, G.-W. & Walcarius, A. Durable cofactor immobilization in sol-gel bio-composite thin films for reagentless biosensors and bioreactors using dehydrogenases. Biosensors & bioelectronics 32, 111–7 (2012).

41. Fernandez-lafuente, R. *et al.* Stabilization of multimeric enzymes via immobilization and post-immobilization techniques. Journal of Molecular Catalysis B: Enzymatic 7, 181–189 (1999).

42. Torchilin, V. P., Trubetskoy, V. S., Omel'Yanenko, V. G. & Mratinek, K. Stabilization of subunit enzyme by intersubunit crosslinking with bifunctional reagents: studies with glyceraldehyde-3-phosphate dehydrogenase. Journal of Molecular Catalysis 19, 291–301 (1983).

43. Scouten, W., Luong, J. & Stephenbrown, R. Enzyme or protein immobilization techniques for applications in biosensor design. Trends in Biotechnology 13, 178–185 (1995).

44. Vandenberg, E., Brown, R. & Krull, U. Immobilized biosystems in theory and practical applications. Food / Nahrung 39, 129 (Elsevier, Holland: 1983).

45. Weetall, H. H. Preparation of immobilized proteins covalently coupled through silane coupling agents to inorganic supports. Applied biochemistry and biotechnology 41, 157–88 (1993).

46. Doretti, L., Ferrara, D. & Lora, S. Enzyme-entrapping membranes for biosensors obtained by radiation-induced polymerization. Biosensors and Bioelectronics 8, 443–450 (1993).

47. O'Driscoll, K. F. Techniques of enzyme entrapment in gels. Methods in enzymology 44, 169–83 (1976).

48. Scouten, W. H. A survey of enzyme coupling techniques. Immobilized Enzymes and Cells Part B 135, 30–60 (1987).

49. Adeyoju, O., Iwuoha, E. I., Smyth, M. R. & Leech, D. High-performance liquid chromatographic determination of phenols using a tyrosinase-based amperometric biosensor detection system. The Analyst 121, 1885 (1996).

50. Scouten, W. H., Luong, J. H. T., Stephenbrown, R. & Brown, R. S. Enzyme or protein immobilization techniques for applications in biosensor design. Trends in Biotechnology 13, 178–185 (1995).

51. Chibata, I. Immobilized enzymes — research and development. Biochemical Education 7, 284 (Wiley & Sons, Incorporated, John: 1978).

52. Avnir, D., Coradin, T., Lev, O. & Livage, J. Recent bio-applications of sol–gel materials. Journal of Materials Chemistry 16, 1013 (2006).

53. Wang, J. Sol–gel materials for electrochemical biosensors. Analytica Chimica Acta 399, 21–27 (1999).

54. Walcarius, A. & Collinson, M. M. Analytical chemistry with silica sol-gels: traditional routes to new materials for chemical analysis. Annual review of analytical chemistry (Palo Alto, Calif.) 2, 121–43 (2009).

55. Ellerby, L. *et al.* Encapsulation of proteins in transparent porous silicate glasses prepared by the sol-gel method. Science 255, 1113–1115 (1992).

56. Gill, I. & Ballesteros, A. Bioencapsulation within synthetic polymers (Part 2): non-sol-gel protein-polymer biocomposites. Trends in biotechnology 18, 469–79 (2000).

57. Pastor, I., Prieto, M. & Mateo, C. R. Effect of sol-gel confinement on the structural dynamics of the enzyme bovine Cu,Zn superoxide dismutase. The journal of physical chemistry. B 112, 15021–8 (2008).

58. Jin, W. & Brennan, J. D. Properties and applications of proteins encapsulated within sol–gel derived materials. Analytica Chimica Acta 461, 1–36 (2002).

59. Seddon, A. M., Curnow, P. & Booth, P. J. Membrane proteins, lipids and detergents: not just a soap opera. Biochimica et biophysica acta 1666, 105–17 (2004).

60. Le Maire, M., Champeil, P. & Moller, J. V Interaction of membrane proteins and lipids with solubilizing detergents. Biochimica et biophysica acta 1508, 86–111 (2000).

61. Vittal, R., Gomathi, H. & Kim, K.-J. Beneficial role of surfactants in electrochemistry and in the modification of electrodes. Advances in colloid and interface science 119, 55–68 (2006).

62. Rusling, J. J. F. Enzyme bioelectrochemistry in cast biomembrane-like films. Accounts of chemical research 31, 363–369 (1998).

63. Nassar, A. E., Willis, W. S. & Rusling, J. F. Electron transfer from electrodes to myoglobin: facilitated in surfactant films and blocked by adsorbed biomacromolecules. Analytical chemistry 67, 2386–92 (1995).

64. Nassar, A. E., Rusling, J. F. & Kumosinski, T. F. Salt and pH effects on electrochemistry of myoglobin in thick films of a bilayer-forming surfactant. Biophysical chemistry 67, 107–16 (1997).

65. Lu, Z., Huang, Q. & Rusling, J. F. Films of hemoglobin and didodecyldimethylammonium bromide with enhanced electron transfer rates. Journal of Electroanalytical Chemistry 423, 59–66 (1997).

66. Mimica, D., Zagal, J. H. & Bedioui, F. Electroreduction of nitrite by hemin, myoglobin and hemoglobin in surfactant films. Journal of Electroanalytical Chemistry 497, 106–113 (2001).

67. Guto, P. M. & Rusling, J. F. Myoglobin retains iron heme and near-native conformation in DDAB films prepared from pH 5 to 7 dispersions. Electrochemistry Communications 8, 455–459 (2006).

68. Rusling, J. F. & Nassar, A. E. F. Enhanced electron transfer for myoglobin in surfactant films on electrodes. Journal of the American Chemical Society 115, 11891–11897 (1993).

69. Zhang, Z., Nassar, A. F., Lu, Z., Schenkman, J. B. & Rusling, J. F. Direct electron injection from electrodes to cytochrome P450cam in biomembrane-like films. Journal of the Chemical Society, Faraday Transactions 93, 1769–1774 (1997).

70. Nassar, A.-E. F., Zhang, Z., Hu, N., Rusling, J. F. & Kumosinski, T. F. Proton-Coupled Electron Transfer from Electrodes to Myoglobin in Ordered Biomembrane-like Films. The Journal of Physical Chemistry B 101, 2224–2231 (1997).

71. Zu, X., Lu, Z., Zhang, Z., Schenkman, J. B. & Rusling, J. F. Electroenzyme-Catalyzed Oxidation of Styrene and cis- -Methylstyrene Using Thin Films of Cytochrome P450cam and Myoglobin. 7372–7377 (1999).

72. Johnson, D. L., Lewis, B. C., Elliot, D. J., Miners, J. O. & Martin, L. L. Electrochemical characterisation of the human cytochrome P450 CYP2C9. Biochemical pharmacology 69, 1533–41 (2005).

73. Udit, A. K., Hindoyan, N., Hill, M. G., Arnold, F. H. & Gray, H. B. Protein-surfactant film voltammetry of wild-type and mutant cytochrome P450 BM3. Inorganic chemistry 44, 4109–11 (2005).

74. Aguey-Zinsou, K.-F., Bernhardt, P. V, De Voss, J. J. & Slessor, K. E. Electrochemistry of P450cin: new insights into P450 electron transfer. Chemical communications (Cambridge, England) 418–9 (2003).at <http://www.ncbi.nlm.nih.gov/pubmed/12613641>

75. Shukla, A., Gillam, E. M., Mitchell, D. J. & Bernhardt, P. V Direct electrochemistry of enzymes from the cytochrome P450 2C family. Electrochemistry Communications 7, 437–442 (2005).

76. Marcus, R. A. & Sutin, N. Electron transfers in chemistry and biology. Biochimica et Biophysica Acta (BBA) - Reviews on Bioenergetics 811, 265–322 (1985).

77. Habermüller, K., Mosbach, M. & Schuhmann, W. Electron-transfer mechanisms in amperometric biosensors. Fresenius' journal of analytical chemistry 366, 560–8 (2000).

78. Guo, L.-H., Allen, H. & Hill, O. Direct Electrochemistry of Proteins and Enzymes. Advances in Inorganic Chemistry 341–375 (1991).

79. Fridman, V. *et al.* Electrochemical investigation of cellobiose oxidation by cellobiose dehydrogenase in the presence of cytochrome c as mediator. Biochemical Society transactions 28, 63–70 (2000).

80. Scheller, F. W. *et al.* Bioelectrocatalysis by redox enzymes at modified electrodes. Reviews in Molecular Biotechnology 82, 411–424 (2002).

81. Léger, C., Bertrand, P. & Le, C. Direct electrochemistry of redox enzymes as a tool for mechanistic studies. Chemical reviews 108, 2379–438 (2008).

82. Kinnear, K. T. & Monbouquette, H. G. Direct electron transfer to Escherichia coli fumarate reductase in self-assembled alkanethiol monolayers on gold electrodes. Langmuir 9, 2255–2257 (1993).

83. Sucheta, A., Cammack, R., Weiner, J. & Armstrong, F. A. Reversible electrochemistry of fumarate reductase immobilized on an electrode surface. Direct voltammetric observations of redox centers and their participation in rapid catalytic electron transport. Biochemistry 32, 5455–5465 (1993).

84. Sucheta, A., Ackrell, B. A., Cochran, B. & Armstrong, F. A. Diode-like behaviour of a mitochondrial electron-transport enzyme. Nature 356, 361–2 (1992).

85. Bianco, P. Electrocatalytic Hydrogen-Evolution at the Pyrolytic Graphite Electrode in the Presence of Hydrogenase. Journal of The Electrochemical Society 139, 2428 (1992).

86. Khan, G. F., Shinohara, H., Ikariyama, Y. & Aizawa, M. Electrochemical behaviour of monolayer quinoprotein adsorbed on the electrode surface. Journal of Electroanalytical Chemistry and Interfacial Electrochemistry 315, 263–273 (1991).

87. Ikeda, T., Matsushita, F. & Senda, M. Amperometric fructose sensor based on direct bioelectrocatalysis. Biosensors and Bioelectronics 6, 299–304 (1991).

88. Burrows, A. L. *et al.* Direct electrochemistry of the enzyme, methylamine dehydrogenase, from bacterium W3A1. European journal of biochemistry / FEBS 199, 73–8 (1991).

89. Guo, L. H., Hill, H. A., Hopper, D. J., Lawrance, G. A. & Sanghera, G. S. Direct voltammetry of the Chromatium vinosum enzyme, sulfide:cytochrome c oxidoreductase (flavocytochrome c552). The Journal of biological chemistry 265, 1958–63 (1990).

90. Paddock, R. M. & Bowden, E. F. Electrocatalytic reduction of hydrogen peroxide via direct electron transfer from pyrolytic graphite electrodes to irreversibly adsorbed cytochrome c peroxidase. Journal of Electroanalytical Chemistry and Interfacial Electrochemistry 260, 487–494 (1989).

91. Armstrong, F. A. & Lannon, A. M. Fast interfacial electron transfer between cytochrome c peroxidase and graphite electrodes promoted by aminoglycosides: novel electroenzymic catalysis of hydrogen peroxide reduction. Journal of the American Chemical Society 109, 7211–7212 (1987).

92. Guo, L. H., Hill, H. A. O., Lawrance, G. A., Sanghera, G. S. & Hopper, D. J. Direct un-mediated electrochemistry of the enzyme P-cresolmethylhydroxylase. Journal of Electroanalytical Chemistry and Interfacial Electrochemistry 266, 379–396 (1989).

93. Yaropolov, A. I., Karyakin, A. A., Varfolomeev, S. D. & Berezin, I. V. Mechanism of H2-electrooxidation with immobilized hydrogenase. Bioelectrochemistry and Bioenergetics 12, 267–277 (1984).

94. E Ferapontova, E. & Gorton, L. Direct electrochemistry of heme multicofactor-containing enzymes on alkanethiol-modified gold electrodes. Bioelectrochemistry (Amsterdam, Netherlands) 66, 55–63 (2005).

95. Barton, S. C., Gallaway, J. & Atanassov, P. Enzymatic biofuel cells for implantable and microscale devices. Chemical reviews 104, 4867–86 (2004).

96. Silveira, C. M. & Almeida, M. G. Small electron-transfer proteins as mediators in enzymatic electrochemical biosensors. Analytical and bioanalytical chemistry (2013).doi:10.1007/s00216-013-6786-4

97. Ronkainen, N. J., Halsall, H. B. & Heineman, W. R. Electrochemical biosensors. Chemical Society reviews 39, 1747–63 (2010).

98. Yamamoto, K., Takagi, K., Kano, K. & Ikeda, T. Bioelectrocatalytic Detection of Histamine Using Quinohemoprotein Amine Dehydrogenase and the Native Electron Acceptor Cytochrome c-550. Electroanalysis 13, 375–379 (2001).

99. Townshend, A. Frontiers in biosensorics, I. fundamental aspects, II practical applications. Analytica Chimica Acta 353, 398 (1997).

100. Ghindilis, A. L., Atanasov, P. & Wilkins, E. Enzyme-catalyzed direct electron transfer: Fundamentals and analytical applications. Electroanalysis 9, 661–674 (1997).

101. Gorton, L. *et al.* Direct electron transfer between heme-containing enzymes and electrodes as basis for third generation biosensors. Analytica Chimica Acta 400, 91–108 (1999).

102. Updike, S. J. & Hicks, G. P. The Enzyme Electrode. Nature 214, 986–988 (1967).

103. Wollenberger, U., Schubert, F., Pfeiffer, D. & Scheller, F. W. Enhancing biosensor performance using multienzyme systems. Trends in biotechnology 11, 255–62 (1993).

104. Spalding, R. F. & Exner, M. E. Occurrence of Nitrate in Groundwater—A Review. Journal of Environment Quality 22, 392 (1993).

105. Manassaram, D. M., Backer, L. C. & Moll, D. M. A Review of Nitrates in Drinking Water: Maternal Exposure and Adverse Reproductive and Developmental Outcomes. Environmental Health Perspectives 114, 320–327 (2005).

106. Carpenter, S. R. *et al.* Nonpoint pollution of surface waters with phosphorous and nitrogen. Ecological Applications 8, 559–568 (1998).

107. Vitousek, P. M. *et al.* Human alteration of the global nirtrogen cycle: sources and consequences. Ecological Applications 7, 737–750 (1997).

108. COMLY, H. H. Cyanosis in infants caused by nitrates in well water. JAMA: The Journal of the American Medical Association 129, 112 (1945).

109. Almeida, G., Tavares, P., Lampreia, J., Moura, J. & Moura, I. Abstracts Poster Presentations (A). Journal of Inorganic Biochemistry 86, 119–130 (2001).

110. Lundberg, J. & Gladwin, M. Nitrate and nitrite in biology, nutrition and therapeutics. Nature chemical biology 5, 865–869 (2009).

111. Shiva, S., Gladwin, M. T. & Gladwin, Æ. M. T. Nitrite mediates cytoprotection after ischemia/reperfusion by modulating mitochondrial function. Basic research in cardiology 104, 113–9 (2009).

112. Hord, N. G., Tang, Y. & Bryan, N. S. Food sources of nitrates and nitrites: the physiologic context for potential health benefits. The American journal of clinical nutrition 90, 1–10 (2009).

113. Van Faassen, E. E. *et al.* Nitrite as regulator of hypoxic signaling in mammalian physiology. Medicinal research reviews 29, 683–741 (2009).

114. Bryan, N. S. Nitrite in nitric oxide biology: cause or consequence? A systems-based review. Free radical biology & medicine 41, 691–701 (2006).

115. Reynolds, J. D. *et al.* Nitrate and nitrite anion concentration in the intact cerebral cortex of preterm and nearterm fetal sheep: indirect index of in vivo nitric oxide formation. Journal of pharmacological and toxicological methods 39, 125–8 (1998).

116. Raat, N. J. H. *et al.* Dietary nitrate and nitrite modulate blood and organ nitrite and the cellular ischemic stress response. Free radical biology & medicine 47, 510–7 (2009).

117. Cosby, K. *et al.* Nitrite reduction to nitric oxide by deoxyhemoglobin vasodilates the human circulation. Nature medicine 9, 1498–505 (2003).

118. Sinha, S. S., Shiva, S. & Gladwin, M. T. Myocardial protection by nitrite: evidence that this reperfusion therapeutic will not be lost in translation. Trends in cardiovascular medicine 18, 163–72 (2008).

119. Jensen, F. B. The role of nitrite in nitric oxide homeostasis: a comparative perspective. Biochimica et biophysica acta 1787, 841–8 (2009).

120. Perlman, D. H. *et al.* Mechanistic insights into nitrite-induced cardioprotection using an integrated metabolomic/proteomic approach. Circulation research 104, 796–804 (2009).

121. Bryan, N. S. *et al.* Dietary nitrite supplementation protects against myocardial ischemia-reperfusion injury. Proceedings of the National Academy of Sciences of the United States of America 104, 19144–9 (2007).

122. Webb, A. J. *et al.* Acute blood pressure lowering, vasoprotective, and antiplatelet properties of dietary nitrate via bioconversion to nitrite. Hypertension 51, 784–90 (2008).

123. Ellis, G., Adatia, I., Yazdanpanah, M. & Makela, S. K. Nitrite and nitrate analyses: a clinical biochemistry perspective. Clinical biochemistry 31, 195–220 (1998).

124. Silveira, C. M. *et al.* An efficient non-mediated amperometric biosensor for nitrite determination. Biosensors & bioelectronics 25, 2026–32 (2010).

125. Almeida, M. G., Serra, A., Silveira, C. M. & Moura, J. J. G. Nitrite biosensing via selective enzymes–a long but promising route. Sensors (Basel, Switzerland) 10, 11530–55 (2010).

126. Bianco, P. The Origin of Bioelectrochemistry: An Overview. Encyclopedia of Electrochemistry, Bioelectrochemistry (Wiley-VCH: 2002).

127. Silveira, C. M., Besson, S., Moura, I., Moura, J. J. G. & Almeida, M. G. Measuring the cytochrome C nitrite reductase activity-practical considerations on the enzyme assays. Bioinorganic chemistry and applications 2010, (2010).

128. Da Silva, S., Cosnier, S., Gabriela Almeida, M. & Moura, J. J. G. An efficient poly(pyrrole–viologen)-nitrite reductase biosensor for the mediated detection of nitrite. Electrochemistry Communications 6, 404–408 (2004).

129. Serra, a S. *et al.* Cooperative use of cytochrome cd1 nitrite reductase and its redox partner cytochrome c552 to improve the selectivity of nitrite biosensing. Analytica chimica acta 693, 41–6 (2011).

130. Almeida, M. G., Silveira, C. M. & Moura, J. J. G. Biosensing nitrite using the system nitrite redutase/Nafion/methyl viologen–a voltammetric study. Biosensors & bioelectronics 22, 2485–92 (2007).

131. Kissinger, P. T. Biosensors-a perspective. Biosensors & bioelectronics 20, 2512–6 (2005).

132. Chen, H. *et al.* Highly sensitive nitrite biosensor based on the electrical wiring of nitrite reductase by [ZnCr-AQS] LDH. Electrochemistry Communications 9, 2240–2245 (2007).

133. Richardson, D. J. & Watmough, N. J. Inorganic nitrogen metabolism in bacteria. Current opinion in chemical biology 3, 207–19 (1999).

134. Moura, I. & Moura, J. J. Structural aspects of denitrifying enzymes. Current opinion in chemical biology 5, 168–75 (2001).

135. Kiang, C. H., Kuan, S. S. & Guilbault, G. G. A novel enzyme electrode method for the determination of nitrite based on nitrite reductase. Analytica chimica acta 80, 209–14 (1975).

136. Scharf, M. *et al.* Electrochemical Studies on Nitrite Reductase toward a Biosensor. Biochemical and Biophysical Research Communications 209, 1018–1025 (1995).

137. Zhang, Z. *et al.* A novel nitrite biosensor based on conductometric electrode modified with cytochrome c nitrite reductase composite membrane. Biosensors & bioelectronics 24, 1574–9 (2009).

138. Silveira, C. M. *et al.* Enhanced Direct Electron Transfer of a Multihemic Nitrite Reductase on Single-walled Carbon Nanotube Modified Electrodes. Electroanalysis 22, 2973–2978 (2010).

139. Strehlitz, B. *et al.* A nitrite sensor based on a highly sensitive nitrite reductase mediator-coupled amperometric detection. Analytical chemistry 68, 807–16 (1996).

140. Strehlitz, B. *et al.* Artificial electron donors for nitrate and nitrite reductases usable as mediators in amperometric biosensors. Fresenius' Journal of Analytical Chemistry 349, 676–678 (1994).

141. Ferretti, S. *et al.* Optical biosensing of nitrite ions using cytochrome cd1 nitrite reductase encapsulated in a sol-gel matrix. The Analyst 125, 1993–9 (2000).

142. Rosa, C. C., Cruz, H. J., Vidal, M. & Oliva, A. G. Optical biosensor based on nitrite reductase immobilised in controlled pore glass. Biosensors & bioelectronics 17, 45–52 (2002).

143. Wu, Q. *et al.* A nitrite biosensor based on a maltose binding protein nitrite reductase fusion immobilized on an electropolymerized film of a pyrrole-derived bipyridinium. Analytical chemistry 69, 4856–63 (1997).

144. Quan, D., Min, D. G., Cha, G. S. & Nam, H. Electrochemical characterization of biosensor based on nitrite reductase and methyl viologen co-immobilized glassy carbon electrode. Bioelectrochemistry (Amsterdam, Netherlands) 69, 267–75 (2006).

145. Sasaki, S. *et al.* Application of nitrite reductase from Alcaligenes faecalis S-6 for nitrite measurement. Biosensors & bioelectronics 13, 1–5 (1998).

146. Astier, Y. *et al.* Sensing nitrite through a pseudoazurin-nitrite reductase electron transfer relay. Chemphyschem: a European journal of chemical physics and physical chemistry 6, 1114–20 (2005).

147. Einsle, O. Cytochrome c nitrite reductase. Handbook of metalloproteins 1–14 (2006).doi:10.1002/0470028

148. Rodrigues, M. L., Oliveira, T. F., Pereira, I. a C. & Archer, M. X-ray structure of the membrane-bound cytochrome c quinol dehydrogenase NrfH reveals novel haem coordination. The EMBO journal 25, 5951–60 (2006).

149. Almeida, M. G. *et al.* The isolation and characterization of cytochrome c nitrite reductase subunits (NrfA and NrfH) from Desulfovibrio desulfuricans ATCC 27774. European Journal of Biochemistry 270, 3904–3915 (2003).

150. Einsle, O. *et al.* Structure of cytochrome c nitrite reductase. Nature 400, 476–80 (1999).

151. Cunha, C. a *et al.* Cytochrome c nitrite reductase from Desulfovibrio desulfuricans ATCC 27774. The relevance of the two calcium sites in the structure of the catalytic subunit (NrfA). The Journal of biological chemistry 278, 17455–65 (2003).

152. Bamford, V. a *et al.* Structure and Spectroscopy of the Periplasmic Cytochrome c Nitrite Reductase from Escherichia coli. Biochemistry 41, 2921–2931 (2002).

153. Einsle, O. *et al.* Cytochrome c nitrite reductase from Wolinella succinogenes. Structure at 1.6 A resolution, inhibitor binding, and heme-packing motifs. The Journal of biological chemistry 275, 39608–16 (2000).

154. Bellamine, A., Mangla, A. T., Nes, W. D. & Waterman, M. R. Characterization and catalytic properties of the sterol 14alpha-demethylase from Mycobacterium tuberculosis. Proceedings of the National Academy of Sciences of the United States of America 96, 8937–42 (1999).

155. Shumyantseva, V. V. *et al.* Electrochemical investigations of cytochrome P450. Biochimica et Biophysica Acta (BBA) - Proteins & Proteomics 1814, 94–101 (2011).

156. Montellano, P. R. O. De cytochrome p450: structure mechanism and biochemistry. (Springer-Verlag New York: 1995).

157. Sadeghi, S. J., Fantuzzi, A. & Gilardi, G. Breakthrough in P450 bioelectrochemistry and future perspectives. Biochimica et biophysica acta 1814, 237–248 (2011).

158. Hlavica, P. Assembly of non-natural electron transfer conduits in the cytochrome P450 system: a critical assessment and update of artificial redox constructs amenable to exploitation in biotechnological areas. Biotechnology advances 27, 103–21 (2009).

159. Shumyantseva, V. V, Bulko, T. V & Archakov, A. I. Electrochemical reduction of cytochrome P450 as an approach to the construction of biosensors and bioreactors. Journal of inorganic biochemistry 99, 1051–63 (2005).

160. Udit, A. K. & Gray, H. B. Electrochemistry of heme-thiolate proteins. Biochemical and biophysical research communications 338, 470–6 (2005).

161. Hara, M. Application of P450s for biosensing: combination of biotechnology and electrochemistry. Materials Science and Engineering: C 12, 103–109 (2000).

162. Todorovic, S., Jung, C., Hildebrandt, P. & Murgida, D. H. Conformational transitions and redox potential shifts of cytochrome P450 induced by immobilization. Journal of biological inorganic chemistry, JBIC: a publication of the Society of Biological Inorganic Chemistry 11, 119–27 (2006).

163. Udit, A. K. *et al.* Spectroscopy and electrochemistry of cytochrome P450 BM3-surfactant film assemblies. Journal of the American Chemical Society 128, 10320–5 (2006).

164. Bonifacio, A. *et al.* Active-site structure, binding and redox activity of the heme-thiolate enzyme CYP2D6 immobilized on coated Ag electrodes: a surface-enhanced resonance Raman scattering study. Journal of biological inorganic chemistry,JBIC: a publication of the Society of Biological Inorganic Chemistry 13, 85–96 (2008).

165. Schneider, E. & Clark, D. S. Cytochrome P450 (CYP) enzymes and the development of CYP biosensors. Biosensors & bioelectronics 39, 1–13 (2013).

166. Alexander I. Archakov & Bachmanova, G. I. Cytochrome P-450 and active oxygen. (1990).

167. Lewis, D. F. V. Guide to Cytochromes P450: Structure and Function. (Informa Healthcare: 2001).

168. Iyanagi, T. Structure and function of NADPH-cytochrome P450 reductase and nitric oxide synthase reductase domain. Biochemical and biophysical research communications 338, 520–8 (2005).

169. Ortiz de Montellano, P. R. Heme Oxygenase Mechanism: Evidence for an Electrophilic, Ferric Peroxide Species. Accounts of Chemical Research 31, 543–549 (1998).

170. Nelson, D. R. *et al.* P450 superfamily: update on new sequences, gene mapping, accession numbers and nomenclature. Pharmacogenetics 6, 1–42 (1996).

171. Im, S.-C. & Waskell, L. The interaction of microsomal cytochrome P450 2B4 with its redox partners, cytochrome P450 reductase and cytochrome b(5). Archives of biochemistry and biophysics 507, 144–53 (2011).

172. Ellis, J. *et al.* Domain motion in cytochrome P450 reductase: conformational equilibria revealed by NMR and small-angle x-ray scattering. The Journal of biological chemistry 284, 36628–37 (2009).

173. Hannemann, F., Bichet, A., Ewen, K. M. & Bernhardt, R. Cytochrome P450 systems–biological variations of electron transport chains. Biochimica et biophysica acta 1770, 330–44 (2007).

174. Walker, F. A. & Murataliev, M. B. Electron transfer by diflavin reductases. 1698, 1–26 (2004).

175. Smith, G. C., Tew, D. G. & Wolf, C. R. Dissection of NADPH-cytochrome P450 oxidoreductase into distinct functional domains. Proceedings of the National Academy of Sciences of the United States of America 91, 8710–4 (1994).

176. Brenner, S. *et al.* Inter-flavin electron transfer in cytochrome P450 reductase - effects of solvent and pH identify hidden complexity in mechanism. The FEBS journal 275, 4540–57 (2008).

177. Aigrain, L., Pompon, D., Moréra, S. & Truan, G. Structure of the open conformation of a functional chimeric NADPH cytochrome P450 reductase. EMBO reports 10, 742–7 (2009).

178. Iyanagi, T., Makino, N. & Mason, H. S. Redox properties of the reduced nicotinamide adenine dinucleotide phosphate-cytochrome P-450 and reduced nicotinamide adenine dinucleotide-cytochrome b5 reductases. Biochemistry 13, 1701–10 (1974).

179. Vermilion, J. L. & Coon, M. J. Purified liver microsomal NADPH-cytochrome P-450 reductase. Spectral characterization of oxidation-reduction states. The Journal of biological chemistry 253, 2694–704 (1978).

180. Zhou, S.-F., Yang, L.-P., Zhou, Z.-W., Liu, Y.-H. & Chan, E. Insights into the substrate specificity, inhibitors, regulation, and polymorphisms and the clinical impact of human cytochrome P450 1A2. The AAPS journal 11, 481–94 (2009).

181. Shumyantseva, V. V., Suprun, E. V., Bulko, T. V., Dobrynina, O. V. & Archakov, a. I. Sensor systems for medical application based on hemoproteins and nanocomposite materials. Biochemistry (Moscow) Supplement Series B: Biomedical Chemistry 4, 25–36 (2010).

182. Wilks, A. Analysis of Heme and Hemoproteins: Methods and Protocols. Heme, Chlorophyll, and Bilins (2002).doi:10.1385/1-59259-243-0:157

183. Gómez-Bombarelli, R. *et al.* Alkylating Potential of Oxetanes. Chemical Research in Toxicology 23, 1275–1281 (2010).

184. Kaplan, İ. H., Dağcı, K. & Alanyalıoğlu, M. Nucleation and Growth Mechanism of Electropolymerization of Methylene Blue: The Effect of Preparation Potential on Poly(methylene blue) Structure. Electroanalysis 22, 2694–2701 (2010).

185. Ni, H., Du, Y., Ma, G., Nagai, M. & Omi, S. Mechanism of Soap-Free Emulsion Polymerization of Styrene and 4-Vinylpyridine: Characteristics of Reaction in the Monomer Phase, Aqueous Phase, and Their Interface. Macromolecules 34, 6577–6585 (2001).

186. Mie, Y., Suzuki, M. & Komatsu, Y. Electrochemically Driven Drug Metabolism by Membranes Containing Human Cytochrome P450. Journal of the American Chemical Society 131, 6646–6647 (2009).

187. Estavillo, C. Epoxidation of styrene by human cyt P450 1A2 by thin film electrolysis and peroxide activation compared to solution reactions. Biophysical Chemistry 104, 291–296 (2003).

188. Bayachou, M., Lin, R., Cho, W. & Farmer, P. J. Electrochemical Reduction of NO by Myoglobin in Surfactant Film: Characterization and Reactivity of the Nitroxyl (NO -) Adduct. Journal of the American Chemical Society 120, 9888–9893 (1998).

189. Chen, X., Hu, N., Zeng, Y., Rusling, J. F. & Yang, J. Ordered Electrochemically Active Films of Hemoglobin, Didodecyldimethylammonium Ions, and Clay. Langmuir 15, 7022–7030 (1999).

190. Matsumura, H., Nakamura, N., Yohda, M. & Ohno, H. The electrochemical properties of thermophilic cytochrome P450 CYP119A2 at extremely high temperatures in poly(ethylene oxide). Electrochemistry Communications 9, 361–364 (2007).

191. Krishnan, S., Schenkman, J. B. & Rusling, J. F. Bioelectronic Delivery of Electrons to Cytochrome P450 Enzymes. The Journal of Physical Chemistry B 0, 8371–8380 (2011).

192. Bartlett, P. N. & Techniques, E. Bioelectrochemistry: fundamentals, experimental techniques and applications. Experimental Techniques (John Wiley & Sons: Chichester, England; Hoboken, NJ, 2008).

193. Nalwa, E. H. S., Bauza, D., Derry, G. N., Miller, R. & Fainerman, V. B. Handbook of Surfaces and Interfaces of Materials. Handbook of Surfaces and Interfaces of Materials 1, xxv–xxviii (2001).

194. Limoges, B. & Savéant, J.-M. Catalysis by immobilized redox enzymes. Diagnosis of inactivation and reactivation effects through odd cyclic voltammetric responses. Journal of Electroanalytical Chemistry 562, 43–52 (2004).

195. Gwyer, J. D., Angove, H. C., Richardson, D. J. & Butt, J. N. Redox-triggered events in cytochrome c nitrite reductase. Bioelectrochemistry (Amsterdam, Netherlands) 63, 43–7 (2004).

196. Dawson, J. Probing structure-function relations in heme-containing oxygenases and peroxidases. Science 240, 433–439 (1988).

197. Liu, S. & Ju, H. Reagentless glucose biosensor based on direct electron transfer of glucose oxidase immobilized on colloidal gold modified carbon paste electrode. Biosensors and Bioelectronics 19, 177–183 (2003).

198. Boccaccini, A. R. *et al.* Electrophoretic deposition of carbon nanotubes. Carbon 44, 3149–3160 (2006).

199. Cho, J. *et al.* Characterisation of carbon nanotube films deposited by electrophoretic deposition. Carbon 47, 58–67 (2009).

200. Goodwin, J. W., Hearn, J., Ho, C. C. & Ottewill, R. H. Studies on the preparation and characterisation of monodisperse polystyrene laticee. Colloid and Polymer Science Kolloid Zeitschrift & Zeitschrift for Polymere 252, 464–471 (1974).

201. Mazurenko, I. *et al.* Electrophoretic deposition of macroporous carbon nanotube assemblies for electrochemical applications. Carbon 53, 302–312 (2013).

202. Plumeré, N., Henig, J. & Campbell, W. H. Enzyme-catalyzed O2 removal system for electrochemical analysis under ambient air: application in an amperometric nitrate biosensor. Analytical chemistry 84, 2141–6 (2012).

203. Alayash, A. I., Patel, R. P. & Cashon, R. E. Redox reactions of hemoglobin and myoglobin: biological and toxicological implications. Antioxidants & redox signaling 3, 313–27 (2001).

204. Nagababu, E. & Rifkind, J. M. Heme degradation during autoxidation of oxyhemoglobin. Biochemical and biophysical research communications 273, 839–45 (2000).

205. Nagababu, E. & Rifkind, J. M. Reaction of hydrogen peroxide with ferrylhemoglobin: superoxide production and heme degradation. Biochemistry 39, 12503–11 (2000).

206. Nagababu, E., Ramasamy, S., Rifkind, J. M., Jia, Y. & Alayash, A. I. Site-specific cross-linking of human and bovine hemoglobins differentially alters oxygen binding and redox side reactions producing rhombic heme and heme degradation. Biochemistry 41, 7407–15 (2002).

207. Almeida, M. G. *et al.* A needle in a haystack: the active site of the membrane-bound complex cytochrome c nitrite reductase. FEBS letters 581, 284–8 (2007).

208. Villegas, J. a, Mauk, a G. & Vazquez-Duhalt, R. A cytochrome c variant resistant to heme degradation by hydrogen peroxide. Chemistry & biology 7, 237–44 (2000).